UNIVERSITY OF PAVIA
Department of Molecular Medicine
Unit of Human Physiology

Trafficking and intracellular processing of exogenous and endogenous proteins: VacA toxin from *Helicobacter pylori* as a tool.

Doctoral degree in Biomedical Sciences
Macro-area of Life Science
XXX Cycle – 2014-2017

PhD candidate: Giulia Sedda
Supervisor: Professor Vittorio Ricci

The important thing is to never stop questioning.
(Albert Einstein)

Summary

List of Figure and Table

Abbreviations

AO	Acridine Orange
Arf	ADP-ribosylation factors
BCF	Broth Culture Filtrate
BFA	Brefeldin A
BoNT	Botulinum Neurotoxin
BSA	Bovine Serum Albumin
CagA	Cytotoxin-associated gene A
CHL	Chloroquine
CTx	Cholera Toxin
CTxA	Cholera Toxin subunit A
CTxB	Cholera Toxin subunit B
DMEM	Dulbecco's Modified Eagle's Medium
DTx	Diphtheriae Toxin
DTxA	Diphtheriae Toxin catalytic domain A
EE	Early Endosome
EEA1	Early Endosome Antigen 1
EGA	2-[(4-Bromophenyl)methylene]-N-(2,6-dimethylphenyl)-hydrazinecarboxamide
EGF	Epidermal Growth Factor
EGFR	Epidermal Growth Factor Receptor
EGTA	Egtazic acid
ER	Endoplasmic Reticulum
ERAD	Endoplasmic-Reticulum-Associated protein Degradation
FBS	Fetal Bovine Serum
FK1	Antibody which recognize polyubiquitinated conjugates
GEEC	GPI-AP-enriched early endosomal compartment
GEF	Guanine nucleotide exchange factor
GFP	Green fluorescent protein
GM1	Monosialotetrahexosylganglioside 1
GPI-AP	Glycosylphosphatidylinositol-Anchored Protein
H^+-ATPase	Proton pump ATPase
HBSS	Hanks' Balanced Salt Solution
HCl	Hydrogen Chloride
HEPES	4-(2-hydroxyethyl)-1-piperazineethanesulfonic acid
Hp	*Helicobacter pylori*
Hsp	Heat shock protein
Htt	Huntingtin protein
HttQ97	Mutated Htt with 97 expansions of the polyglutamine tract
ICC	Immunocytochemistry analysis
IF	Immunofluorescence analysis
IHC	Immunohistochemistry analysis
IPOD	Insoluble Protein Deposit
JUNQ	Juxtanuclear Quality Control compartment
LAMP1	Lysosomal-Associated Membrane Protein 1
LBs	Lafora Bodies

LE	Late Endosome
LTx	Lethal Toxin
MG132	Benzyloxycarbonyl-Leu-Leu-Leu-aldehyde
Microscope Olympus	Microscope Olympus IX83 with X-Cite120W fluorescence illuminator system and inverted unit
$Mouse^{KO}$	Mouse knock out
MT	Microtubule
NaCl	Sodium Chloride
NH_4Cl	Ammonium Chloride
NRU	Neutral Red dye Uptake assay
p62	Sequestosome 1 protein
PaCS	Particle-rich Cytoplasmic Structure
PBS	Phosphate Buffered Saline
PM	Plasma Membrane
PolyQ	Polyglutamine tract
Rab	Ras related protein
RPTP α/β	Receptor Protein-Tyrosine Phosphatases α and β
SDS	Sodium Dodecyl Sulphate
SEM	Standard Error of Mean
STx	Shiga-like Toxin
STxB	Shiga-like Toxin subunit B
T4SS	Type IV Secretion System
TBST	Tris-Buffered Saline with Tween 20
TEM	Transmission Electron Microscopy
TGN	Trans-Golgi Network
Ub	Ubiquitin
UPS	Ubiquitin-Proteasome System
VacA	Vacuolating cytotoxin A
V-ATPase	Vacuolar-type H^+-ATPase
VHL	Von Hippel Landau tumor suppressor

ABSTRACT

INTRODUCTION

Eukaryotic cells are complex systems, which require a continuous flow of communication and material exchange between the intracellular and extracellular environments. The importance of a precise and fine-tuned cellular organization is demonstrated by the development of intracellular aggregates, such Particle-rich Cytoplasmic Structure (PaCS), as a result of altered trafficking or the failure of the degradation quality system to manage misfolded proteins. PaCSs were firstly identified in *Helicobacter pylori* (Hp) infected human superficial gastric epithelium and are present in a variety of cultured cell lines and ex vivo tissue. Inside PaCSs, it was found out the presence of Vacuolation toxin A (VacA), which has been recognized to be the key of the bacterium's ability to adapt in a hostile environment. VacA is a multifunctional toxin, with a similar structure and cleavage to the AB family of bacterial toxins. Intracellularly VacA can promote the formation of large vacuoles, arising from late endosome, but can alter also mitochondria functioning and intracellular calcium signaling, suggesting that the toxin could achieved the Endoplasmic Reticulum (ER).

AIM

The aims of this work are: to deeply characterize aggregates such as PaCSs, Lafora Bodies (LBs), Justanuclear Quality Control (JUNQ) and Insoluble Protein Deposit (IPOD) in order to investigate their nature and development; to elucidate the effect of trafficking inhibitor on VacA-induced vacuolization; to investigate VacA trafficking at different time.

RESULTS

Our results demonstrated that these aggregates are different inclusions, even if they share some similarities either structural or cytochemical. We observed that PaCSs and LBs are glycogen and laforin positive. A comprehensive analysis of JUNQ and IPOD showed that these aggregates have different ultrastructure from PaCSs and that they are mutually exclusive. Considering that inside PaCSs, VacA is accumulated together with polyubiquitin proteins and proteasome components, we evaluate if the toxin is ubiquitinated inside cells. Using histidine-tagged ubiquitin and metal affinity purification, we found out two bands, which might represent ubiquitinated VacA. We next analyzed the effect of eight different trafficking inhibitors, among which, EGA virtually abolish VacA-induced vacuolization. EGA effects was achieved also when vacuolization was already promoted, but it did not prevent toxin binding or internalization process. Binding-on-ice results support the idea that VacA can exploit the retrograde movement to reach ER. A preincubation time with EGA showed that the inhibitor can relocated the toxin to other organelles.

CONCLUSION

We demonstrated that PaCSs are unique aggregates and that VacA could be ubiquitinated inside cytoplasm. Our VacA ubiquitination and trafficking results supports the idea that the toxin could escape ER, reach the cytoplasm, ubiquitinated and later accumulated inside PaCSs. This approach could be a cell's tool to prevent VacA cytotoxic effect and promote degradation, making vacuoles only an intermediate step of toxin trafficking. Moreover, we found out that EGA, a newly inhibitor with a powerful effect on several toxins, virtually abolished the toxin activity in all experiments. Its effects, associated to a low toxicity in mouse model, make it look like a potent inhibitor and interesting tool to develop therapeutic strategy against bacterial toxins.

INTRODUCTION

Vesicles mediated intracellular trafficking

Eukaryotic cells are complex systems composed by several organelles which require continuous communication between them and between the intracellular and extracellular environment. Cellular compartmentalization in organelles is maintained through the organization of multiple intracellular structures surrounded by membrane, which guarantee distinct identity and function (Watson et al., 2005). The indispensable network among the different structures is allowed by an elaborate and coordinate budding and engulfing of small vesicular compartments and transient components, which constitute the endomembrane network (Mishev et al., 2013). The dynamic system moved materials from the different organelles inside the cells and from/to the Plasma Membrane (PM). For instance, polarized cell (i.e. cells that compose epithelial tissues or neurons) possesses distinct PM domains, to which selective vesicles must be directed. For this reason, the uptake of extracellular material and the endomembrane system work together to well orchestrate the correct direct of vesicles containing lipids, proteins or other cellular components to its final target (Alberts et al., 2005; Tokarev et al., 2009).

The correct communication among organelles depends on the intracellular membrane trafficking and its two main components: the outwards exocytic pathway and the inwards endocytic pathway (Tokarev et al., 2009; Watson et al., 2005). The exocytic pathway, also known as secretion pathway, elucidate by Palade and coworkers in 1960s, is responsible for delivery of newly synthetized proteins, to export communication components and for removal of waste substances. Instead the endocytic pathway, which was described in early 1970s by Brown and Goldstein (Tokarev et al., 2009), controls the engulf of extracellular materials, to receive signals from the outside environment, and of intracellular materials, to allow proper communication between the organelles. These two pathways are largely interconnected and allowed a continuous and dynamic movement between compartments (Mishev et al., 2013). As proposed by Watson and colleagues (Watson et al., 2005), there are no truly resident component inside the compartments: the constant movement of component between the different organelles allow to define only a balance of trafficking materials between them, on steady-state (Figure 1).

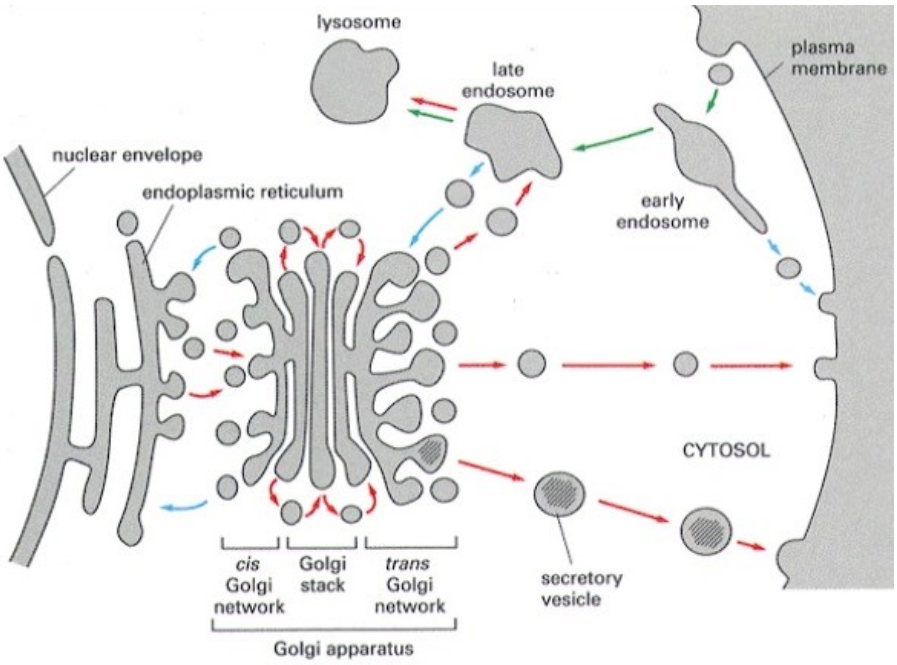

Figure 1. Summary of the exocytic pathway (red) and the endocytic pathway (green and blue). From Alberts et al., 2005.

The endocytic system

Macromolecules that cannot diffusely spontaneously through PM, such as macromolecules, to be internalized are engulfed by PM and leads to the formation of carrier vesicles. This process is the first step of endocytic pathway and it is essential for the uptake of nutrients as well as for signaling and cellular communication. Furthermore, cells are dependent on endocytosis for organism's development, immune responses and homeostasis (Conner & Schmid, 2003; Kumari et al., 2010). Endocytosis on the PM require an invagination and pinching-off of the membrane and can include the internalization of fluid and solutes, also known as "pinocytosis", or of solid particles larger than 0.5 µm of diameter, the so called "phagocytosis" (Conner & Schmid, 2003). To selectively control molecules entry into the cell and cellular responses to stimuli, cells develop different kind of endocytosis that are highly regulated. Moreover, the endocytic process does not involve only the PM, but it is also used by membrane of several organelles to obtain cellular products that needed to be modify. For instance, newly synthetized proteins that are secreted by the Endoplasmic Reticulum (ER) reach the Golgi apparatus for post-translational modification. To this purpose, vesicles budding from the ER needed to be sorting to the Golgi apparatus, where they can be internalized thanks to the vesicle-organelles membrane fusion.

As supposed by Palade in 1975 (Palade, 1975) small trafficking vesicles are essential for internalization, transport and exchange between organelles. Nowadays these small vesicles are

known as endosomes. Endosomes constitute a complex system of tubule-vacuolar membrane with two major elements: Early Endosomes (EEs) and Late Endosomes (LEs) (Johannes & Wunder, 2011). They are distinguished by the time for endocytic material to reach them, by markers and by morphology (Saimani & Kim, 2017; Stenmark, 2009).

EEs are the first endocytic compartment in which internalized material is accumulated after few minutes and are located in the peripheral cytoplasm. EEs receive endocytic cargo throughout different endocytic mechanism, including clathrine-mediated pathway or uncoated mechanisms (Huotari & Helenius, 2011). Inside EEs ligands dissociate form their receptors, due to the acidic luminal pH around 6.8 - 6.1 (Huotari & Helenius, 2011), and the unoccupied receptor usually recycle back to the cell surface via the recycling endosome (marked by Ras-related protein (Rab) 4 and 11) as for the transferrin receptors (Watson et al., 2005). EEs are heterogenous in morphology, localization, composition, and function. Most of them consist of dynamic small vesicles with tubular domains, that moves using cell Microtubules (MT) components. On the tubular extension there are domains enriched for several markers necessary for the correct sorting and targeting, including Rab5 and Early Endosome Antigen 1 (EEA1) (Huotari & Helenius, 2011; Watson et al., 2005). EEs are the major station of sorting of endocytic materials: from EEs molecules can be recycling back to the cell surface, sent to the Trans-Golgi Network (TGN) or to degradation pathway (Scott et al., 2014).

As the number of intraluminal vesicles increases, EEs mature into LEs. Mature LEs are bigger than EEs (with a diameter around 250 - 1000 nm) and they have low floating density and different lipid membrane components (Saimani & Kim, 2017). Their membrane is characterized by the so called “Rab conversions”, since contains Rab7 and is marked also by the Lysosomal-Associated Membrane Protein 1 (LAMP1) (Hu et al., 2015). Rab7 is essential for LEs maturation and allow endosomes to move along MT to the perinuclear region and promote pH drops (Girard et al., 2014). Proton pump ATPase (H^+-ATPase), known as Vacuolar ATPase (V-ATPase) is responsible for LEs acidification (where the pH drops to 6.0 to 4.8 range). V-ATPase is a unique class of ATPase essential for the endocytic pathway, vesicular trafficking and homeostasis, as demonstrated by its (Hu et al., 2015; Johnson et al., 1993). The drop of pH associated with several changing into the membrane component, morphology and fusion partners are necessary for shutting the recycling function of EEs and allow to direct the endosomal component to the degradative compartment (Huotari & Helenius, 2011). Mature LEs can fuse with lysosomes to promote the degradation of its cargo molecules. Lysosomes are the major degradation site for internalized materials and cellular proteins, that needed to be dismissed. Thanks to their hydrolytic enzymes and the acidic pH (around 4.5-5.0) they

can degrade biomolecules such as peptides, nucleic acids, carbohydrates and lipids. Furthermore, they can cooperate with phagosomes and promote autophagy, which allows to degrade unnecessary or dysfunctional components of the cells (Huotari & Helenius, 2011). Instead useful materials from LEs is sorted and transported throughout the TGN or to the PM and escape degradation (Hu et al., 2015).

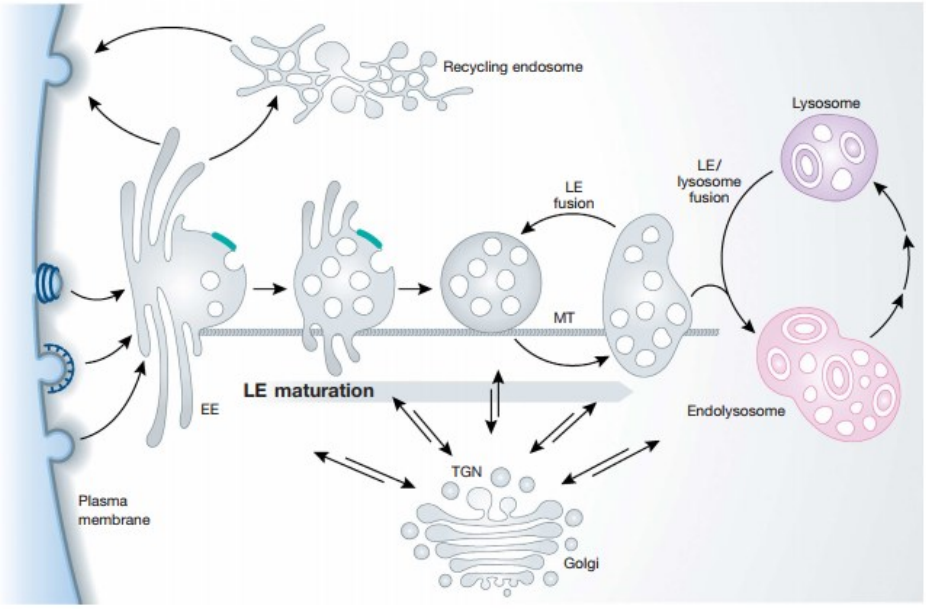

Figure 2. Summary of the endosome system, maturation and trafficking. From Huotari & Helenius, 2011.

The trafficking of endosome to TGN, which both EEs and LEs can achieved in parallel, following the exocytic pathway in the reverse direction, is known as retrograde transport (Johannes & Wunder, 2011). It is opposed to the classical anterograde trafficking by which newly synthetized proteins are produced in ER, sent to Golgi apparatus for post-translational modification and, throughout TGN which produces clathrin-coated transport vesicles, delivered as mature proteins (Personnic et al., 2016). Retrograde trafficking from endosome to the TGN is nowadays considered a critical intracellular pathways to several function, as for sorting receptors or enzymes, organelle biogenesis and functional integrity and intracellular glucose homeostasis (Chia et al., 2013; Johannes & Wunder, 2011; Personnic et al., 2016). Retrograde transport could also promote the trafficking of some proteins to the ER to allowed their function: for instance Mammalian Protein Sulfatase Modifying Factor 1 and the Autocrine Motility Factor receptor employ the retrograde movement to reach ER and interact with their substrates (Kumari et al., 2010). Evidence in the literature has demonstrated that bacterial and plant toxins, as well as some nonenveloped viruses, take advantage of the retrograde pathway to trafficking inside the cells (Chia et al., 2013; Sivan et al., 2016; Watson

et al., 2005). For instance Cholera Toxin (CTx) once internalized and accumulated inside EEs is retrograde transport to ER where it exploit ER-Associated protein Degradation (ERAD) pathway to reach its final cytoplasmic target (Progida et al., 2010; Wernick et al., 2010). In fact, retrograde targeting of cellular molecules to the ER, is a cell method which allowed to promote ERAD physiologically retro-translocation of misfolded or misassembled proteins to the cytosol (Johannes & Popoff, 2008). Inside the cytosol, misfolded proteins are ubiquitinated and sent to the proteasome for cleavage (Stringer, 2010). Moreover, ER was classically considered an organelle whose main interactions was with the outer nuclear membrane and its main task includes protein folding, lipid biosynthesis and calcium storage. However, Raiborg and colleagues (Raiborg et al., 2016) recently reported that ER may act as an interchanging platform for different organelles, making abundant contacts with multiple membranes, including endosomes and mitochondria. The recognized functions of ER-endosome contact sites include cholesterol transfer, receptor dephosphorylation and endosome fission. The fission between endosomes and the ER allows molecules flowing and it could be a pathway exploited by proteins and also several pathogen toxins.

Toxins

In order to colonize and survive inside the host, pathogens have developed key factors known as virulence factors. These factors protect bacteria from the host immune system, enable them to cross mucosal barriers and survive inside cells (Ramachandran, 2014).

Some of the most important bacterial virulence factors are toxins. Toxins can be divided in two main group: endotoxin and exotoxin. Endotoxins are relatively heat stable lipopolysaccharide-protein components of the outer membrane of bacteria that are released after the bacterium lysis (Fleck, 2006) or through membrane vesicle budding, generating bacterial outer membrane vesicles (Kulp & Kuehn, 2012). Lipopolysaccharides are now included in the pathogen-associated molecular patterns which recognized Toll-like receptor and trigger the innate immune response. Exotoxins, nowadays known as bacterial protein toxins (Boquet & Ricci, 2014), instead are usually heat sensible and highly antigenic proteins secreted by the bacterium and exert their action on the host cell. Usually pathogenic strains of the bacterium produce toxin while the non-pathogenic strains do not, and toxin production is one of the features that determines it degree of virulence (Todar, 2009). It should be emphasized that not all toxin effects are lethal for the host: even though some toxins cause events that culminate with the death of the host (i.e. Botulinum Neurotoxin (BoNT) secreted by *Clostridium botulinum*), other induce a well-orchestrated response that can allowed a successful chronic colonization (Peterson, 1996).

Interestingly, some gram-negative pathogens are able to secret outer membrane vesicles containing both endotoxins and bacterial protein toxins, combining or balancing their effects.

Considering their action, bacterial protein toxins can be divided in three different classes (Figure 3): signaling toxins acting on cell surface receptor, pore-forming toxins which oligomerized and form a pore on the membrane of the target cell and intracellular acting toxins (Boquet & Ricci, 2014).

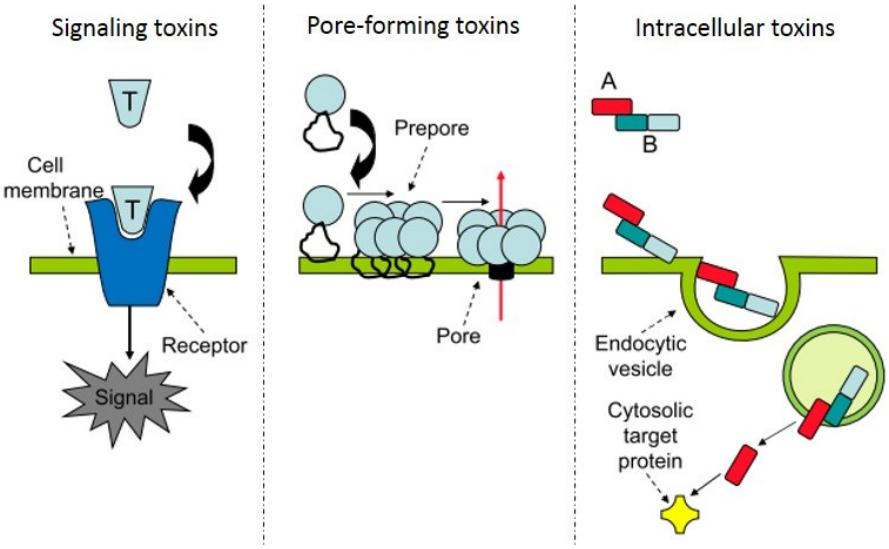

Figure 3. Cartoon of the three classes of bacterial protein toxins. Modified from Boquet & Ricci, 2014.

Among toxins which act on cell surface, are the superantigenic toxins produced by *Staphylococcus aureus* and *Staphylococcus pyogenes* mainly related to human sepsis. The pore-forming toxins instead, which provokes ion leakage throughout pore forming channel, includes hemolysins and cytolisins which are able to destroy host cell membranes and insecticidal toxins (Boquet & Ricci, 2014; Ramachandran, 2014).

The last group of intracellular acting toxin are known as AB family of toxins, due to their binary structure and includes Shiga, Cholera and Anthrax Toxins. These kind of toxins are characterized by A-component carry effective (usually enzymatic) activity which act on specific intracellular target and B subunit that is devoted to cell binding and intracellular translocation (Cover, 1998). The A subunit is not active until it is released form the native (A+B) structure and can have different effects, such as protein synthesis alteration (Shiga Toxin produced by *Shigella dysenteriae*), signal transduction (Pertussis Toxin secreted by *Bordetella pertussis*) or neurotransmitter release (BoNT) (Boquet & Ricci, 2014). Isolated A or B moiety, that lack of their toxicity, are useful tool both on medical or research purposes.

AB toxins can use two different mechanisms to be internalized: the first is direct entry, as the B subunits bind the receptor on the target cell and induce the formation of a pore in the membrane, throughout which the A component is inserted to the cell cytoplasm (Henkel et al., 2010). The other mechanism required active endocytosis clathrin-dipendent or independent of the AB toxins (Sandvig et al., 2004). Once internalized the toxin is accumulated inside EEs. The maturation of EEs into LEs, associated to a decrease in the pH of the vesicle, allow a change in conformation of the AB toxin which promote the separation of the two subunits. Since that these toxins need to pass inside acidic compartments to be cleaved and fully active, they are also known as pH-dependent bacterial toxin (Slater et al., 2014). Afterward, B subunit is translocated into the membrane where is able to insert into lipid membrane and produce a pore that allowed the passage of the A component that can reach its cytosolic target. Some toxins, such as Shiga-like Toxin (STx) secreted by *Escherichia coli,* are transported via the retrograde pathway before enters actively the cytosol (Johannes & Popoff, 2008; Sandvig & Van Deurs, 2002).

Furthermore, studies regarding cytotoxic effect (Sandvig et al., 2004) revealed that some of the toxins differ their internalization mechanism when infecting different cell types. For instance Diphtheria Toxin (DTx) secreted by *Corynebacterium diphtheriae* can be internalized both in clathrin-dependent and non-clathrin-dependent vesicles (Lencer & Tsai, 2003). This dual input mechanism has been shown to be dependent, not only on cell type, but also on the concentration of the toxin, suggesting an efficient adaptive evolution (Johannes & Popoff, 2008; Todar, 2009).

One of most studied AB toxins is CTx secreted by *Vibrio cholerae,* an oligomeric polypeptidic toxin which targets small intestine and induce an high volume of secretory diarrhea (Odumosu et al., 2010). As part of the AB family it consists of two subunits: the larger A (CTxA) subunit of approximately 27 kDa located centrally, while the five B subunits (CTxB, each of 10.6 kDa) are located peripherally (Bharati & Ganguly, 2011). Furthermore, studies have shown that CTxA component is further divided in two moieties, CTxA1 and CTxA2, linked by a disulfide bond. The CTxA1 component is responsible of the CTx toxicity (Odumosu et al., 2010), thanks to its ADP-ribosylating activity. CTx binds to the monosialotetrahexosylganglioside 1, also known as ganglioside GM1, located on the outer apical membranes of intestinal epithelial cells (Henkel et al., 2010). The binding of CTxB to the GM1 promote its clusterization and GM1 shows preferential association with lipid rafts, composed by gangliosides, cholesterol and sphingomyelin (Wernick et al., 2010). Moreover, Panasiewicz and colleagues (Panasiewicz et al., 2003) reported that one molecule of CTx

can bind up to five GM1 thanks to CTxB pentameric structure, and this type of binding increase the affinity of GM1-CTx, supporting the idea that lipid raft are crucial for CTx toxicity (Yukako Fujinaga et al., 2004). Confirm this hypothesis is the reduced trafficking of CTx and cytotoxicity in cells depleted of membrane cholesterol or sphingomyelin (Wernick et al., 2010).

The internalization of CTx can be done through different pathway: lipid raft mediated endocytic pathway (mainly in Hela cells for instance), clathrin mediated endocytic pathway, or ADP-ribosylation factor 6 (Arf6)-associated endocytic pathway (Bharati & Ganguly, 2011). After internalization CTx traffics from the PM to the TGN and ultimately reaches the ER (Wernick et al., 2010), bypassing the Golgi apparatus, that is not necessary for the development of cytotoxic effect (Feng et al., 2004; Spooner et al., 2008). On the contrary, the correct transport from EEs to the TGN is essential for its final destination targeting, and requires the association with detergent resistant membrane microdomains (Spooner et al., 2008). Inside ER, CTxA1 subunits take advantage of ERAD. Even though, it is not been detailed yet, the low content of lysine, an essential marker for ubiquitination, could allow CTxA1 to escapes degradation despite the passage through ERAD by subversion of the Sec61p complex, that physiologically forms a channel which allows the movement of proteins across ER membranes (Chong et al., 2008; Hazes & Read, 1997; Schmitz et al., 2000). Inside the cytosol, CTxA1 acts as a ADP-ribosyltransferase and leads to ADP-ribosylation of G protein, that promote the constitutive activation of the adenylate cyclase which produce cyclic cAMP. Increased level of intracellular cAMP activates protein kinase A, which phosphorylates the cystic fibrosis transmembrane conductance regulator and leads to an increasing active secretion of chloride ions (Henkel et al., 2010). The increase of chloride ions into the gut lumen associated with a decreased influx of sodium ions, cause a massive osmotic water flow through the intestinal cells and the pathological outcome of CTx.

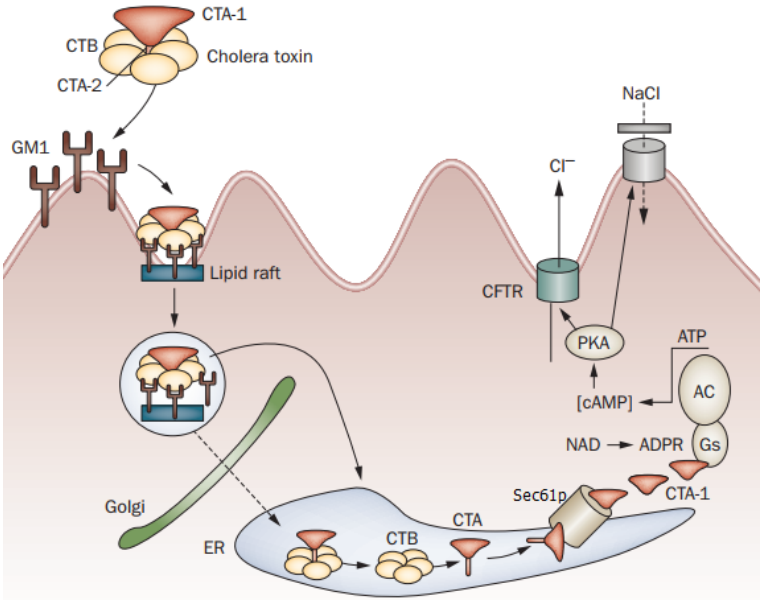

Figure 4. Summary of CTx intoxication. Modified from Clemens et al., 2011.
AC: adenylate cyclase; ADPR: ADP ribose; CTA: Cholera Toxin subunit A; CTB: Cholera Toxin subunit B; CTFR: cystic fibrosis transmembrane conductance regulator; GS: GTP-binding protein GS; NAD: nicotinamide adenine dinucleotide; PKA: protein kinase A.

The severe dehydration, electrolyte abnormalities and metabolic acidosis associated with CTx intoxication, leads to almost inevitably death of the patient in case that are not treated (Bharati & Ganguly, 2011). CTx intoxication approximately affect around 3-5 million of people, particularly in the developing countries, since it is passed on through drinking water or food that has been contaminated. Considering the massive and epidemic public health problem several attempts to understand toxin effect has been done. For instance, to investigate the trafficking of CTx and better understand its final target and action, several studies were performed using CTxB fluorescent marked (Day & Kenworthy, 2012; Matsudaira et al., 2015; Snider et al., 2010; Stechmann et al., 2010). CTxB fluorescence marked is structurally similar to CTxB and is able to bind to its receptor and traffic back to ER, even though it does not induce the cytotoxicity. Thus it is an useful tool to better understood CTx target and it was also used to develop a successful vaccine against cholera disease (Clemens et al., 2011; Odumosu et al., 2010; Todar, 2009).

Inhibitors

In early 2000s scientist studied small organic molecules with several chemical structures with modulators effect, known as inhibitors, to prevents cytotoxicity toxin related effects. These inhibitors, due to their ability to interfere with the intracellular movement, have proven to be useful to investigate endomembrane trafficking inside cells.

The first and most studied inhibitor is Brefeldin A (BFA), a hydrophobic fungal metabolite that interfere with anterograde transport by disrupting the Golgi apparatus (Driouich et al., 1993). BFA promote rapid and prominent disorganization of Golgi structure (Figure 5-2b), which manifested by the complete disassembly of cisternal stacks and their replacement by vacuoles, and the gradual redistribution of Golgi proteins to ER (Lippincott-Schwartz et al., 1989).

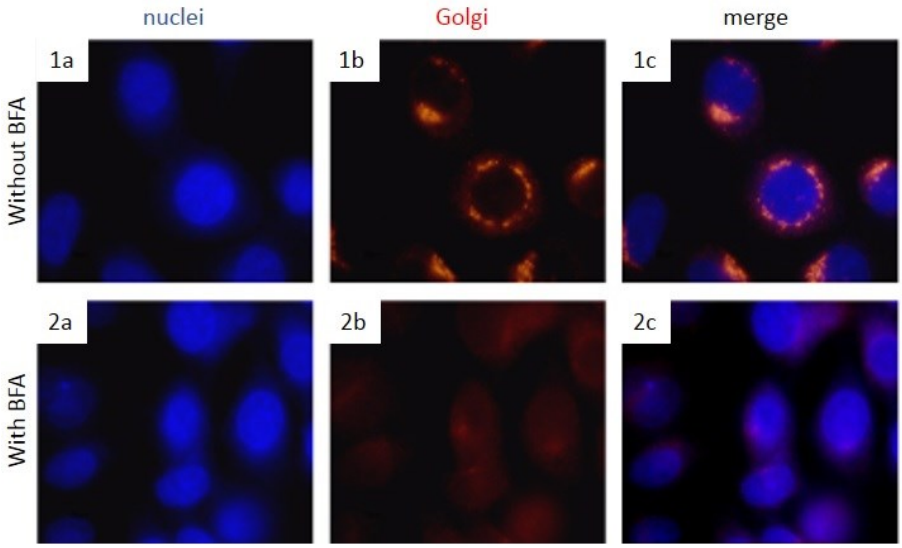

Figure 5. Hela cells left untreated (1) or with BFA (2) for 1 hour, revealed that Golgi (red) disassembly (1b versus 2b). a) Nuclei are counterstained in blue. Merge of nuclei and Golgi in c). Propriety of Alomone labs report.

All these alterations are reported to occur without affecting other events (i.e. endocytosis or protein synthesis) and are reversible, since that Golgi stacks regenerate after BFA removal (Ito et al., 2012). The main target of BFA in mammalian cells has been identified to be the guanine nucleotide exchange factor, called GBF1. This factor is a member of Arf family and it is responsible for the regulation of Arf1p GTPase: once GBF1 bind to its target, the GTPase change to an active form that recruits coat proteins necessary for proper vesicle formation and transport. BFA reversibly inhibits the function of GBF1 by uncompetitively binding to the GTPase inactive form. Due to lack of vesicle budding, Golgi membrane collapse and it is promoted Golgi fusion with the ER membrane nearby (Niu et al., 2005). BFA was used for several studies including trafficking studies, Golgi regeneration or Golgi-related proteins distribution (Alvarez-Miranda et al., 2015; Alvarez & Sztul, 1999; Doms et al., 1989; Ito et al., 2012). The inhibitor is currently used as a tool for studying membrane traffic and vesicle transport dynamics between the ER and Golgi apparatus.

Other inhibitors which are useful for dynamic trafficking studies, have been recognized to be able to block toxin related cytotoxicity. For instance, Stechmann and colleagues (Stechmann et al., 2010) found out that two inhibitors, called Retro-1 and Retro-2, are able to selectively inhibits STx and, even if in a less prominent way, ricin (found inside seeds of the castor oil plant *Ricinus communis*). Once internalized these toxins trafficking form EEs to ER via the Golgi apparatus (Johannes & Popoff, 2008). Using the B subunit of STx, termed STxB, they showed that Retro-1 and Retro-2 are able to induce an 80% decrease of trafficking to the TGN, and that STxB accumulates in the EEs of cell treated with inhibitors. Furthermore, their results reveal that these inhibitors did not induce any morphological changing of ER, EEs or LEs/lysosome and the anterograde transport was not affected. Interestingly Retro-1 and Retro-2 did not show any additive or synergistic effect, suggesting a possible common target inside the cells. They speculate that these compounds interact with glycolipids, which are needed by the toxin to be internalize. The stronger protective effect on STx toxicity than against ricin, could be due to the ability of ricin to trafficking between endosome and TGN by binding to several receptors, maybe bypassing the glycolipids anchors.

EGA

Gillespie and collaborators (Gillespie et al., 2013) in 2013 where conducting a high throughput screen of 30000 inhibitors in order to identify a compound able to block the Lethal Toxin (LTx) secreted by *Bacillus anthracis*. LTx is composed by two subunits consisting of a protective antigen with receptor role and lethal factor, a zinc metalloprotease which promote cell death (Slater et al., 2014). The protective antigen undergoes a conformational change upon exposure to low pH inside endosomes and form a pore through which the lethal factor is translocated into cytosol where it can exert its action. They were able to identify a potent compound, 2-[(4-Bromophenyl)methylene]-N-(2,6-dimethylphenyl)-hydrazinecarboxamide, which they called EGA. EGA was able to rescue viability to up to 100% of controls when measured 3 hours after toxin addition. Furthermore, EGA could protects cells even if was added 15 minutes after the intoxication. Their results revealed also that this inhibitor completely blocked the formation of Sodium Dodecyl Sulphate (SDS) resistant oligomers, which results from the acid-induced conformational change, but not affected the toxin ability to bind to PM. Using Epidermal Growth Factor (EGF) and examining trafficking of his receptor (EGFR), they found out that EGA effect could be overcome by excess ligand stimulation during longer periods of time. Moreover, since that in cells treated with EGA, EGF was retained in enlarged EEs, they suggest that EGA blocks the maturation from EEs to LEs. The same result on toxin assembly and

functioning was obtained studying Cytolethal Distending Toxins, secreted by several gram-negative bacteria such as *Shigella dysenteriae, Haemophilus ducreyi and Escherichia coli*, also confirm by another group (Dixon et al., 2015). Several bacteria toxins and viruses are known to require a low pH to develop their cytotoxic effect, explaining why they traffic from EEs to LEs. They suggest that EGA ability to prevent the maturation between these two compartments could also affect the toxin activity.

Starting from these data, Azarnia Tehran and colleagues (Azarnia Tehran et al., 2015) investigate the effect of EGA on BoNT. These toxins are neurospecific metalloproteases which act inside peripheral nerve terminals with potent and deadly effects. They showed that EGA was able to reduce BoNTs activity on neuronal cultures and also that was effective to prevent neurotoxicity in vivo. They found out that EGA maximal effect was reached at a final concentration of 12,5 μM (without any cytotoxic related effect) and that EGA could prevent neurotoxic effects when added before BoNTs intoxication. Using Lysotracker Red DND-99 a highly sensitive probe of acid organelles in cell, they show that EGA did not interfere with the maturation of acidic compartments or with BoNTs binding and internalization. Instead they underling that EGA prevents the trafficking of BoNTs to its target, therefore blocking the toxin action.

The group of Schnell in 2016 reported two different studies (Schnell A and B, 2016) on EGA with DTx and Clostridium Toxin.

In the first study (Schnell A, 2016), they analyzed EGA effect on the transport of the catalytic domain of DTx (DTxA), from the endosomal lumen into the host cytoplasm. They reported that preincubation time with EGA protects cells from DTxA cytotoxic effects. They found out also that a prolonged preincubation time with EGA (up to 6 hours) did not enhance the effect compared to a 1-hour preincubation period. Moreover, they confirm that EGA added up to 15 minutes after intoxication can develop the same protective effect as a preincubation treatment. Schnell groups revealed that EGA inhibits the pH-dependent transport of DTxA inside cells, by endosomes acidic environment mimicked assay. From their data, they speculated that EGA may block the transmembrane pore formation or inhibit host cell factor which are involved in DTxA translocation.

Regarding the effect of EGA on Clostridium Toxins (Schnell B, 2016) they analyzed three different kind of ADP-ribosylating toxins, known as CDT, iota and C2 secreted respectively by *Clostridium difficile, perfringens* and *botulinum*. These toxins are AB toxins and EGA was able to prevent the effect of toxins CDT, iota and C2 once internalized and assembly but did not prevent their binding or internalization. They demonstrated that EGA inhibits the pH-dependent transport of the

enzymatic component across cell membrane. Using the same endosomes acidic environment mimicked assay as for DTxA, they were able to mimics the condition in the lumen of acidified vesicle on the surface of living cells. Taking together these results, they speculated that EGA blocks the formation of heptameric translocation channel, as for LTx, or interfere with the correct conformation folding of the toxin.

Trafficking and misfolded proteins

Vesicle mediated intracellular trafficking is responsible not only for the movement of cellular materials in physiological condition or to ensure organelles integrity, but play an important role in response to several stressors. Damage proteins or proteins which cannot achieve their proper folded conformations and exceeds cell refolding and degradative capacities, are accumulated and leads to the development of intracellular aggregates (Miyazaki et al., 2016). Intracellular aggregates are oligomeric complexes of misfolded or altered proteins which can develop during hyperthermia, osmotic and oxidative stress or are due to mutation, RNA modification and translation misincorporation (Kopito, 2000). As a result of these alterations, misfolded or unassembled proteins can expose hydrophobic surfaces, which are usually buried in the interior domain during correct conformation process, to the aqueous environment of the cytosol. Such exposure can ease interaction between single proteins which can polymerized and form aggregates (Johnston et al., 2012). In some cases, these aggregates are surrounded by a membrane, with an organization organelle-like.

Altered proteins are actively delivered to aggresome by a dynein-dependent retrograde transport on MT. As demonstrated by Johnston and colleagues (Johnston et al., 2012), trafficking trough MT is responsible for removing potentially toxic misfolded proteins which have escaped the degradation system, and accumulated inside aggregates together with other components, such as the Ubiquitin-Proteasome System (UPS), molecular chaperons and polyubiquitinated proteins.

The UPS is a complex mechanism that functions as a quality control system and it is responsible for the degradation of more than 80% of normal and abnormal intracellular proteins. The degradation of misfolded proteins, is promoted by attaching to the target protein a Ubiquitin (Ub) moiety of 8.5 kDa: this bond is a multistep process that requires three different kind of enzymes (Ub-activating, conjugating and ligating enzymes) and involves the presence of lysine residues on the target protein. The Ub targeted protein is then sent to the proteasome, where is degraded by proteolytically cleavage (Shames & Finlay, 2012). The other major degradative system inside the cells is the

autophagy mechanism. Autophagy is a cellular pathway by which intracellular cargo are sent to lysosomes for degradation. It intervenes as physiological process to regulate homeostasis, as quality control system degrading cytoplasmic components and it also plays an innate immune defense role (Raju & Jones, 2010; Ricci, 2016). Classically stressor and starvation strongly induce autophagy, thus its role is also linked to aggregates.

Cytosolic aggregates are the hallmark of many severe human disease, as for amyloidosis, Alzheimer's disease, Parkinson's disease, Huntington's disease and alcoholic liver disease (Bersuker et al., 2013; Kopito, 2000; Takalo et al., 2013). Even though these inclusions were classical considered an harmful response of cell, there are increasing evidences that these aggregates might be an useful tool of the cell to avoid any more damage and promote proteins degradation by gather together altered proteins and degradative components (Kaganovich et al., 2008). Moreover, it has been shown that some of these aggregates can be dynamic and reversible: this could suggest a temporary role to prevent cellular deterioration and would allow a subsequent refolding afterwards. It has been speculated that, as well as the sequestration role, those aggregates can serve also to facilitate interaction with other degradative cellular compartments, such as lysosome or autophagic structure, which are delivered by MT to the same cellular region (Johnston et al., 2012). The cell death and extracellular lesions associated to many degenerative diseases could be due to an altered quality control or, for instance, due to loss of cytoprotective role of aggregates beyond cell tolerance limits (Kopito, 2000).

Particle-rich cytoplasmic structure

Recently, a new cytoplasmic structure has been described: it is called 'Particle-rich Cytoplasmic Structure' or PaCS (Necchi et al., 2010). PaCSs were firstly identified in *Helicobacter pylori* (Hp) infected human superficial–foveolar gastric epithelium (Figure 6a) and selectively concentrates several bacterial products and bodies as well as oncogenic proteins, nucleotide-binding oligomerization domain-containing protein 1 receptor, glycogen, Ub-activating enzyme E1, polyubiquitinated proteins and proteasome components (Necchi et al., 2010). The presence of PaCSs in gastric pre-neoplastic lesions associated with the selective colocalization with putative oncogenic factors, members of the mitogen-activated protein kinase signaling system and UPS, suggests a possible role in cancer origin or progression (Mani & Gelmann, 2005). Further studies have also revealed the presence of PaCSs in a variety of cultured cell lines, neoplastic or non-neoplastic, and ex vivo tissue cells (normal, chronically infected, mutated and neoplastic) (Necchi et

al., 2007; Solcia et al., 2014). PaCSs are constitutive in many cell lines (i.e. HeLa (Figure 6b), HL60, SHS5Y5 cells) and are positive for proteasome, polyubiquitinated proteins and glycogen (Sommi et al., 2013). Under Transmission Electron Microscopy (TEM), PaCS appears as a collection of barrel-like particles of about 13 nm thick and 13–20 nm long, in a relatively clear cytoplasmic area without cytoskeleton fibrils and usually surrounded by ribosomes (Solcia et al., 2014).

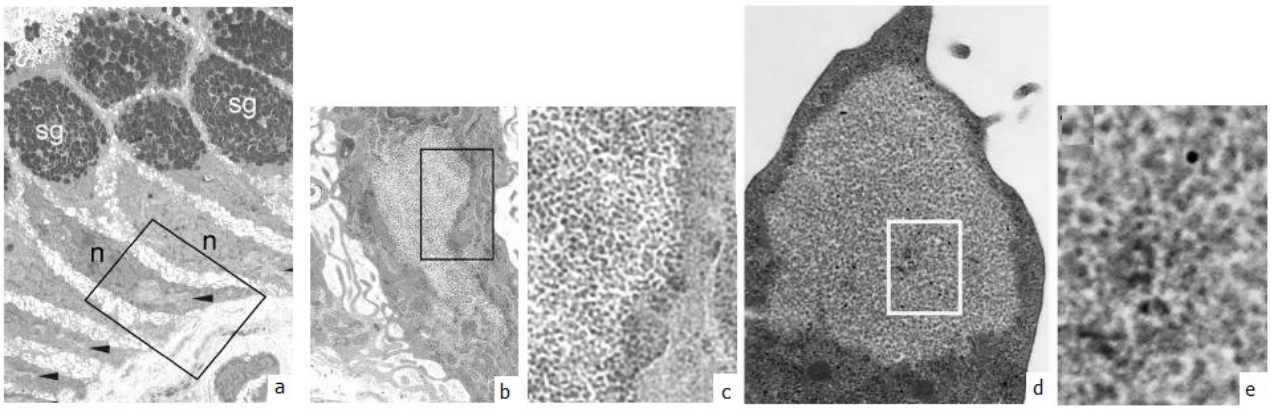

Figure 6. a) Hp-colonized non-neoplastic human gastric epithelium, from Necchi et al., 2010. Enlarged in b) and c) to show the particles characteristic (n, nucleus; sg, secretory granules; arrowheads, PaCSs). d) Glycogen immunoreactivity (bar, 1 µm) of PaCS in HeLa cell, magnified in e (bar, 100 nm) from Sommi et al., 2013.

PaCSs were found frequent in topographic relationship with sequestosomes in HeLa cells (Figure 7), amorphous structures largely destined to autophagy, but they are different both cytochemically and ultrastructurally, and are also distinct from dendritic cell aggresome-like induced structures (Solcia et al., 2014; Sommi et al., 2013).

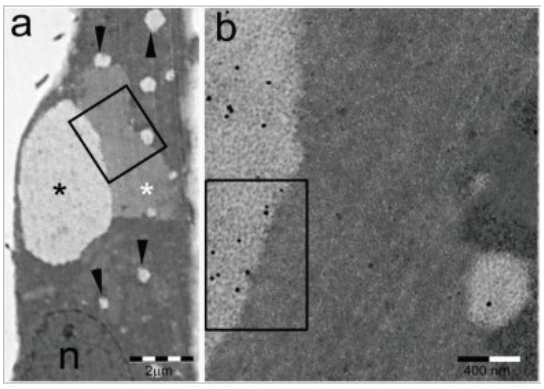

Figure 7. PaCSs and sequestosomes in HeLa cells cultured under basal conditions from Solcia et al., 2014. a) Ultrastructural image (bar, 2 µm; n, nucleus) of a sequestosome (white asterisk) next to a PaCS (black asterisk). Several other smaller PaCSs are highlighted by arrowheads. The boxed area is enlarged in b) to show distinctive barrel-like particles and antibody reactivity for polyubiquitinated proteins (bar, 400 nm).

Moreover Montagna and colleagues revealed that PaCSs can be induced by cytokines in human dendritic cells undergoing differentiation from their monocyte precursors (Montagna et al., 2017) and have been found in differentiating tissues of mouse fetus and human embryo (Necchi et al., 2014).

Lafora Bodies

Alternative structures that shows similar accumulation of glycogen and are positive for laforin primary antibody like PaCSs, are Lafora Bodies (LBs). LBs are present primarily in neurons, but can be found in multiple tissues, such as skeletal muscle, heart, liver, etc. (Minassian, 2001). LBs are pathognomonic of Lafora disease (OMIM #254780), a progressive autosomal recessive neurometabolic disease characterized by myoclonus epilepsy, cognitive deficit and physical deterioration, with an onset between 8 and 18 years of age. Symptoms gradually worsen and become intractable and are accompanied by progressive cognitive decline, resulting in dementia (Turnbull et al., 2012). About 10 years after onset, affected individuals are in near-continuous myoclonus with absence seizures, frequent generalized seizures, and profound vegetative state. Lafora disease is caused by a mutation in two genes NHLRC1 and EPM2A, which encodes respectively two proteins: malin (E3-Ub ligase) and laforin (a serine-threonine phosphatase). These proteins interact functionally to promote the degradation of glycogen synthase, in order to prevent the synthesis of glycogen. Gentry and colleagues (Gentry et al., 2005) revealed that laforin is polyubiquitinated in a malin-dependent manner, which promote its degradation. Mutation of NHLRC1 gene, resulting in loss of the E3 ligase activity of malin, abolished the laforin polyubiquitination and degradation, thus altering the laforin protein concentrations. Mutation of malin or laforin induced an increase of glycogen content and the presence of abnormally branched malformed and insoluble glycogen molecules called polyglucosan (Figure 8), whose latter accumulate into masses and forms LBs (Turnbull et al., 2012). The over-accumulation of polysaccharide inside LBs can causes cytotoxicity and neuronal apoptosis (Duran et al., 2014).

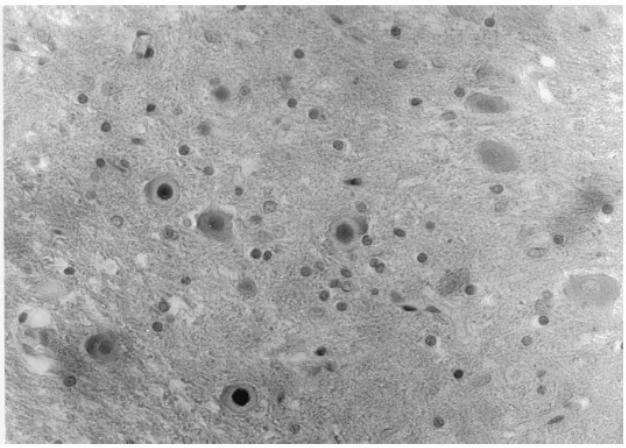

Figure 8. Hematoxylin-eosin stain of LBs with a dark core and paler peripheral zone in dentate nucleus of the brain. From Minassian, 2001.

The association between glycogen accumulation and LBs development was also confirmed by Duran and colleagues (Duran et al., 2014), whose generated a double-transgenic mouse model in which malin was deleted in all tissues and glycogen synthase was specifically deleted in the brain (mouse model malin^{KO}). Moreover, their findings reveal that glycogen accumulation impaired also autophagy.

Juxtanuclear Quality Control compartment and Insoluble Protein Deposit

A different intracytoplasmic structure that show similar characteristics to PaCS, regarding the accumulation of polyubiquitinated proteins and the proteasome, is the Juxtanuclear Quality Control compartment or JUNQ. When the proteasome is impaired, soluble polyubiquitinated proteins which were destined for degradation, are sorted into JUNQ. The sequestration is reversible, so the proteins that accumulate in JUNQ maybe refolded or degraded afterwards. The Von Hippel Landau tumor suppressor (VHL) for instance, has often been used as a model substrate to study proteins aggregation in yeast and mammalian cells (Amen & Kaganovich, 2015). Kaganovich (Kaganovich et al., 2008) reported that VHL folds only after binding to its cofactor and that mutations impairing cofactor binding or expression in cells lacking the cofactor, leads to misfolded VHL ubiquitination. Inhibition of the proteasome with benzyloxycarbonyl-Leu-Leu-Leu-aldehyde, also known as MG132, leads to the formation of a single juxtanuclear VHL inclusion in association with proteasome and UPS component. It has been speculated that, by concentrating proteasome, chaperones and ubiquitination machinery, the cell could gains efficiency in degradation of proteins (Amen & Kaganovich, 2015). Therefore JUNQ is rather a dynamic functional compartment than a deposition or storage site showing a turnover of misfolded proteins (Ogrodnik et al., 2014). Moreover the same

groups (Kaganovich et al., 2008) revealed that, in yeast, prolonged exposure to high levels of stresses causes JUNQ to increase in size, become less mobile and accumulate Heat shock protein (Hsp) 104. Furthermore, when JUNQ achieve that new proprieties, actin filaments redistribute around it, suggesting a possible recruitment of lysosomes, thus moved JUNQ to autophagic degradation as a last cellular effort (Ogrodnik et al., 2014). A classical model of studies, used in several investigation (England & Kaganovich, 2011; Ogrodnik et al., 2014; Weisberg et al., 2012) to promote the induction of JUNQ in mammalian cells, is the overexpression of proteins by transient or stable transfection. Under these stress-promoting conditions cells accumulated proteins inside aggregate inclusion and develop reliable JUNQ (Bagola & Sommer, 2008).

Misfolded proteins that are not ubiquitinated are instead sent to perivacuolar compartment known as Insoluble Protein Deposit or IPOD (Amen & Kaganovich, 2015; Ogrodnik et al., 2014). For instance, mutated expansion (40-100 against physiological 15-35 repeats) of the polyglutamine tract (polyQ) at the N-terminus of Huntingtin protein (Htt) promoted protein aggregation and accumulation inside IPOD, along with other proteins, such as several chaperones (Hsp42 or Hsp104) or autophagic markers. Aggregation of Mutated Htt (polyQ-Htt) becomes pathologic (Giacomello et al., 2011; Goehler et al., 2004) and leads to a neurodegenerative disorder called Huntington's disease. Kaganovich and collegues (Amen & Kaganovich, 2015) revealed that proteins within the IPOD are immobile and no ubiquitin or proteaosomal signal can be detected within these structures. IPOD sequestration of proteins, such as disease-linked amyloidogenic proteins that if aggregates can be toxic and the colocalization with protective cofactors, supports the idea of IPOD protective role (Amen & Kaganovich, 2015).

JUNQs and IPODs (Figure 9) are both dependent on MT for development. Benomyl, a drug that promote the depolymerization of MT, leads to the accumulation of proteins in small puncta through the cytosol (Bagola & Sommer, 2008) preventing JUNQ and IPOD development. This could imply that these aggregates are both formed by an active mechanism that require a specific intracellular trafficking. Furthermore, both compartments colocalized with Hsp104, a cytosolic chaperone which interacts with misfolded and aggregated proteins (Glover & Lindquist, 1998).

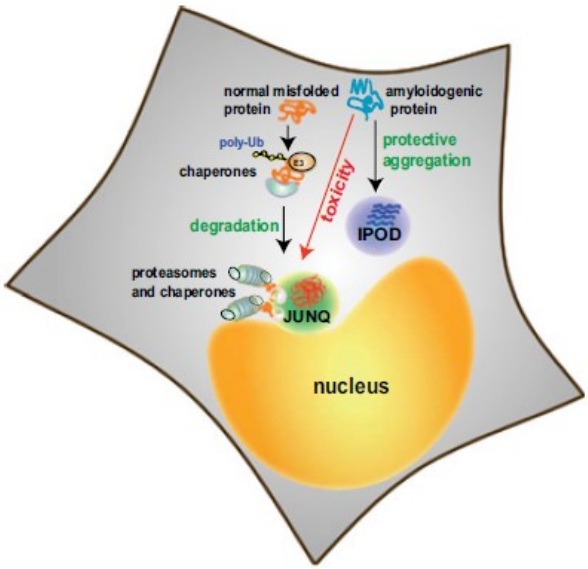

Figure 9. Model of JUNQ or IPOD development and functioning inside the cell. From Weisberg et al., 2012.

However they share these common features, as suggest by Bagola and Sommer (Bagola & Sommer, 2008), they are morphological and functional different: JUNQ appears as a temporary storage site under stress condition for misfolded and ubiquitinated proteins and IPOD, instead, is the result of accumulation of aggregation-prone not ubiquitinated components to prevent any cytotoxic effect.

Helicobacter pylori

Hp, previously known as *Campylobacter pylori*, is a microaerophilic, spiral shaped, Gram-negative bacterium (Figure 10) which represents the most common bacterial infection worldwide (Blaser & Atherton, 2004).

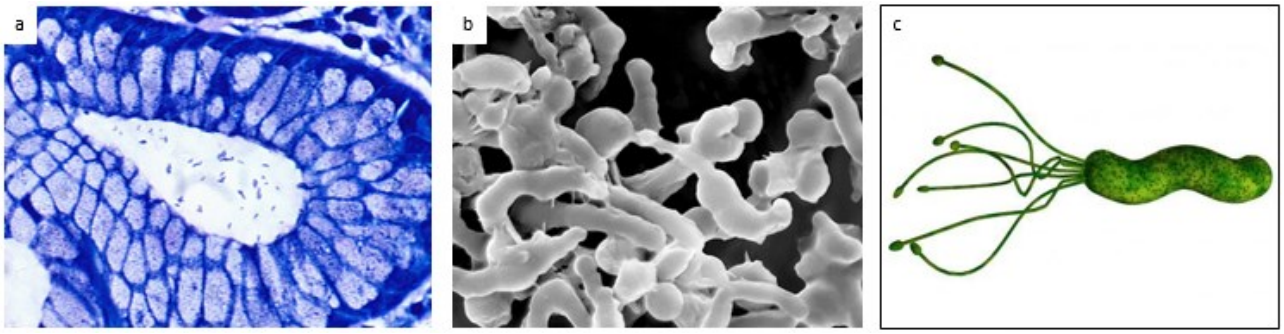

Figure 10. a) Giemsa staining of Hp infected gastric layer. b) Scanning electron micrograph of Hp. c) Illustration enhancing structure of the bacterium. Property of a) Klein M b) Kunkel D c) Marshall W.

Although Hp is not a commensal bacterium, its infected about half of the world's population, with rates of 70% in the developed world (Hatakeyama, 2017; Kim et al., 2011). Typically, the infection is acquired during childhood, usually trough gastric-oral route within families, even if the acute

infection with the bacterium is rarely diagnosed. The infection can persist during the host's life if untreated with drugs and progress in chronic gastritis, that are develop in almost all persistently colonized individuals, 90% of whom will remain asymptomatic. The coexisting chronic inflammation can possibly evolve in more severe disease such as atrophic gastritis, peptic ulcer or gastric adenocarcinoma (Atherton, 2006; Kuipers, 1997; Romano et al., 2006; Zarrilli et al., 1999). The link between Hp and peptic ulcers was discovered by Marshall in 1984, later appointed with Nobel Prize in 2005 for his discovery (Marshall, 2008).

Hp infection is the strongest known risk factor for gastrointestinal malignancies which arise within the stomach: in 1994, the International Agency for Research on Cancer classified Hp as a carcinogen I in human (IARC, 2012). It is now well accepted that Hp is the single greatest risk factor for the development of gastric cancer and causes 75% of all gastric cancers (Parkin, 2006). It has been calculated that the risk of gastric adenocarcinoma and lymphoma of gastric mucosal associated lymphoid tissue in Hp infected individuals is 3- to 6-fold higher than in those who are uninfected (Kim et al., 2011). Gastric adenocarcinoma is the fifth most common cancer, the second leading cause of cancer death and the fourteen most common cause of death around the world, with annual deaths that overcomes 700.000 people (Hatakeyama, 2017; Herrera & Parsonnet, 2009; Herszényi & Tulassay, 2010). Early stages of the disease are often clinically silent: patients at diagnosis have an advanced stage disease, with survival rates at 5 years approximately around 20% (Correa et al., 2004). The host response to Hp infection may contribute to gastric carcinogenesis by promoting a chronic inflammation which contributes to mucosal cell damage, interfering with the mechanisms of proliferation and survival that regulate epithelial cell homeostasis (Peek et al., 2002; Peek & Crabtree, 2006). Randomized prospective studies demonstrated that eradication significantly reduced the presence of premalignant gastric lesions, providing additional evidence that Hp has an effect on early stages of gastric carcinogenesis (Mera et al., 2005; Wong et al., 2004).

The bacterium target inside the stomach is the surface mucus layer in which can adhere to mucus-secreting cells especially close to intercellular junctions (Hazell et al., 1986). The mucus is about 300 µm thick and its pH increases gradually, reaching neutral conditions at the epithelium in contrast with the acidic stomach lumen where the pH is as low as 2 (Schreiber et al., 2005).

To survive in the harsh environment of the stomach, Hp has developed the ability to adapt to gastric conditions and modified his colonization skills to persist inside the host. For instance, Hp secretes an enzyme called urease, common to all clinical isolates (Ricci et al., 1997), which catalyzes the hydrolysis of urea to carbon dioxide and ammonia, thus allowing the bacterium to buffer the gastric

environment (Amieva & El-Omar, 2008). Furthermore the spiral shaped morphology and the unipolar flagella guarantee the bacterium movement within the gastric mucous layer, which is less acidic than the inside space, overlaying gastric epithelial cells (Sycuro et al., 2011). This enable also to deliver bacterial products (i.e. proteases, phospholipase, and other virulence factors) to the epithelium, that can modulate its activity and inflammatory response for Hp own benefit (Amieva & El-Omar, 2008; Ricci et al., 2002). For instance, when adherent, Hp can inject a protein encoded by the Cytotoxin-associated gene A, known as CagA, into the host cell. The effector protein CagA is encoded by the cagA gene within the cytotoxin-associated pathogenicity island, approximately 40 kilobase genomic segment. CagA is secreted as 120–145 kDa protein (due to structural polymorphism in the carboxy-terminal (C-terminal) region) together with a type IV secretion system (T4SS), a multiprotein complex which allows the bacterium to inject the toxin inside the target cell (Atherton, 2006; Romano et al., 2006). The T4SS apparatus and CagA itself interact with β1 integrin and several other receptors on host cells. Expression of CagA in cultured gastric epithelial cells, for instance consequently to Hp infection, induces a unique cell phenotype called “hummingbird phenotype” (Figure 11). The infected cell is morphologically characterized by an elongated shape with elevated cell motility and cell scattering (Segal et al., 1999).

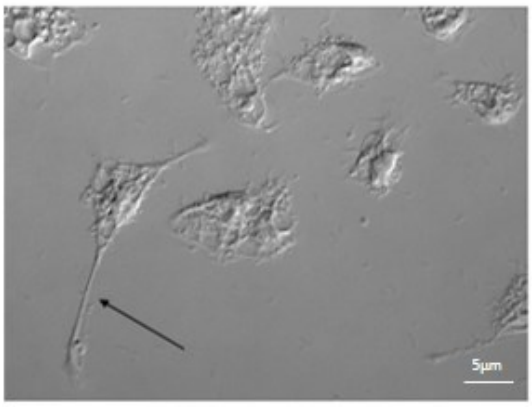

Figure 11. Hp intoxication for 24 hours induced "hummingbird phenotype" (enhanced by the black arrow) in adenogastric carcinoma cells (bar, 5 µm).

CagA has various effects on cells, including altering cell signaling and polarity, disruption of cell-cell junctions, abnormal cell proliferation and destruction of gastric mucosa to induce pro-oncogenic process (Hatakeyama, 2017). Indeed, CagA is a highly immunogenic protein that elicits serum antibody responses used for the detection of $CagA^+$ strains: in fact, only 60% of wild-type Hp strains secreted CagA, and these strains are linked to more harsh inflammation and increased possibility of advancement to gastric cancer compared with CagA negative strains (Ahn & Lee, 2015; Ricci et al.,

1993; Sommi et al., 1996). Hatakeyama and colleagues (Hatakeyama, 2004) showed that CagA delivery inside the cells, throughout its T4SS, promoted the early event of gastric carcinogenesis. Furthermore, it has been demonstrated that systemic expression of the toxin inside transgenic mice can induce gastrointestinal malignancies, supporting a oncogenic role of CagA inside mammalian cells (Ohnishi et al., 2008).

The Vacuolation toxin A

The Vacuolation toxin A (VacA) secreted by Hp, has been recognized to be the key of the bacterium's ability to adapt to gastric conditions (e.g. acidic environment) and the colonization abilities in a hostile environment (Ricci, 2016). All the HP strains encode a protein about 140 kDa in mass composed by a signal sequence, a passenger domain and an autotransporter domain. During secretion, the protoxin can be processed (Figure 12a) in a mature form that can be further cleaved in two fragments (33 kDa and 55 kDa), that remain non-covalently associated and may represent two distinct subunits or domains (p33 and p55) with a different role (Cover & Blanke, 2005). The C-terminal p55 domain is responsible for VacA binding to host cells and assembly into oligomeric structures (Figure 12b) required for pore formation, and the N-terminal fragment of 33 kDa, together with 100 amino acids of the p55 domain, is sufficient to induce intracellular vacuolation (De Bernard et al., 1998; Junaid et al., 2016).

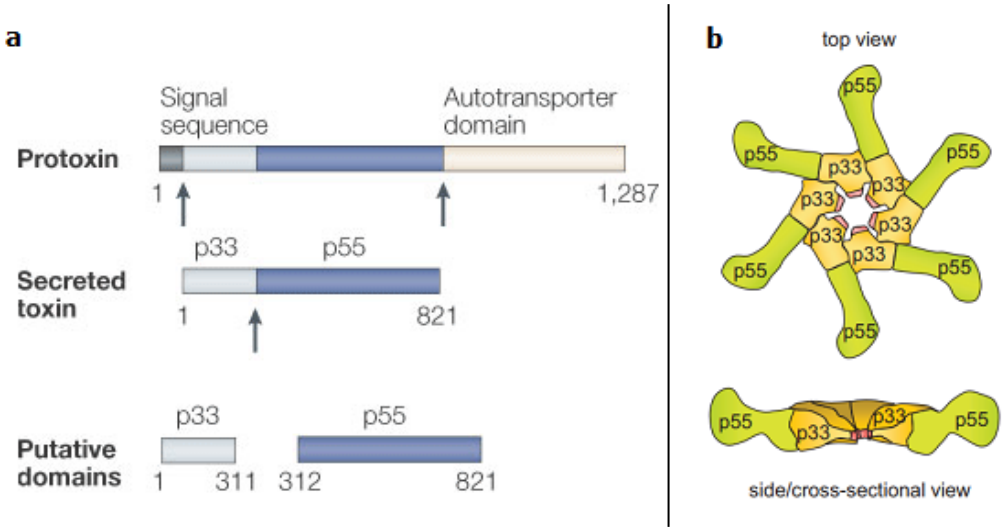

Figure 12. a) VacA structure and processing from Cover & Blanke, 2005.
b) Model of VacA oligomeric assembly proposed by Kim & Blanke, 2012.

This type of cleavage in subunits is characteristic of other bacterial protein toxins of the AB type such as LT, DTx and CTx. Two main difference regarding VacA and AB family of toxins, are the binding process and toxin effect, which for VacA are dependent from both fragments and concern a pore

forming effect (Torres et al., 2005). For these reasons it was proposed that VacA represents the prototype of a new class of AB toxins (Boquet & Ricci, 2012).

The genetic variability among Hp strains is relatively high and three VacA regions exhibit a prominent allelic diversity: N-terminal signal region (s1 and s2 alleles), intermediate region in the p33 domain (i1 and i2), and the mid-region in the p55 domain (m1 and m2) (Chung et al., 2010). Further, bacteria with the s1/m1 genotype have been associated with the most virulent strains, those with s1/m2 have been linked with less virulent strains, and strains which have s2/m2 are known to be the minimum virulent (Atherton, 2006). The first alleles of the three regions also correlate with the presence of CagA, thus with a more severe disease outcome (Chung et al., 2010).

The mid-region subtypes in p55 have different affinities for cell-surface receptors and show different cell specificities. In epithelial cells, VacA binds to several receptors on target cells including phospholipids, glycosphingolipids, sphingomyelin and heparan sulphate. EGFR was observed to mediated VacA uptake in HeLa cells (Seto et al., 1998) instead Receptor Protein-Tyrosine Phosphatases α and β (RPTPα/β) were also identified as receptors on kidney and stomach epithelium cells. Other receptors included glycosaminoglycan, Glycosylphosphatidylinositol-Anchored Protein (GPI-AP), low-density lipoprotein receptor-related protein-1, fibronectin, β-integrin and lipid rafts (Backert & Tegtmeyer, 2010; Junaid et al., 2016; Sewald et al., 2008). In addition, lipid rafts are associated with VacA-induced apoptosis, which is also controlled by low-density lipoprotein receptor-related protein-1 (Yahiro et al., 2016). Furthermore, binding of VacA to lipids and association with lipid rafts is enhanced upon acid activation of the water-soluble oligomeric toxin (Junaid et al., 2016).

Internalization and effects

After binding VacA is internalized by a common pathway shared by epithelial and gastric cells that is clathrin-independent but temperature, energy and actin dependent and the toxin is concentrated inside endosome (Gauthier et al., 2004; Ricci et al., 2000). VacA is found in GPI-AP-enriched Early Endosomal Compartments (GEECs) 10 minutes after internalization, within 30 minutes in EEs and reach LEs within 120 minutes (Gauthier et al., 2007). In these endomembranes, VacA oligomerizes to form anion-selective channels that can conduct chloride, bicarbonate, and small organic molecules. In solution, VacA oligomerizes to form flower- or snowflake-shaped structures (Figure 13). These structures are double-layered (dodecamers and tetradecamers) as well as single layer structures (mainly hexamers and heptamers). Several evidence indicate that VacA oligomerization

is required for VacA induced vacuolization and that single layered VacA oligomers resemble the structure of VacA membrane channel (Foegeding et al., 2016).

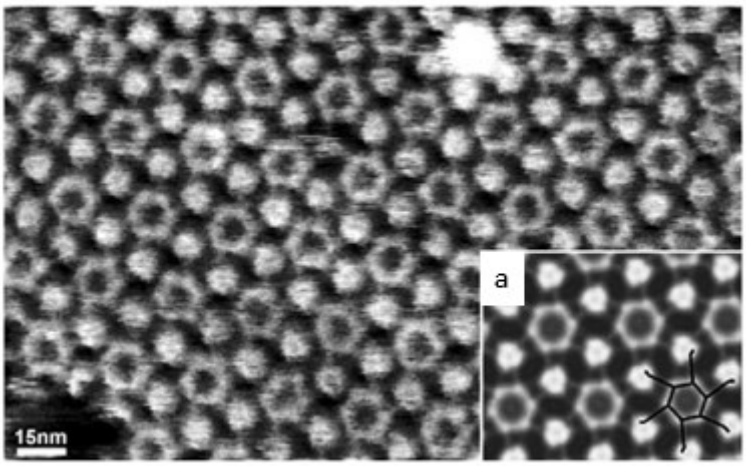

Figure 13. VacA hexameric pores assembled into lipid bilayer (bar, 15 nm). a) Magnification and correlation of structural details with the toxin structure. Modified from Müller et al., 2002.

The exposure of VacA oligomers to acid pH or alkaline pH, results in oligomer disassembly and inactivation and, once exposed to low or high pH, VacA preparation has greater cytotoxic effects (Cover et al., 1997). Therefore, this could suggest that VacA first interacts as a monomer with the membrane of the host cell and then oligomerizes and insert to form the channel. VacA mutant proteins unable to assemble, also lack the vacuolating toxin activity and similar results are obtain using chemical inhibitor of chloride channel (Tombola et al., 1999; Vinion-Dubiel et al., 1999). The increasing in intraluminal chloride concentration inside LEs, triggers the enhancement of V-ATPase causing a decrease in intraluminal pH (Foegeding et al., 2016). Membrane-permeant weak bases, like ammonia, diffuse into LEs where are protonated and trapped. As a consequence (Figure 14a), LEs undergo osmotic swelling, resulting in cell vacuolation (Cover et al., 1992; Kern et al., 2015). In absence of weak bases VacA does not induce prominent cells vacuolation but still promote other alterations which include inhibition of intracellular degradation of EGF and procathepsin D maturation, perturbation of transferrin recycling, and in immune cells, inhibition of antigen presentation (Cover & Blanke, 2005). Vacuoles can reach a diameter of up to 5 µm and take up a large part of the cytoplasm; its membranes can be stained for the markers typically found in LEs membranes (i.e. Rab7 and LAMP1) suggesting that the vacuoles arise from LEs (Papini et al., 1994). Moreover, while accumulating inside the endosomal-lysosomal compartment, a large amount of VacA avoids the classical lysosomal degradative processes and retains its apparent molecular

integrity. This is supported by the VacA protonation, which takes place inside the acidic endosomal compartments in order to avoid toxin cleavage or degradation (Sommi et al., 1998).

VacA namesake cellular effect and the first to be discovered is the induction of vacuoles inside cells. VacA-induced vacuoles were discovered in early '90, when Leunk and colleagues found out that Hp Broth Culture Filtrates (BCFs) added to cultured eukaryotic cells (Figure 14b), caused the development of vacuoles inside cells (Leunk et al., 1988) and similar vacuoles were also found in gastric biopsy (Figure 14c) of Hp infected patients (Necchi et al., 2010). Many cultured cells, including primary human gastric epithelial cells, transformed cell lines derived from different type of human tissue and cell line derived from mammalian cells, develop vacuoles after VacA incubation (Cover & Blanke, 2005). Vacuolation can be observed within a few hours after addition of VacA in the medium. Instead the addition of VacA oligomers to cells does not promote vacuolation (Cover et al., 1992). Interestingly, even though vacuolation is the first discover and most prominent VacA effect, their purpose of the vacuoles is still unknown.

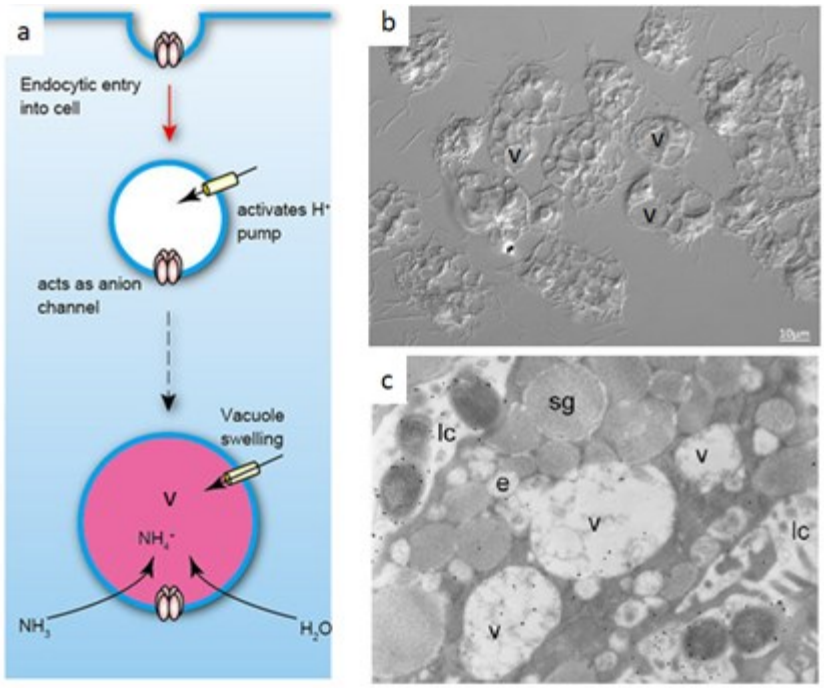

Figure 14. a) Model of VacA action from Miyashita et al., 2016. b) Adenogastric carcinoma cells infected with BCF showing vacuoles development (v, vacuole; bar, 10 µm). c) Superficial gastric epithelium colonized by Hp (v, vacuole; e, endosomal vesicle; lc, luminal cleft; sg, secretory granules) modified from Necchi et al., 2010.

In addition to vacuoles, VacA can alter multiple intracellular site, for instance mitochondria. Although studies have not yet been exhaustive, the greater effect that so far has been identified is

variations in membrane permeability and the induction of apoptosis (Boquet et al., 2003). Apoptosis may lead to a faster turnover of the cells, providing more nutrients for Hp and suppresses the immune response to promote the host colonization (Rassow & Meinecke, 2012). Supporting this hypothesis is also the role of VacA on macrophages: VacA impairs vesicular maturation, leading to the formation of large vesicular compartments called megasomes (Utsch & Haas, 2016). This could prevent the bacteria eradication therefore contribute to Hp survival and colonization. Furthermore in B-cells, VacA interferes with antigen presentation, possibly altering vesicular trafficking (Djekic & Müller, 2016). Moreover, VacA effect on mitochondria have been reported to result in reduction of ATP concentrations, impaired cell-cycle progression and reactive oxygen species increasing (Cover & Blanke, 2005; Rassow & Meinecke, 2012). Interesting the development of mitochondrial alteration requires longer period of incubation and higher VacA doses than for VacA-induced vacuolation (Willhite & Blanke, 2004). This could possibly suggest that VacA actions on mitochondria are the indirect consequence of toxin cytotoxicity. However, other studies localized the toxin inside mitochondria, suggesting a possibly direct role on mitochondria (Galmiche et al., 2000). All these hypotheses are still a matter of debate, considering also that it is not clear whether both the p33 and p55 subunits are required for pore-formation at the inner mitochondrial membrane and the route exploit by the toxin from the LEs to the mitochondria (i.e. release via channels or by vacuole swelling and destruction) (Palframan et al., 2012). It was also demonstrated that VacA can promote endosome-mitochondria juxtaposition before inducing the formation of mitochondria apoptotic channels or the activation of proapoptotic proteins (Calore et al., 2010). Moreover, colocalization between VacA and mitochondria was confirm as VacA inside mitochondria can induced functional alteration which results in mitochondria lost typical spaghetti-like morphology, consider to be a signal of mitochondria integrity (Oldani et al., 2009).

Immunostaining analysis found out also the involvement of VacA in intracellular calcium signaling. VacA was shown to cause a rapid, transient increase in cytosolic calcium concentrations in adenocarcinoma gastric cells also leading to pepsinogen secretion (Chan et al., 1996). This important role can explain the etiology of chronic active gastritis and peptic ulcer Hp-induced. More evidence come from VacA effect on proliferation of T lymphocyte: during T-cell activation, intracellular calcium is abundant and binds calmodulin, enabling it to activate calcineurin, but as reported by Sundrud and colleagues (Sundrud et al., 2004) VacA inhibits calcineurin in order to blocks T-cells proliferation, evading the adaptive immune response and establish chronic infection. They also

demonstrated that, VacA-mediated inhibition of T cell proliferation requires an intact N-terminal hydrophobic region necessary for the formation of anion-selective membrane channels.

Interestingly, VacA induced alteration on intracellular calcium suggests a possible trafficking of VacA from endosomes to Golgi apparatus and ER, which is the major storage for intracellular calcium. This might imply that the toxin, once internalized, may follow not only the classical endocytic pathway to finally reach lysosomes but also the so-called "retrograde pathway", that is the exocytic pathway in the reverse direction, passing from the TGN to the ER. This movement is indeed the pathway followed by some bacterial toxins (such as CTx and Shiga Toxin) to intoxicate their target. Supporting this hypothesis is also the found of Kern and colleagues that demonstrated how VacA colocalize with Sec61p complex, responsible for transmembrane movement of proteins and exploit by toxins such as CTx (Kern et al., 2015). Finally, there might be two or more parallels pathways exploited by the toxin, as already demonstrated for other toxins, depending on the amount of toxin internalized by the cell (Johannes & Popoff, 2008).

Moreover, considering the recently findings about ER (Raiborg et al., 2016) we can speculate that fission between endosomes and the ER allows molecules flowing and it could be a pathway exploited by VacA, as for other bacterial and plant toxins and some nonenveloped viruses (Sivan et al., 2016).

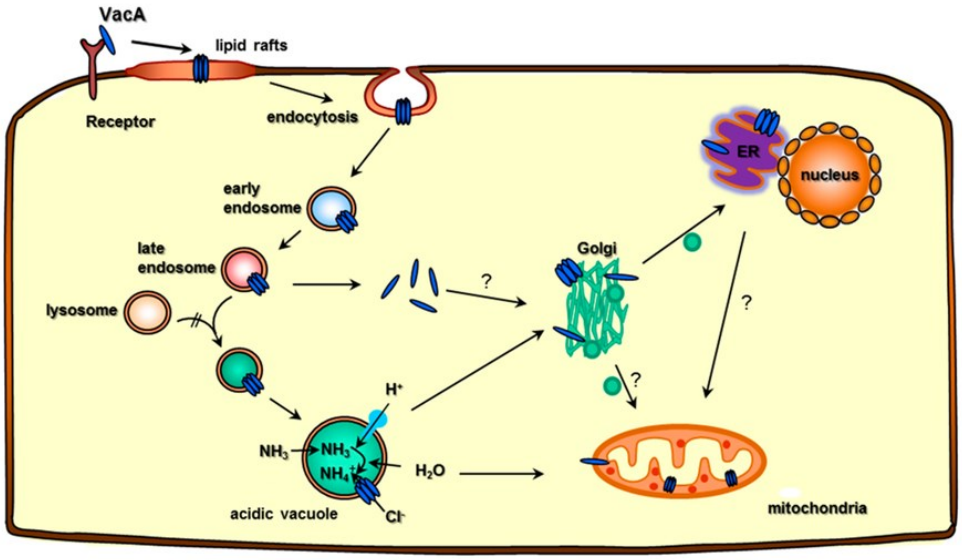

Figure 15. Schematic representation of VacA suppose trafficking inside the cell based on its known effect. Modified from Kern et al., 2015.

VacA & CagA interaction

Hp seems to be evolved to maximize genetic diversity by mutation and recombination of the genetic information within the population, as an adaptive mechanism. Several evidences suggest the importance of the relationship between VacA and CagA to promote Hp successful colonization of the host stomach. For instance, CagA decreases VacA-induced vacuolation and promote apoptotic activity impairment. Moreover, CagA was shown to inhibit VacA internalization into cells and also to interfere with intracellular VacA trafficking, blocking VacA in GEECs and preventing its progression into LEs and mitochondria (Oldani et al., 2009). On the other hand, VacA reduces hummingbird phenotype promoted by CagA, interfering with EGFR activation and endocytosis (Akada et al., 2010; Argent et al., 2008). These actions are not functional related as suggest by the data of Ricci and colleagues (Ricci et al., 1996), that showed how undialyzed Hp BCF inhibited cell migration and proliferation throughout a VacA- and CagA-independent mechanisms.

Remarkably were demonstrated not only antagonistic effects: for instance, in polarized epithelial cell monolayers CagA promotes uptake and internalization of the iron transporter transferrin while VacA promote transferrin shift to sites of bacterial attachment: thus the two virulence factors can act together to provide specific nutrients, such as iron, to facilitate Hp attached to the apical cell pole (Tan et al., 2011). This behavior suggest a possible relationship devoted to increase the bacterium fitness and growth and could also explained why the type I strains, which produce an active VacA and carry the cytotoxin-associated pathogenicity island, is associated with severe clinical outcomes (Argent et al., 2008; Blaser & Atherton, 2004).

The interaction of the two main Hp virulence factors could be a cooperative role by which they can regulate and influence each other and could fall within the mechanism of chronic and persistent infection played by the bacterium (Shames & Finlay, 2012).

AIM OF THE STUDY

Inside cells, intracellular trafficking allows a continuous communication between organelles, which compose the complex eukaryotic systems. This network is guarantee by a coordinate and transient budding and engulfing of the endomembrane systems (Mishev et al., 2013). There are two most trafficked routes inside the cell: the anterograde movement of newly synthetized components, such as proteins, which are sent from the ER to the Golgi apparatus to undergo post transcriptional modification and then routed to its target and the so-called “retrograde pathway”, that is the exocytic pathway in the reverse direction, passing from the TGN to the ER (Bannykh et al., 1998). The importance of a precise and fine-tuned cellular organization is demonstrated by the development of intracellular aggregates as a result of altered trafficking or the degradation quality system failure to manage misfolded proteins. LBs (Minassian, 2001; Turnbull et al., 2012), JUNQs (Amen & Kaganovich, 2015; Kaganovich et al., 2008), IPODs (Moldavski et al., 2015; Ogrodnik et al., 2014) and the newly described PaCSs (Necchi et al., 2013, 2010) arise in cells, from proteins and cellular components aggregation as a response to stressor or metabolism modification. Furthermore, cytosolic aggregates are common to several other human diseases, as for amyloid diseases, Alzheimer’s disease and Parkinson’s disease (Bersuker et al., 2013; Kopito, 2000; Takalo et al., 2013).

Additionally, the intracellular trafficking delivers not only useful component for the cells, but it is exploit by pathogen components, such as toxins. In order to understand and prevent their cytotoxic effects and also elucidate their movement inside the cell, several trafficking inhibitors have been tested in recent years (Driouich et al., 1993; Park et al., 2012; Stechmann et al., 2010; Yang et al., 2016). Among them, EGA was found out to be able to block the action of LT, Cytolethal Distending Toxins, BoNTs, DTx and Clostridium Toxins (Azarnia Tehran et al., 2015; Dixon et al., 2015; Gillespie et al., 2013; Schnell A, 2016; Schnell B, 2016; Slater et al., 2014). These toxins have different actions on cells, but they all belong to the AB toxins family (Henkel et al., 2010; Odumosu et al., 2010).

Even though there are differences in binding and function (Torres et al., 2005) between VacA and the AB family of toxins, it has been suggested that VacA could represents the prototype of a new class of AB toxins, since its similar structure and cleavage (Boquet & Ricci, 2012). VacA is considered to be the key of the bacterium's ability to adapt to gastric conditions and surviving in a hostile environment (Ricci, 2016). Intracellularly VacA can promote the formation of large vacuoles arising from LEs (Leunk et al., 1988; Papini et al., 1994; Rassow & Meinecke, 2012), but can alter also mitochondria functioning and intracellular calcium signaling (Boquet et al., 2003; Chan et al., 1996).

Furthermore, has been supposed that calcium level alteration, which for instance affects T lymphocyte functioning (Sundrud et al., 2004), could be achieved by the toxin inside ER. Thanks to the juxtaposition of ER and endosome membranes, recently described by Raiborg and colleagues (Raiborg et al., 2016), VacA could escape EEs or LEs and reach its target. This kind of interaction might explain also why some toxins, such as CTx, are able to bypass the Golgi structure and route directly to the ER (Sivan et al., 2016). This route could be the reasons why VacA is found inside PaCSs in gastric biopsy of Hp infected patients (Necchi et al., 2010). The toxin could escape ERAD degradation, as CTx does, and be moved into the cytosol, where it could be ubiquitinated and accumulated inside PaCSs.

The aims of this work are: I) to deeply characterize aggregates such as PaCSs, LBs, JUNQs and IPODs in order to investigate their nature and development; II) to elucidate the effect of trafficking inhibitor on VacA-induced vacuolization; III) to investigate VacA trafficking at different time.

MATERIALS AND METHODS

MATERIALS

Reagents and inhibitors

All reagents were purchased from Sigma-Aldrich, unless otherwise stated.

Inhibitors used were BFA (final concentration 1 µg/mL), Retro-2 (final concentration 25 µM), 2-[(4-Bromophenyl)methylene]-N-(2,6-dimethylphenyl)-hydrazinecarboxamide (EGA, final concentration 12,5 µM). Retro-2 cyclic (final concentration 30 µM), RN-3-122 (final concentration 5 µM), Compound 20 (final concentration 50 µM), Retro-1 (final concentration 20 µM), HA-432 (final concentration 5 µM) kindly provided by Dr. Daniel Gillet (Commissariat à l'Energie Atomique, France).

Plasmids

Plasmids used were: pcDNA3.1-HttQ97-mRFP2.1 (HttQ97, mutated Htt with 97 expansion of the polyglutamine tract) and pcDNA3.1-VHL-GFP (VHL) kindly provided by Prof. Daniel Kaganovich (Hebrew University of Jerusalem, Jerusalem, Israel), plasmid pDsRed-Mito (DsRed Mito) by Prof. Patricia Boquet (University of Nice, Nice, France) and pRBG4-6His-myc-Ub (pCW7) by Prof. Ron Kopito (Stanford University, Stanford, United States).

Antibodies

Primary antibody used for Immunohistochemistry (IHC), Immunocytochemistry (ICC) in light or Immunofluorescence (IF) analysis or TEM were directed against: Bcl2-associated athagene 3 (Bag3, ProteinTech, rabbit polyclonal); Calnexin AF18 (ThermoFisher, mouse IgG); c-Myc tagged protein (c-myc, Thermoscientific, mouse IgG); Early Endosome Marker 1 (EEA1, Abcam, mouse IgG); Giantin (Abcam, mouse IgG); Golgin97 (ThermoFisher, mouse IgG); Heat shock protein 70 (Hsp70, Santa Cruz, goat polyclonal); Laforin (Millipore, rabbit polyclonal); Lysosomal-associated membrane protein 1 (LAMP1, BD Pharmingen, mouse IgG); poly-Q expansion disease (poly-Q, Epitomics, mouse IgG); Polyubiquitinated conjugates (FK1, Enzo Life Sciences, mouse IgM); Proteasome 20S (Enzo Life Sciences, mouse IgG); Rab7 (Sigma self-made custom, mouse IgG); Sequestosome 1 protein (p62, Santa Cruz, rabbit polyclonal); VacA (VacA 958, kindly given by Prof. Timothy L. Cover, Vanderbilt University, United States, rabbit IgG).

Secondary antibody for IF were anti-mouse IgG Alexa Fluor 488 labelled, anti-mouse IgM Alexa Fluor 647, anti-goat Alexa Fluor 488-labelled or anti-rabbit Fluor Cy5-labelled (all purchase from

Jackson Immunoresearch). For TEM secondary antibody was labelled with colloidal gold particles (5–20 nm diameter, British BioCell). For western blot analysis, anti-mouse IgG (Amersham) or IgM (Abcam) and anti-rabbit (Amersham) horseradish peroxidase (HRP) conjugated were used.

Cells lines and bacterial strains

HeLa (ATCC CCL-2, from human cervix adenocarcinoma), HEK 293 and HEK 293T/17 (ATCC CLR-1573 and CRL-11268, Human Embryonic Kidney 293 and 293T/17) cells were cultured in complete medium Dulbecco's Modified Eagle's medium 4.5 g/L (DMEM, Lonza) supplemented with 10% heat-inactivated Fetal Bovine Serum (FBS, Gibco) and2mM Glutamine (Lonza). Cultures were maintained at 37°C and 5% CO_2 in humidified.

Three Hp strains were used: wild type 60190 (ATCC #49503, producing both VacA and CagA) and its isogenic mutant $CagA^-/VacA^+$ (lacking CagA gene, 60190:M22), $picB/cagE^-/VacA^+$ (unable to translocate CagA inside the cell, 60190:C-) kindly given by Prof. Timothy L. Cover (Vanderbilt University, United States). All Hp strains were grown in Brucella broth medium (Difco), supplemented with 5% of heat-inactivated FBS (Gibco) and 1% of VITOX (Oxoid) at 37°C in a thermostatic shaker under micro-aerophilic conditions. The absence of contamination (e.g. by *Escherichia coli*) was evaluated using the Urease test, which involves a colorimetric indicator (Urea-indole, Bio-Rad).

METHODS

Bacterial filtrates production and VacA preparation

To obtain BCFs, bacteria were removed through centrifugation (12000 g-force (g) for 10 minutes at 16°C) and supernatants were sterilized by passage through a 0,22 µm cellulose acetate filter (Nalge Co). In order to assess the efficiency of the filtrate, subconfluent Hela cell were washed twice with Hanks' Balanced Salt Solution (HBSS, Euroclone) and then incubated for 24 hours with Hp BCF diluted 1:3 in HBSS. VacA-induced vacuolization and absence of cellular toxicity were evaluated by microscopic analysis in light microscopy.

VacA was purified from BCF C- by ammonium sulphate precipitation and gel filtration chromatography using Superose 6 10/300 GL column (Amersharm Bioscience) in accordance with Cover (Cover et al., 1997). The concentration was determined using the DC protein assay kit (Bio-Rad) and the correct purification was verified by Comassie blue and Western Blotting analysis using anti-VacA antibody.

After purification, VacA is oligomerized and thus biologically inactive (McClain et al., 2000). Before all intoxication experiments, purified VacA was activated by dropwise acidification to pH 3.0 with 0.2 N of Hydrogen Chloride (HCl).

Vacuolation assay

Neutral red is an acidotropic membrane permeant amine, which accumulates in the vacuolar lumen. Neutral red dye uptake (NRU, Figure 16) is a widely accepted in vitro assay for evaluating Hp-induced vacuolation (Cover et al., 1992).

We used NRU assay to give a score of inhibitors effect on VacA-induced vacuoles.

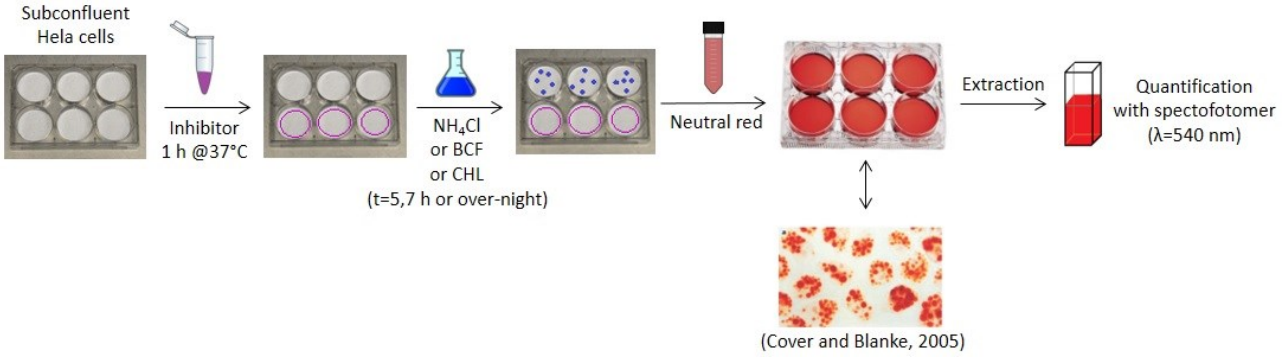

Figure 16. Schematic representation of Neutral Red Uptake assay.

In accordance with Cover (Cover et al., 1994), Hela cells were seeded two days before the experiment in 6-well culture plates (BD Falcon). Subconfluent Hela cells were washed with HBSS and the medium was replaced with HBSS or HBSS supplemented with Ammonium Chloride (NH_4Cl, 5 µM), BCF C- (diluted 1:3 in HBSS) or Chloroquine (CHL, 1 mM). The inhibitor was added 1 hour before the addition of the conditioned medium, instead the controls were left inhibitor free. In vacuoles regression experiments, EGA was added after 5 hours of vacuolation promoted by BCF or CHL. For the assessment of vacuoles induction after treatment with EGA and cell recovery, cells were preincubated with EGA for 1 hour, washed abundantly and let recover for 1 hour. Then BCF or CHL were added to the medium to promote vacuolization. NRU analysis was performed as usual. In all the experiments, after the intoxication period (5 hours for early vacuolization, 7 hours or overnight incubation for a total of 16 hours) the degree of cells vacuolation, evaluated also by light microscopy, was determined by incubating cells for 5 minutes with neutral red solution (0,5% in saline solution 0,9% composed of sodium chloride (NaCl) in deionized water) diluted 1:40 in HBSS. Cells were then washed twice with saline solution, then the neutral red inside vacuoles was extracted by the addiction of 1% acid acetic in ethanol 50%. The absorbance was measured with

Du-64 Spectrophotometer (Beckman) at 540 nm (Cover et al., 1994), and was expressed as µg of neutral red per µg cell proteins (Ricci et al., 1993) evaluated in accordance with Lowry (Lowry et al., 1951) or as a proportion of the control values.

EGA effect analysis

EGA is an aryl semi carbazone inhibitor, that has been reported to block several toxins (Slater et al., 2014). To investigate the effect of EGA on VacA-induced vacuoles, Hela cell were preincubated with the inhibitor for a time ranging from 1 hour to 10 minutes, then cells were wash abundantly, and the vacuolization was promoted adding BCF C- diluted 1:3 in the medium without FBS. Cells were visualized at different time and images were taken after 24 hours of intoxication in light microscopy "*in vivo*" with microscope Olympus IX83 with X-Cite120W fluorescence illuminator system (microscope Olympus) 20X magnification (20X).

For the vacuoles regression experiments, Hela cells were seeded on a µ-Dish 35 mm with a glass bottom and an imprinted 500 µm relocation grid (IBIDI). The grid allows to recognize the same cell before and after treatment. Cells were seeded two days before the experiment on the grid and allow to grow to 60% of confluence. Then BCF diluted 1:3 was added and the vacuolization was allowed for 5 hours and then EGA was added to the medium and images were taken at 2 and 4 hours of treatment "*in vivo*" with microscope Olympus 60X magnification with oil immersion objective (microscope Olympus 60X).

Acridine Orange staining

Acridine Orange (AO) is a metachromatic dye able to cross the PM and staining nucleic acids as DNA or RNA to cytoplasm or nucleoli. Furthermore, AO can accumulate inside the acid compartment where becomes protonated and trapped inside. The constant influx of AO molecules results in increasing of AO concentration, aggregation and a red shift of emission and self-quenching. In the event that pH becomes more basics AO molecules can cross again the membrane of acid compartments due to the deprotonation. Moreover, AO uptake and organelles staining is linearly associated with concentration (Lovelace & Cahill, 2007; Pierzyska-Mach et al., 2014). For these reasons, AO is considered to be a good acidic compartments pH indicator.

To investigate the effect of EGA on the acid compartments and pH alteration, at the end of cells treatments acid compartments were stained with AO. Cells were washed three times with Phosphate Buffered Saline (PBS, Euroclone), stained with AO solution (10 mM in PBS) for 10 minutes

at 37°C. Then, cells were washed abundantly with PBS and immediately observed "*in vivo*" with microscope Olympus 60X.

Colocalization study and ICC analysis.

The colocalization studies (Figure 17) were performed using VacA purified and concentrated (final concentration 4 µg/mL) and Cholera Toxin Subunit B-Alexa Fluor 555 (CTxB-Alexa 555, final concentration of 2 µg/mL, ThermoFisher).

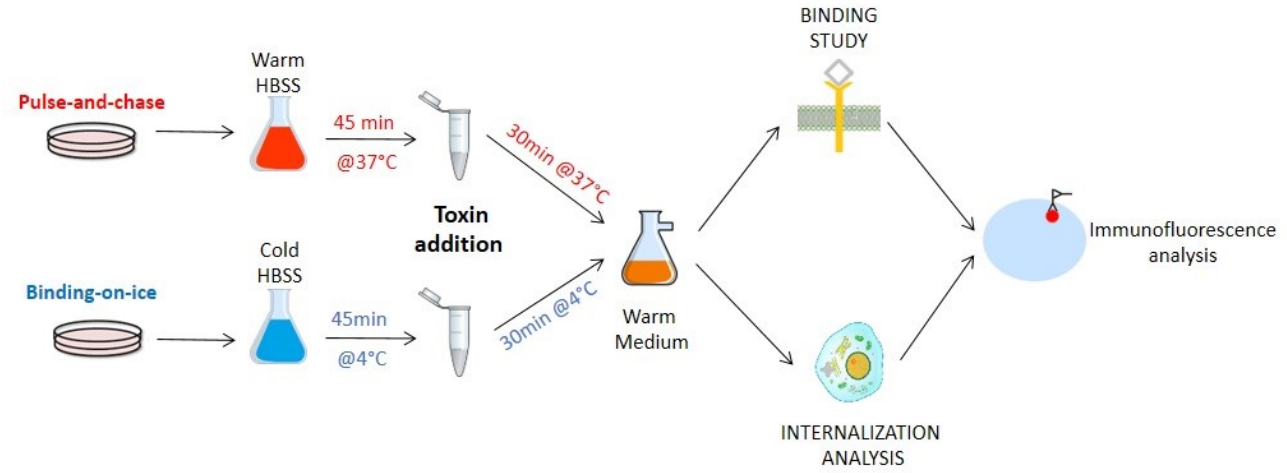

Figure 17. Schematic representation of pulse-and-chase and binding-on-ice protocols.

For pulse and chase experiments, before toxin addition, the medium was changed with warm HBSS and the cells were placed for 45 minutes at 37°C. The toxin was then added, and binding was promoted for 30 minutes at 37°C. Once the binding time ended, the cells were washed with a warm medium and moved at 37°C for a variable time depending on the protocol (30 minutes, 1 hour, 2 hours, 5 hours). The binding-on-ice protocol instead was performed using cold medium and the preincubation time was done on ice at 4°C. In the experiments in which inhibitor was used, it was added 1 hour before the toxin and maintained throughout the experiment.

At the end of the incubation time or treatment, cells were fixed with 4% paraformaldehyde, permeabilized with Triton 0,1% and ICC analysis was performed. Then, IF analysis was conducted with primary antibody against VacA, Golgin97, Calnexin AF18, LAMP1. Secondary antibody fluorescent labelled were chosen accordingly to the primary antibody. Hoechst 33258 was used for nuclear counterstaining. For binding analysis, the cells were subsequently fixed after binding-on-ice period, without internalization allowed.

Microscopy analysis was carry out in collaboration with Centro Grandi Strumenti (TCS SP2 confocal laser scanning microscope, Leica, equipped with a 63x oil-immersion objective). Analysis of

colocalization was performed on all stacks using ImageJ (National Institute of Health) and Fiji's plugin (Schindelin et al., 2012).

Plasmid preparation and trasfection

Plasmids were grown in *Escherichia coli* strain cultured in Liquid Broth miller (Life Technologist) supplemented with Kanamycin (50 mg/mL) and purified using Qiagen Plasmid Maxi Kits (Qiagen) following manufacturer's instructions.

For IF analysis of transient transfections, cells were grown to 70% of confluence in 35 mm^2 Petri dish (BD Falcon, on poly-L-Lysine only for HEK293T/17) and transfected using jet-PRIME (Polyplus Transfection) according to manufacturer's instructions. To obtained cells transfected with both HttQ97 and VHL plasmids, Hela cells were transient transfected combining both plasmids into the trasfection procedure. Cells were observed "*in vivo*" in light and fluorescence microscopy (microscope Olympus 20X) to check the correct trasfection rate and then treated as necessary.

To promote JUNQ development, cells were treated with MG132 (Calbiochem), which effectively blocks the proteolytic activity of the proteasome complex (Han et al., 2011), at final concentration of 10 µM diluted in complete medium for 24 hours at 37°C.

For colocalization analysis with transfected mitochondria, trasfection was performed 24 hours before the experiments.

Aggregates analysis

Since that PaCSs share some characteristics with LBs, JUNQ and IPOD, we deeply characterized these aggregates (Figure 18).

Firstly, we analyzed differences or similarities between PaCSs and LBs. To this purpose eight mice aged between 7 and 11 weeks (four were $malin^{KO}$ and four controls) kindly provided by Dr. Jordi Duran (Institute for Research in Biomedicine, Barcelona, Spain) were used. This mouse model was previously generated for the Lafora disease study (Valles-Ortega et al., 2011) and $malin^{KO}$ mice showed polyglucosan accumulations in several brain areas. For light microscopy studies brain, heart, skeletal muscle, kidney, liver and lungs were collected. All samples for light microscopy were fixed with 10% formalin in acetate buffer for 24 hours at room temperature and then processed. IHC analysis was performed using brain samples and primary antibodies directed against Laforin, Proteasome 20S, FK1, Hsp70, Bag3. Secondary antibodies against rabbit, mouse or goat were chosen accordingly. Half brain, sectioned in different parts (hippocampus, cerebellum and cortex) and cut to thicknesses suitable, was collected to perform TEM analysis. The samples were placed in

Karnovsky fixative 2,5% (2.5% glutaraldehyde and 2% formaldehyde in cacodylate buffer, pH 7.3) and left 4 hours at 4°C followed by 3% osmium tetroxide for 1 h at room temperature. After dehydration in ethanol and propylene oxide, the specimens were embedded in Epon–Araldite resin. Thin (~1 µm) sections were stained with uranyl–lead or underwent immunogold procedures followed by uranyl–lead staining. The primary antibodies were the same of IHC analysis and secondary antibodies were labelled with colloidal gold particles (British BioCell). Specimens were analyzed by a Jeol JEM-1200 EX II TEM (Joel Ldt) equipped with an Olympus CCD camera Mega View III (Olympus Soft Imaging Solution GmbH) available at the Centro Grandi Strumenti of the University of Pavia.

To evaluate differences and similarities between IPOD, JUNQ and PaCSs, we used HEK293T/17 as cellular model. After 26-29 hours of transfection, cells were fixed with 2% of paraformaldehyde for 15 minutes at room temperature and ICC analysis was performed with primary antibodies against Proteasome 20S and FK1 and secondary antibody used was α-mouse IgG Alexa Fluor 488. Cells were then mounted on slides with Mowiol and observed with microscope Olympus 60X. For TEM, 24 hours after transfection, cells were pelleted and fixed for 1 hour at 4°C in Karnovsky fixative, followed by 1.5% osmium tetroxide for 1 hour at room temperature. After dehydration in ethanol and propylene oxide, the specimens were embedded in Epon–Araldite resin. Thin (~70 nm) sections were stained with uranyl–lead or underwent immunogold procedures followed by uranyl–lead staining (Necchi et al., 2010). ICC was performed with primary antibodies against Proteasome 20S, FK1, polyQ, p62; secondary antibodies were the same of IHC analysis, labelled with colloidal gold particles (British BioCell). Specimens were analyzed as mouse sections.

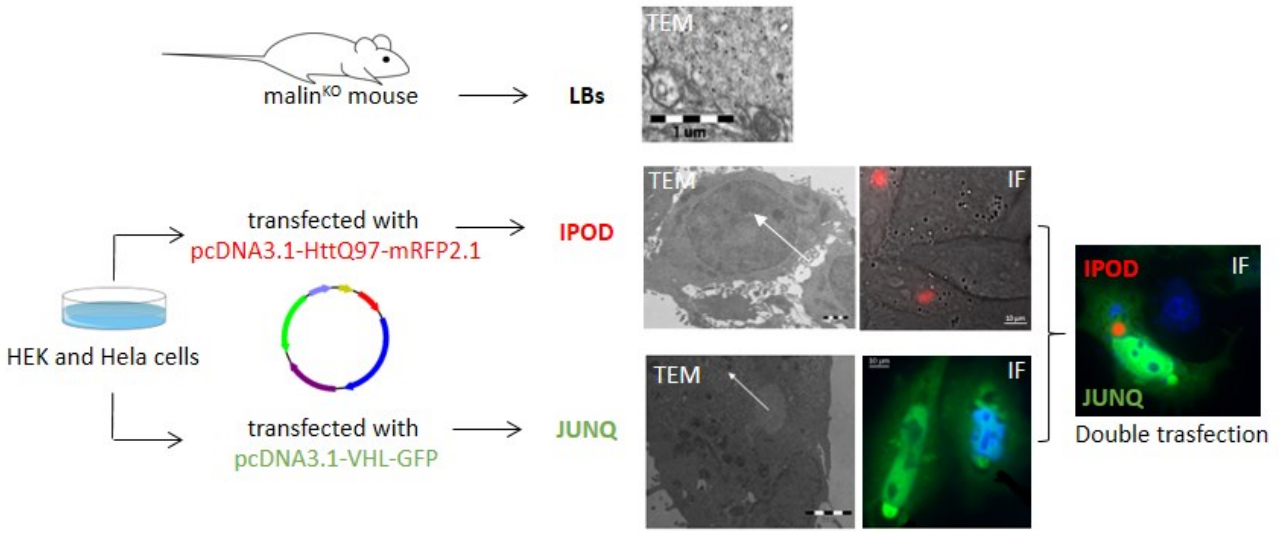

Figure 18. Summary of LBs, IPOD and JUNQ origin and analysis.

Ubiquitination assay

For ubiquitination assay (Figure 19), $1x10^6$ Hela cell plated on a 10 cm Petri dish were transient transfected with Jet-Prime with plasmid pCW7, according to manufacturer's instructions. The correct expression of the plasmid was assessed 24 hours after transfection by IF analysis with primary antibody against c-myc and secondary antibody Alexa Fluor 488 labelled.

For VacA analysis, 24 hours after transfection and before the lysis, cells were treated with BCF 60190 diluted 1:3 in the medium without FBS; the control was left untreated. In both case, 6 hours before the lysis, cells were either untreated or treated with 20 µM of MG132 to increase protein ubiquitination.

At the end of treatment period, cells were washed once in PBS and scraped at room temperature in 1 mL of buffer (BU) composed by 8 M Urea, 20 mM Tris hydrochloride (pH 7.5, Tris-HCl), 200 mM NaCl, 10 mM Imidazole, 0,1% Triton x-100 and 100 µM PR-619 (Ubiquitylating enzymes inhibitor) at room temperature. An aliquot of 50 µL was collected as "total lysate" and mixed with 2X SDS sample buffer (SDS sample, 150 mM Tris-HCl, 300 mM Dithiothreitol, 3% SDS, 0.06% Bromophenol blue, 3% Glycerol). Samples were then vortex and centrifuged for 10 minutes at 15000g at room temperature. An aliquot of 50 µL was collected as "total proteins" and mixed with 2X SDS.

At the same time, cobalt beads (Clontech) were prepared: 60 µL of slurry bead for assay was washed with 1 mL of BU, centrifuged for 2 minutes at 12000g at room temperature and then supernatant was removed. Beads were then saturated for 1 hour in 1 mL of BU supplemented with 2 mg/mL Bovine Serum Albumin (BSA) on a rotating plate. Beads were then washed twice in 1 mL of BU, centrifuged for 2 minutes at 12000g at room temperature and the supernatant was removed. The final volume obtained was adjusted with BU to 100 µL/assay.

At the remaining supernant sample was added 100 µL of beads and the binding was promoted at room temperature for 1 hour on a rotating plate. An aliquot of 50 µL was collected from the supernatant, as "first supernatant" post centrifugation and mixed with 2X SDS. Then beads were washed five time in BU (all washes were sampled as "n° of washing" and stored to further analysis), measured and resuspended in 2X SDS as "ubiquitinated proteins".

Proteins were resolved on a 7.5% SDS-Polyacrylamide Gel Electrophoresis (SDS-page) and polyubiquitinated proteins were visualized by immunoblotting with antibody against c-myc, FK1 and VacA.

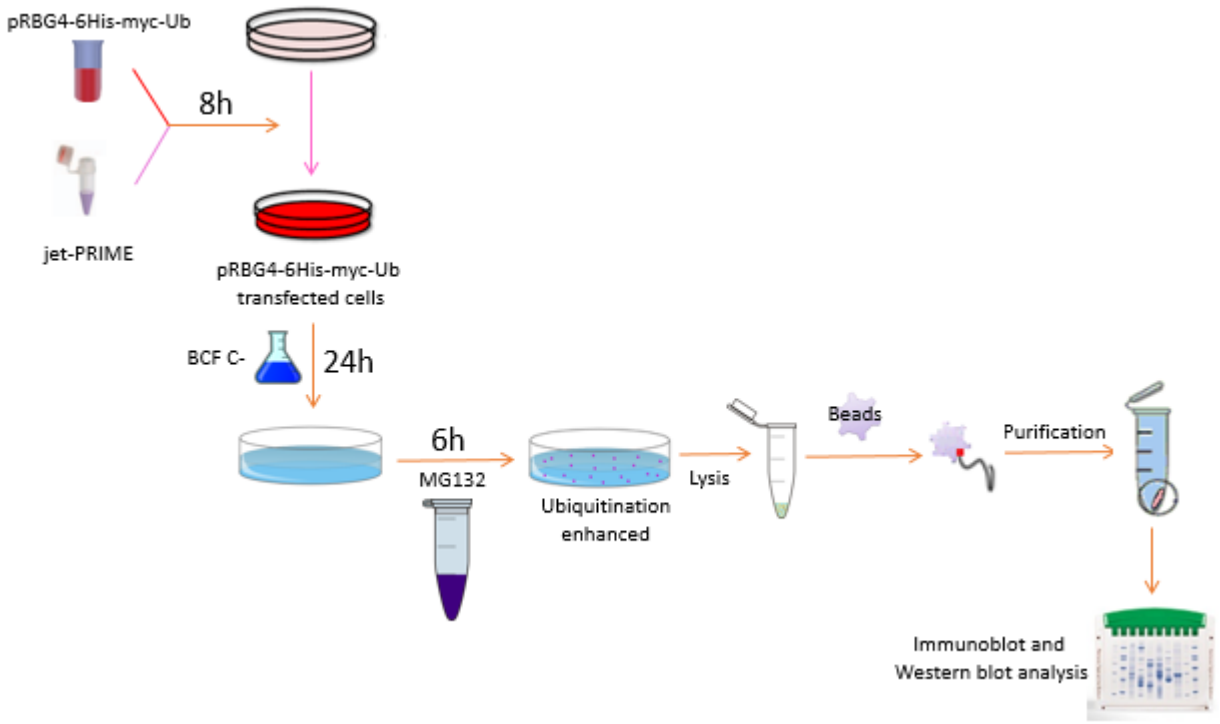

Figure 19. Schematic representation of ubiquitination assay. Protocol modified from Doye et al,2002.

Protein biochemical methods

Samples preparation

In order to be able to compare different cell lysates, samples were prepared in a standardized manner. Cells were cultured in 10 cm^2 Petri dish for two days and treated as required. After treatment cells were washed with washing buffer (Sodium Vanadate and Diisopropylfluorophosphate in PBS) and then lysate for 30 minutes on ice in lysis buffer (50 mM 4-(2-hydroxyethyl)-1-piperazineethanesulfonic acid (pH 7.5, HEPES), 1% Triton X-100, 5 mM Egtazic Acid (EGTA), 50 mM NaCl, 50 mM Sodium Fluoride, 20 mM Sodium Pyrophosphate, 1 mM Sodium Vanadate, 2 mM Phenylmethylsulphonyl Fluoride, 0.2 mg/mL Complete Protease Inhibitor and 8 mM Diisopropylfluorophosphate). Lysate was cleared at 10,000 g for 15 minutes, measured and diluted 1:3 in 3X SDS sample.

For protein concentration determination was used 10 µL of the lysate before SDS was added. A colorimetric assay was employed to measure the concentration of protein solutions. Sample preparation and a dilution series of BSA (0 to 2 mg/mL) were assayed in triplicate with Protein Assay Dye Reagent Concentrate (Bio-Rad) according to the manufacturer's instructions. Absorbance at 750 nm was measured in 96-well plates (Corning) using a Model 680 Microplate Reader (Biorad).

SDS-PAGE and immunoblot analysis

Proteins were separated according to size via SDS-PAGE. Protein samples were boiled (5 minutes at 95°C) before loaded into the gel. Fifty micrograms of proteins were separated on a precast SDS/polyacrylamide gel (percentages and gradients of polyacrylamide depending on the size of the protein of interest, Bio-Rad) together with 10 µL of Precision Plus Protein (Bio-Rad) as standard. The gel was running with a Mini-Protean III vertical gel electrophoresis system (Bio-Rad) in running buffer (25 mM Tris, 192 mM Glycine, 0.1% SDS) and transferred to polyvinylidene fluoride blotting membranes (GE Healthcare) overnight at 4°C in Transfer buffer (20 mM Tris, 150 mM Glycine, 20% Methanol). Proteins transfer was checked with Ponceau S red stain (0.5% Ponceau S in 1% acetic acid). Membranes were blocked with 5% BSA or non-fat milk for 4 hours at room temperature and incubated with the correct primary antibody overnight at 4 °C. After washing abundantly with Tris-Buffered Saline supplemented with Tween 20 (TBST 0,1%, Tris-HCl 20 mM, NaCl 150 mM, 0.1% Tween 20) membranes were incubated with the appropriate peroxidase-conjugated secondary antibodies (Millipore) for 1 hour at room temperature. Reactive proteins were visualized by enhanced chemiluminescence (GE Healthcare) according to the manufacturer's recommended protocol. The film images obtained were scanned to a digital image and the relative amounts of soluble protein of interest for each condition were evaluated by densitometry analysis with ImageJ (National Institute of Health).

Coomassie blue staining

In order to check the correct VacA purification on SDS polyacrylamide gels, gels were stained with Coomassie solution (0.275% Coomassie Brilliant Blue R450 (Biomol), 50% Methanol, 10% Acetic acid) for 20 minutes at room temperature and subsequently treated with de-staining solution (10% Acetic acid, 10% Isopropylic acid) until all relevant bands were visible (16 hours). After abundant water washing, gels were scanned and evaluation of VacA purification was made with ImageJ (National Institute of Health).

Statistics

Data are expressed as mean ± Standard Error of Mean (SEM). All experiments were performed in triplicate. The statistical significance of the results was explored using analysis of variance followed by ad hoc multiple comparisons tests such as Tukey's test or Student-Newman-Keuls's test. Significance was defined at $p < 0.05$ (*).

RESULTS

Strain selection and characterization

Since we wanted to analyze VacA activity and trafficking, we selected three VacA produced Hp strain, to obtain BCFs containing VacA and to further characterized them in "*in vitro*" cell culture experiments.

We cultured wild type CagA$^+$/VacA$^+$ 60190 and its isogenic mutants CagA$^-$/VacA$^+$ (60190:M22), picB/cagE-/VacA+ (60190:C-). These two mutants are respectively mutated for the gene that produce CagA and for the gene that encoded the component necessary to translocate CagA inside cells (Marlink et al., 2003). The absence of contamination, for instance by *Escherichia coli*, was evaluated using the Urease test, which involves a colorimetric indicator that switch from orange to pink, thanks to the Hp striking urease activity.

To evaluate vacuoles induction by the three strains, we performed biological tests on Hela cells incubated with BCFs diluted 1:3 in Hanks' balanced salt solution (HBSS) for 24 hours. The vacuolation induced by VacA and absence of cellular toxicity were evaluated by microscopy analysis in light microscopy.

In cells treated with BCFs, the presence of vacuoles due to the action of VacA toxin produced by the bacterium, was clearly recognizable. This effect was identifiable at phase-contrast microscopy after 4 hours of cell incubation. The analysis of the biological vacuolation 24 hours after Hp incubation (Figure 20) showed a predominant effect on vacuolization induced by VacA by the strain 60190:C- (Figure 20c). For this reason, we proceeded using this strain and its filtrates, in the further stages of the experiments.

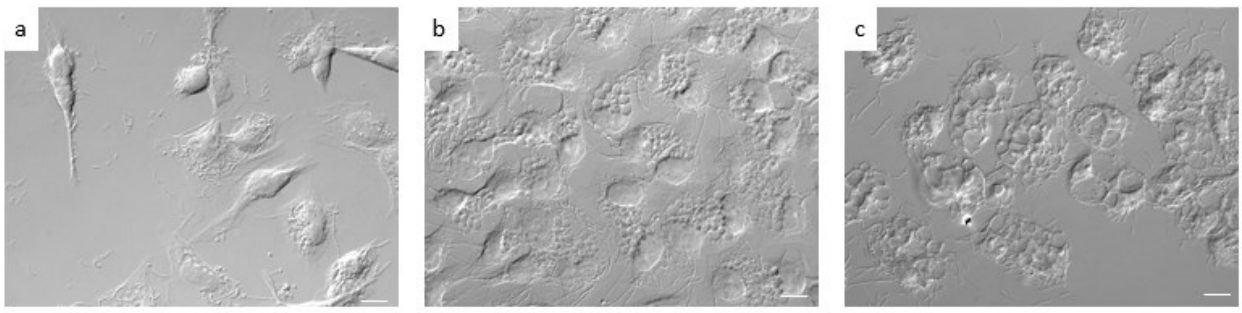

Figure 20. Hela cell infected for 24 hours with Hp (bar, 10 µm). a) CagA+/VacA+ 60190 b) CagA-/VacA+ 60190:M22 c) picB/cagE-/VacA+ 60190:C-.

Purified VacA was necessary for several experiments conducted, so one part of the BCF C- obtained was used to purify and concentrate VacA.

VacA purification was done with ammonium sulphate precipitation and gel filtration chromatography. The correct purification and the single fraction quality were assed combined biological assay, Coomassie staining and SDS-PAGE (Figure 21) with immunoblot analysis using anti VacA specific antibody.

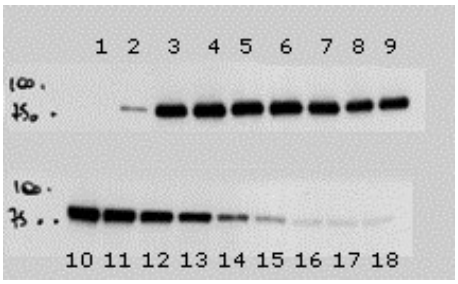

Figure 21. The eluted VacA fractions were applied to a 7,5% SDS polyacrylamide gel. VacA bands were identifiable just around 88 kDa.

The best purified fractions, as determined by the three combined investigations, have been pooled to a final concentration of 4 µg/mL for next experiments. Since that, after purification VacA is oligomerized and thus biologically inactive (McClain et al., 2000), purified VacA was acid activated with HCl before all experiments. Purified acid activated VacA was analyzed for toxin activity in a biological assay before used in further step of the experiment.

Trafficking alterations and misfolded proteins

Considering the similar positivity to glycogen, Hsp and polyubiquitinated proteins between PaCSs and some intracellular aggregates as LBs, JUNQ and IPOD we firstly investigated similarity and difference between them. Moreover, considering that PaCSs store highly soluble components that are poorly preserved by common aldehyde fixatives, was necessarily performed a combined light and electronic analysis with aldehyde-osmium fixation for ultrastructural analysis.

PaCSs vs LBs

We start examining the Lafora disease mouse malin^{KO} model that was previously used for other studied (Duran et al., 2014; Valles-Ortega et al., 2011). In order to identify LBs in the brain, presence of laforin was evaluated by IHC and subsequently by light microscopy. IHC performed on formalin-fixed paraffin embedded tissues showed several cytoplasmic areas positive for PaCS markers, such as glycogen, 20S, FK1, Hsp70, bag3 and laforin (data not shown). The amount of positivity was found

to be different between different areas of samples, with portions of the preparation more positive than other.

Next, starting from this information, half brain of the younger (7 weeks older) mouse malin^{KO} was analyzed by TEM. We found that there was more immunogold reaction in aggregates (primary antibodies against FK1, BAG3 and laforin) inside the sample of cerebellum (the area of Purkinje neurons and five nearby areas labeled with colloidal gold) than the cortex or hippocampus. Analyzed at a high magnification (Figure 22b), LBs appeared as heterogeneous structures with dense granules and short fibrils.

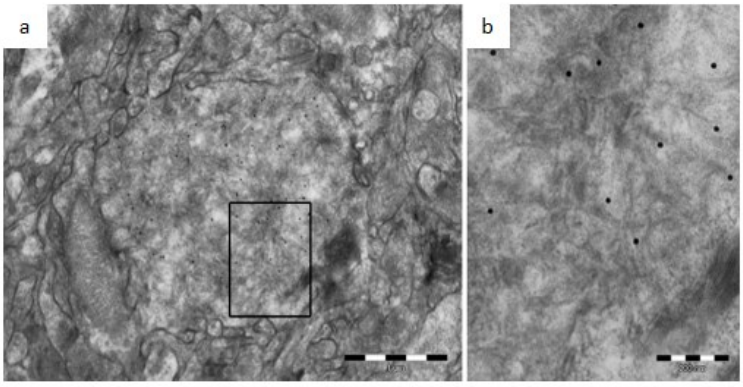

Figure 22. a) Resin section of hippocampus from malin^{KO} mouse (bar, 1 µm).
b) The enlarged boxed area shows the positivity for FK1 antibody (bar, 200 nm).

Ultrastructural analysis showed a different organization of LBs (Figure 23-2a and b), less order than PaCSs (Figure 23-1a and b), and there was no evidence of the classical accumulation of cuboid and fibrillar particles characteristic of PaCSs. Moreover, no PaCSs were found in all sections analyzed.

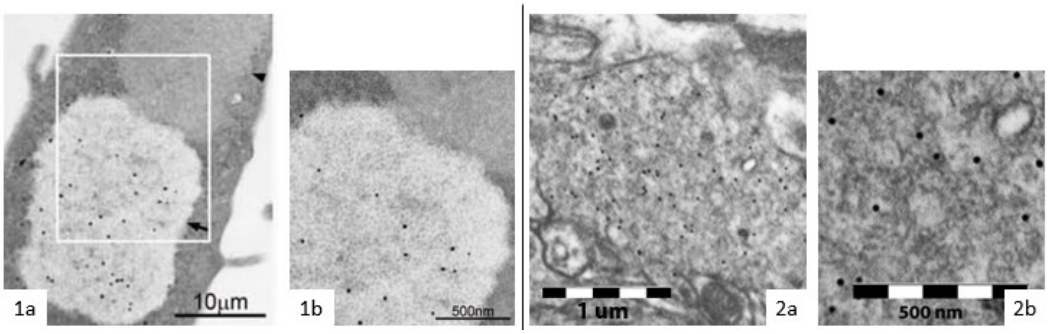

Figure 23. PaCS inside Hela cells (1a; bar, 10 µm) FK1 reactivity compared to LBs (2a, from cerebellum of mouse malin^{KO}; bar, 1 µm). b) Magnification of the ultrastructure of both aggregates (bar, 500 nm).

PaCS vs JUNQ and IPOD

JUNQ and IPOD were firstly described in yeast model and later in mammalian model, particularly in HEK293 cells (Kaganovich et al., 2008). To characterized them we transient transfected HEK293 and HEK293T/17 cells to promote the development of aggregates.

First, TEM analysis of HEK293 and HEK293T/17 cells grown under physiological condition reveal that these cells line did not show the presence of PaCSs (Figure 24). Furthermore, PaCSs did not develop even after transfection with HttQ97, which usually accumulates in IPOD.

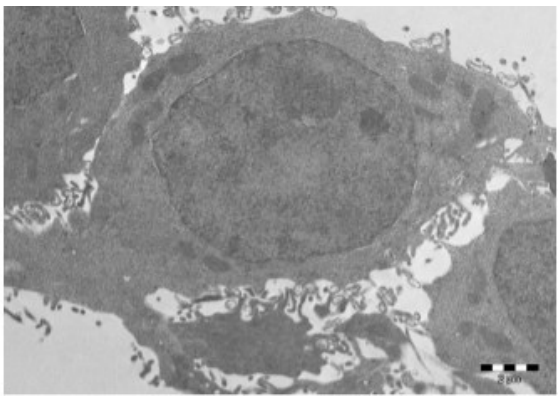

Figure 24. HEK293 cells showed no PaCSs structure (bar, 2 µm).

Instead in transfected cells, cytoplasmic inclusions probably IPOD, appeared. They were shown as circles slightly convex on the cell surface, recognizable even "*in vivo*" in bright microscopy. When observed in fluorescence microscopy they appeared as circle with a quite distinct and intense red fluorescence. Using transfection by jetPRIME it was possible to see IPOD in 40% of the cells, one for each cell (Figure 25).

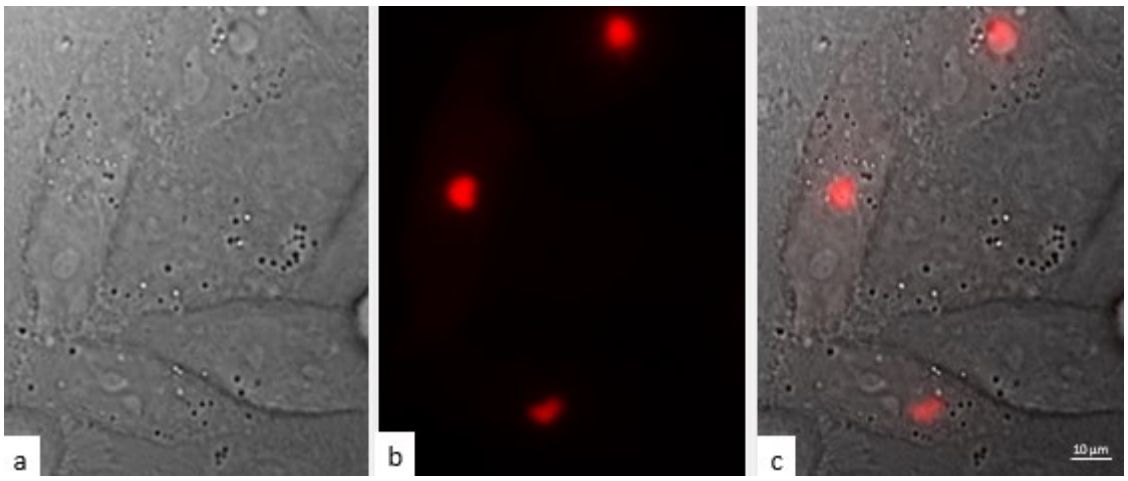

Figure 25. HttQ97-transfected Hela cells showing IPOD (red; 60X after fixation; bar, 10 µm). a) DIC (differential interference contrast microscopy) revealed great cytoplasmic bodies which correspond to the fluorescent Htt bodies (b). c) Overlapping of DIC and fluorescent photographs.

ICC analysis showed a diffuse signal for Proteasome 20S. In some cases, the immunoreactive seems to surround IPOD, even if the co-localization did not seem specific (Figure 26a). The positivity for FK1 showed a signal less intense. Also in this case, the positivity sometimes seems to surround IPOD (Figure 26c).

Transient transfected HeLa cells showed IPOD comparable to HEK293 and HEK293T/17 cells.

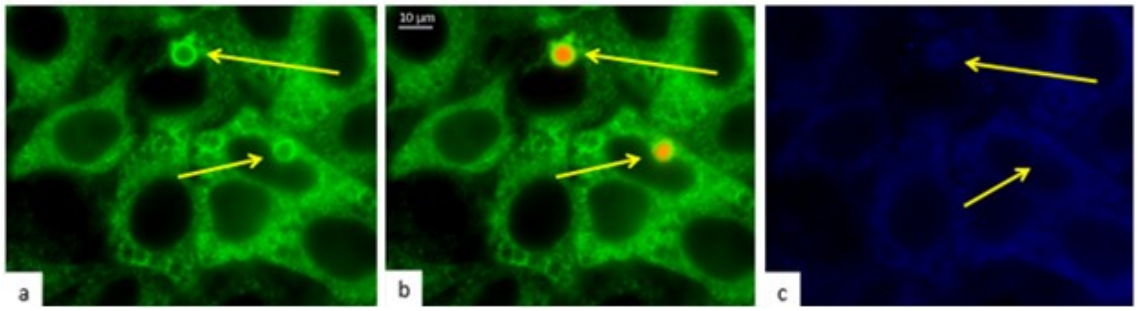

Figure 26. HttQ97-transfected HeLa cells (red; 60X magnification; bar, 10 µm). Primary antibodies against a) FK1 (green) and c) 20S (blue). b) Merge of the two images. Yellow arrows indicate IPODs (red).

Since that Hela cells showed the development of clearly identifiable IPODs as HEK cell line, and considering that they constitutively develop PaCSs, we used this line to perform TEM analysis of both aggregates in the same cells.

The analysis of transfected HeLa cells by TEM (Figure 27), showed the appearance of aggregation bodies inside cells, that were not present in cell grown under physiological condition.

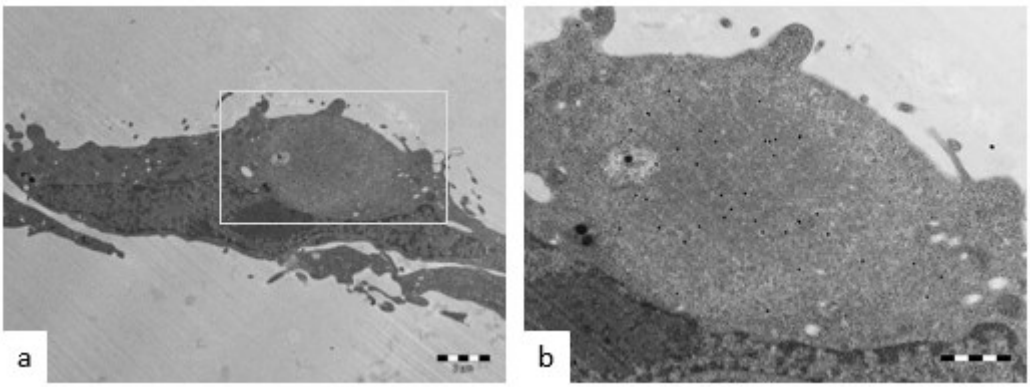

Figure 27. HttQ97-transfected HeLa cells showing IPOD development (a; bar, 2 µm) magnified in b (bar, 500 nm) which is positive for polyQ antibody.

These inclusion bodies had a different texture than the cell cytoplasm and a sharp border. The intracytoplasmic body appeared more dense in the center and less dense to the periphery. They had a particulate ultrastructure more osmiophilic than PaCS and were positive for polyQ antibodies

direct against HttQ97. Moreover, these aggregates had immunogold negativity against FK1 and 20S, instead positivity for primary antibody against polyQ and p62.
Considering all these evidences these bodies were ultrastructurally different from PaCSs, but they interestingly resemble "B structure" or sequestosomes, already identified within HeLa cells (Solcia et al., 2014; Sommi et al., 2013).

An interesting data comes from ICC analysis of consecutive semithin resin sections of the same cells analyzed in TEM (Figure 28). HeLa cells which showed FK1 positive bodies (PaCSs) never revealed reactivity for polyQ antibodies; conversely cells which had HttQ97 positive inclusions (IPOD) did not react for FK1.

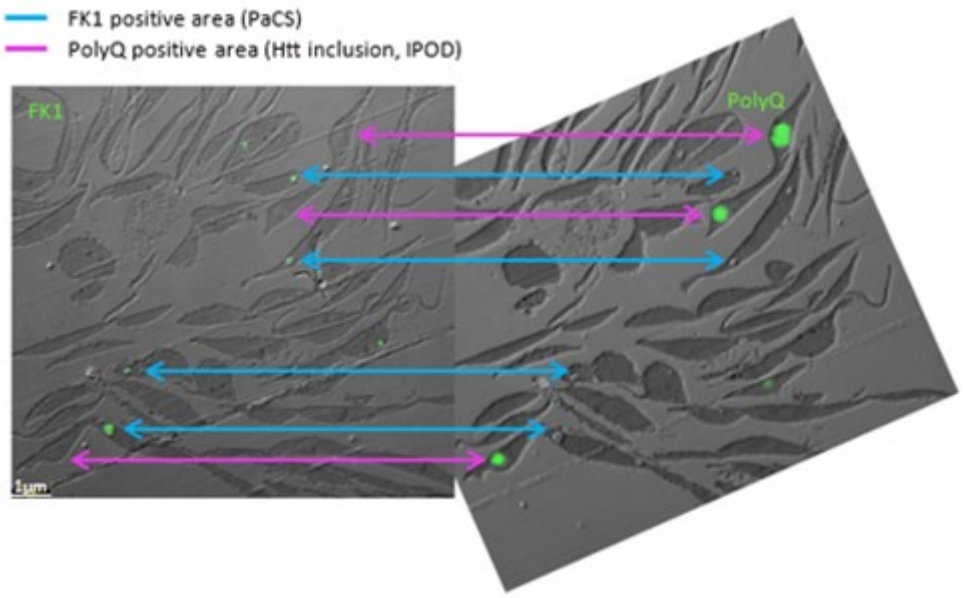

Figure 28. IF on consecutive semithin fixed resin sections (bar, 1 µm) of HttQ97-transfected HeLa cells showed that PaCS (FK1) and IPOD (polyQ) are different structures.

The development of JUNQ has been much more difficult than IPOD. Since that the VHL has often been used as a model substrate to study protein aggregation, we transient transfected Hela and HEK293 cells with VHL plasmid to promote the development of JUNQ. Despite several attempts and longtime of trasfection cells did not show the development of identifiable JUNQ. We move then to HEK293T/17 cells, that are HEK293 derivates with a greater transfection efficiency. These cells showed a good level of transfection but have a low level of adhesion, even if seeded on poly-lysine or other solvents that promote cell adhesion. The association of 47 hours of VHL-transfection associated with 23 hours of 10 µM of MG132, that promote stress since its action as a potent

membrane-permeable proteasome inhibitor (Han et al., 2011; Lee, 1998), allowed us to identify probably JUNQ, localized around the ER and nucleus (Figure 29).

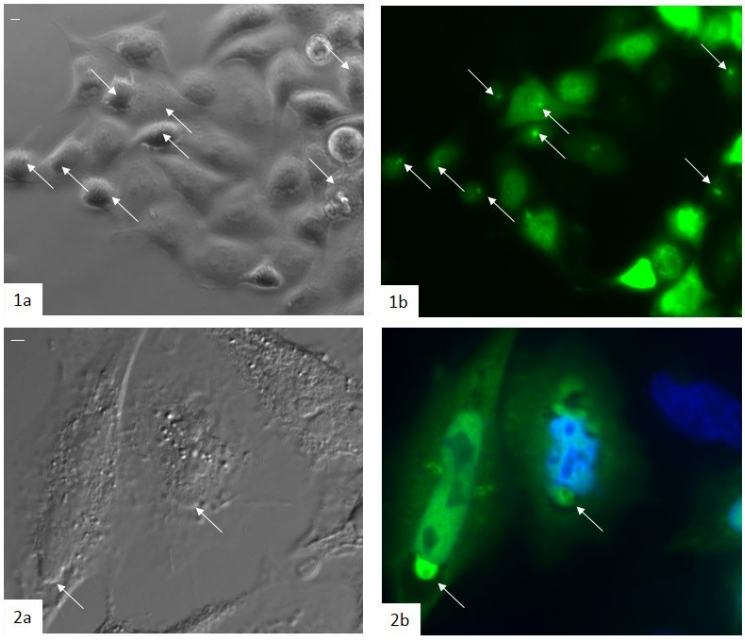

Figure 29. VHL-transfected HEK293T/17 cells showed the development of JUNQ (green, enhanced by the arrows). 1) 20x "in vivo" 2) 60X after fixation (bar, 10 µm). Nuclei are depicted in blue.

TEM analysis of JUNQ bodies revealed, as for IPOD, ultrastructural characteristic different for PaCSs. Starting from the optimal condition establish to develop JUNQ in HEK293T/17, we were able to transient transfected Hela cells, that constructively shows PaCSs development (Figure 30-1), with VHL plasmid (Figure 30-2).

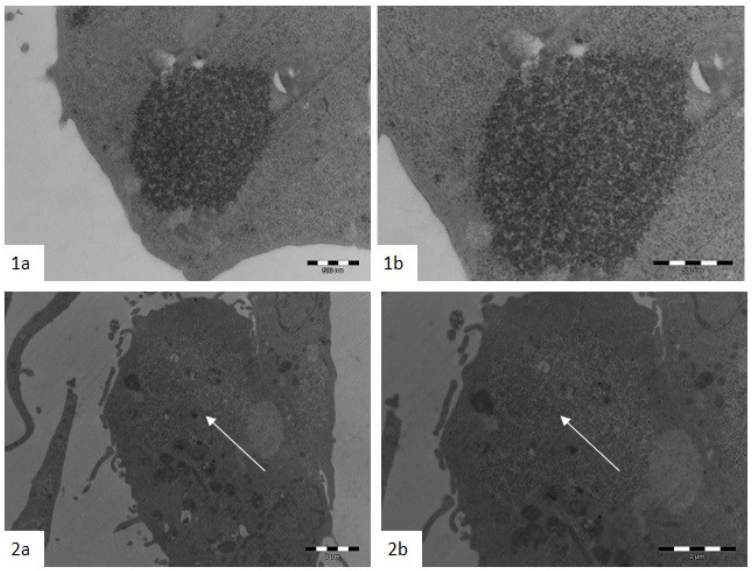

Figure 30. Hela cells which constitutively express PaCS (1; bar, 500 nm) compared to VHL-HeLa cell showing JUNQ development (2a enhanced by the arrow, magnified in 2b) positive for anti VHL antibody (bar, 2 µm).

Furthermore, combining a double trasfection, we promoted the formation of JUNQ and IPOD (Figure 31) and, with TEM analysis, data confirmed that these aggregates have ultrastructurally and immunoreactivity characteristic different from PaCSs (data not shown). Moreover, at TEM analysis, cells that exhibited JUNQ and IPOD did not showed any PaCSs and vice versa.

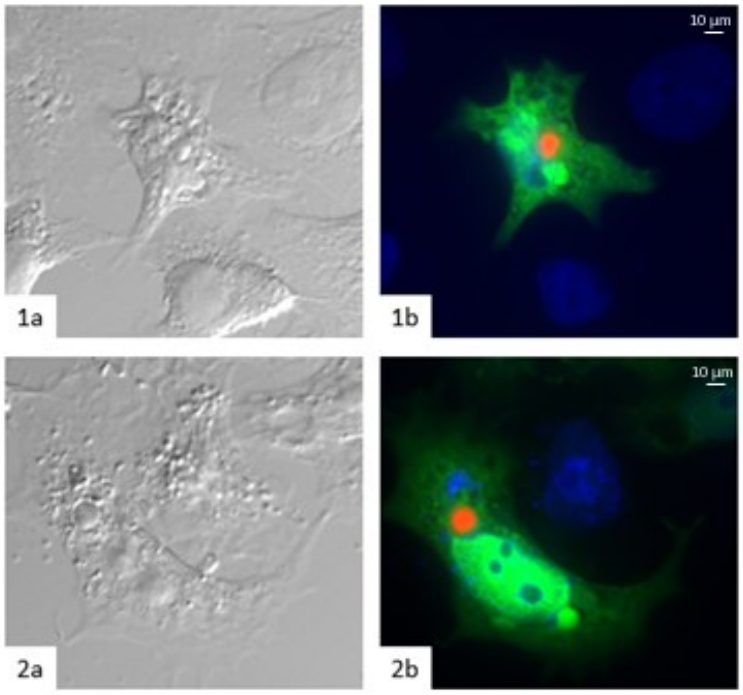

Figure 31. Htt and VHL-transfected Hela cells showed the development of IPOD (red) and JUNQ (green). 60x after fixation (bar, 10 µm): a) DIC, b) merge of two aggregates fluorescence. Nuclei are depicted in blue.

VacA ubiquitination assay

Since that VacA has been reported to accumulate inside PaCSs, together with polyubiquitinated proteins and proteasomal components (Necchi et al., 2010), suggesting the possibility that the toxin could escape the ER and be ubiquitinated for proteasomal degradation, we investigate the ubiquitination levels of VacA throughout ubiquitination assay.

We used the approach of Doye and colleagues (Doye et al., 2012), which transient transfected cells with hexameric-histidine-tagged Ubiquitin (His-Ub), followed by a metal affinity purification in denaturing conditions. After that, the samples obtain are visualized by SDS-PAGE and immunoblot analysis. This approach allows to establish the quantity of protein target by ubiquitination.

Briefly, cells expressing His-Ub were left untreated (control) or treated with 20 µM MG132 for 6 hours before lysis, to increase the rate of ubiquitinated proteins. The proteins were then processed for His-Ub purification by metal affinity precipitation with cobalt beads. Proteins were resolved on a 7.5% SDS-PAGE and visualized by immunoblotting with anti-c-myc and FK1 primary antibodies.

The correct purification (Figure 32) was checked using anti-c-myc antibody which identified His-tagged proteins. The five consecutives washing after purification were also loaded and no His-Ub tagged proteins were found inside it (data not shown). The control showed a good rate of purification, recognizable by the large amount of purified proteins in the third line (Figure 32 "His-Ub tagged proteins"). Furthermore, treatment with MG132 for 6 hours after trasfection (Figure 32 "+ MG132") allowed to increase the total amount of polyubiquitinated proteins.

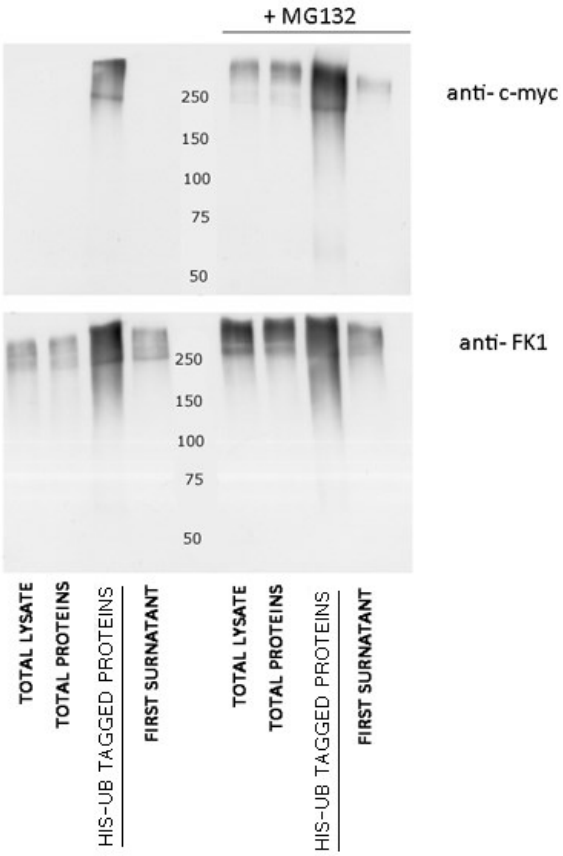

Figure 32. Immunoblot anti-c-myc and FK1 of His-Ub tagged proteins from cells left untreated or treated with MG132 (+MG132) for 6 hours before lysis.

Then we used the same protocol to quantify ubiquitination levels of VacA. To this purpose, 24 hours after trasfection, cells were treated with BCF 60190 diluted 1:3 in the medium without FBS. 18 hours after intoxication and 6 hours before lysis, cells were treated with 20 µM of MG132 or left untreated as a control.

Immunoblot analysis (Figure 33) with c-myc antibody showed the correct purification process. The amount of polyubiquitinated proteins in presence of MG132 was greater than the control left untreated. VacA antibody identify two lines (recognizable only with MG132) in the range of 50-75 kDa, lower than the line of VacA, which is around 88 kDa. As for the control without BCF, the five

washing after purification were loaded and no His-Ub tagged proteins were found inside it (data not shown).

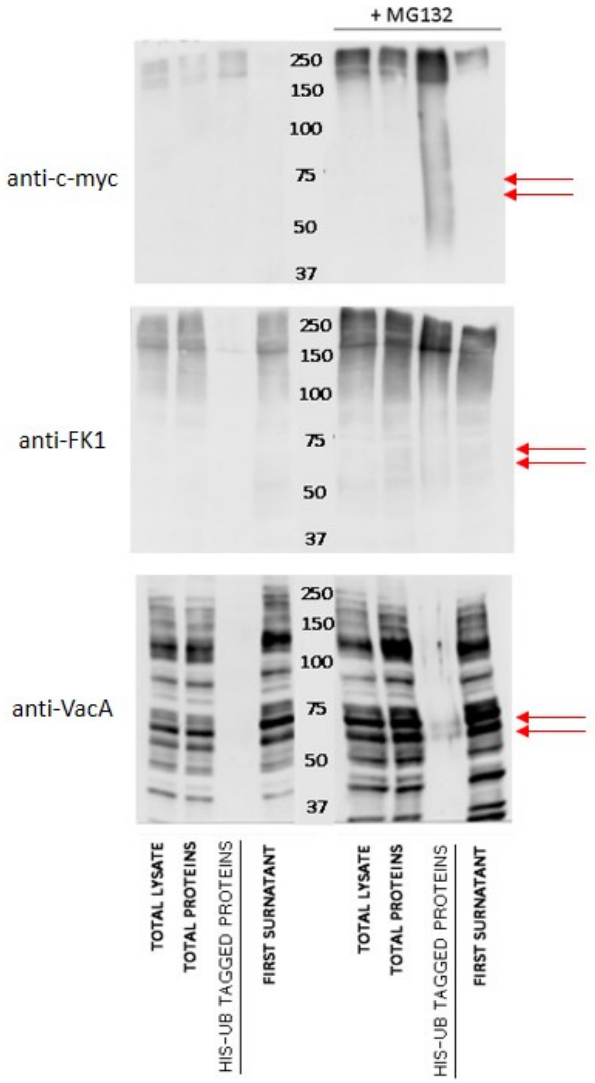

Figure 33. Immunoblot anti-c-myc, FK1 and VacA of samples obtained from cells treated with BCF 60190 for 24 hours. Right lines (+MG132) identified samples of cells treated with MG132 for 6 hours before lysis.

Vacuolation assay and inhibitors effect

Since vacuoles are acidic, their time-dependent development can be assessed quantitatively by the NRU assay. Neutral red dye is a membrane-permeable weak base that accumulated inside vacuoles, where it is protonated and trapped. NRU is widely accepted as "in vitro" assay for VacA-induced cell vacuolation (Cover et al., 1992; de Bernard et al., 1997; Ricci et al., 2002; Sun et al., 2010).

Since VacA-induced vacuoles can be stained with neutral red dye, we were able to quantify the toxin activity and also the effect of several different trafficking inhibitors on the toxin. The inhibitors tested are reported in Table 1.

Inhibitors	Function
BFA	Anterograde transport inhibitor which cause the collapse of Golgi apparatus (Barbier et al., 2012).
EGA	Possibly inhibitor of the trafficking and maturation from EEs to the LEs (Gillespie et al., 2013).
Retro-1	Inhibitor of the retrograde transport between EEs and the TGN (Barbier et al., 2012).
Retro-1.1 (HA-432)	New generation inhibitor of retrograde trafficking.
Retro-2	Inhibits the endosome-to-Golgi retrograde transport (Park et al., 2012).
Retro-2 cyclic	New generation inhibitor of retrograde trafficking.
Retro-2.1 (RN-3-122)	New generation inhibitor of retrograde trafficking.
Compound 20	New generation inhibitor of retrograde trafficking.

Table 1. List of inhibitors used.

The studies were carried out with short treatments of 5 hours, in order to assess the effect on early vacuolization induced by VacA, and overnight treatments. Moreover, we compared the effect on cells treated only with HBSS and BCF C-untreated as controls, with NH_4Cl and with CHL, two weak base that are able to induce cellular vacuolization.

In short-term treatment (Figure 34) only Retro-1.1, added to HBSS treated cells, was able to induce a statistic significant reduction on vacuolation. Instead in cells treated with HBSS supplemented with NH_4Cl only COMPOUND 20 was able to induce a decrease. In cells intoxicated with BCF C- Retro-1, 1.1, Retro-2.1 and Retro-2 cyclic, COMPOUND 20 were able to induce a statistical significant reduction on NRU results. Additionally, EGA virtually abolished the toxin vacuolation activity.

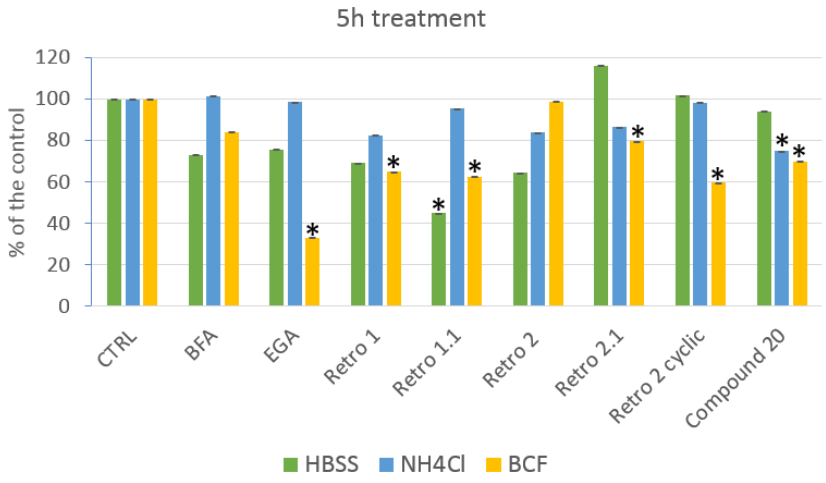

*Figure 34. Cells treated with different inhibitors and with HBSS or with HBSS supplemented with NH_4Cl or BCF C- for 5 hours. Data are expressed as rate of the corresponding control. NRU analysis performed 5 hours after the treatment. * = $p < 0.05$.*

Starting from this information we analyzed the effect of these inhibitors on overnight-treatment (o/n treatment, Figure 35).

In cells left untreated, the spontaneous vacuolation was reduced by inhibitors Retro-2, 2.1 and 2 cyclic, BFA and EGA. Instead cells treated with HBSS supplemented with NH_4Cl did not show the reduction on vacuolization with any inhibitor. Cells treated with BCF C- Retro-1 and 1.1, Retro-2 cyclic, COMPOUND 20, BFA were able to induce a reduction on NRU results. As for the short treatment, EGA virtually abolish the toxin activity.

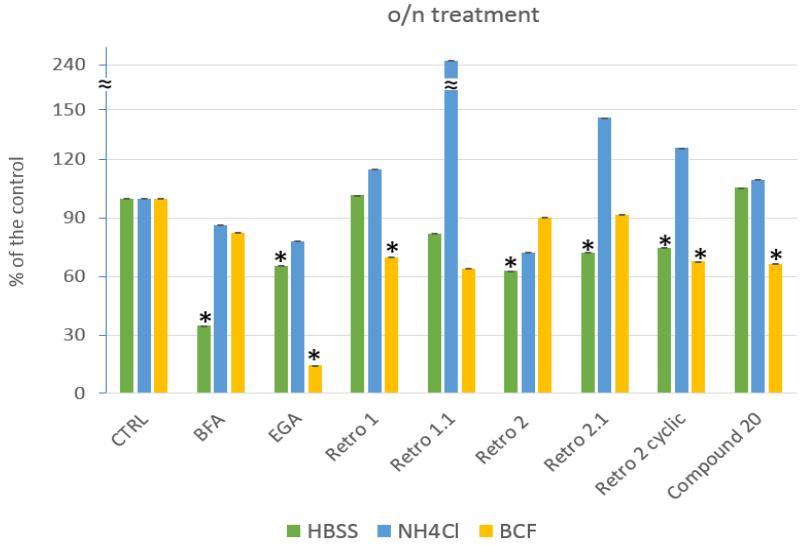

*Figure 35. Cells treated with different inhibitors and with HBSS or with HBSS supplemented with NH_4Cl or BCF C- for 16 hours. Data are expressed as rate of the corresponding control. * = $p < 0.05$.*

Then we tested the effect of the inhibitors on CHL, a weak amine base which cause the dilation of endosome by altering the hydrogen balance across the membrane (Alvarez & Sztul, 1999). Cells treated with CHL (Figure 36) for 7 hours revealed a vacuolization like VacA-intoxicated cells. Inhibitors Retro-1, 1.1 and 2.1, Retro-2, COMPOUND 20 blocked the CHL-induced vacuolization. As for VacA-induced vacuoles, EGA virtually abolish CHL related vacuolization.

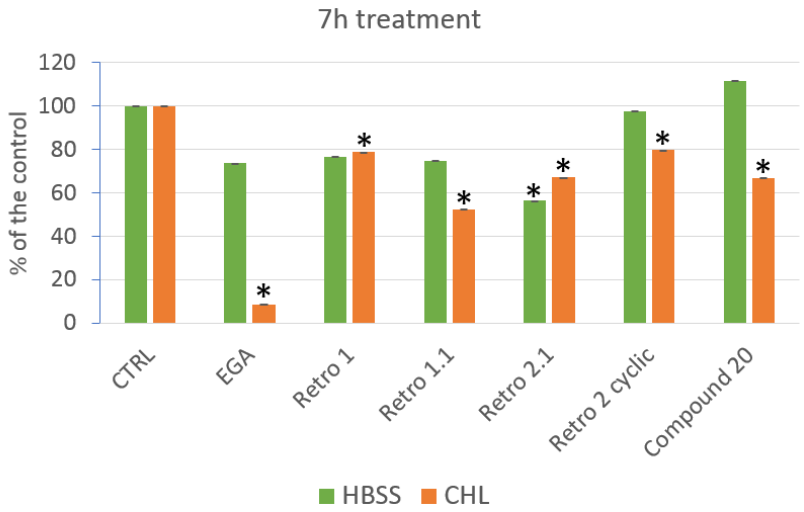

*Figure 36. Cells treated with different inhibitors and with HBSS or with HBSS supplemented with CHL for 7 hours. Data are expressed as rate of the corresponding control. * = p < 0.05.*

Considering the result on short- and long-term treatment on VacA-induced vacuolization and the prominent effect of EGA among the different inhibitors, we focalized our attention on this inhibitor and we further investigate its effect (Figure 37).

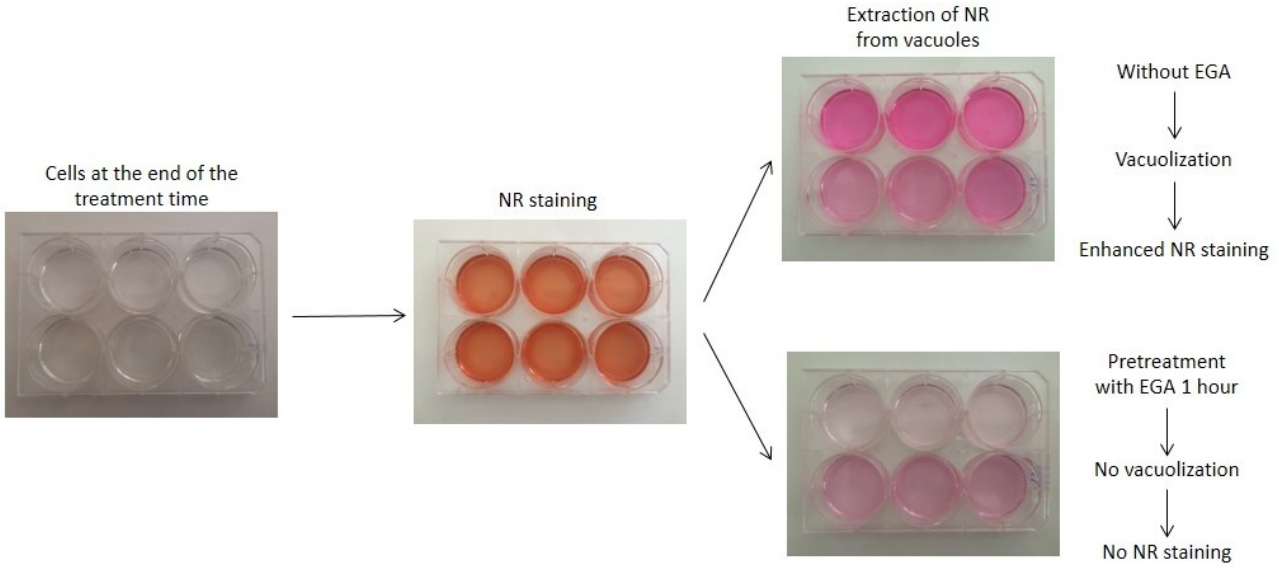

Figure 37. Summary of NRU variations in presence of EGA.

In cell treated with NH_4Cl for 5 hours throughout all the experiment EGA wasn't able to induce any statistical variation. Instead in the event that the vacuolization was promoted for 5 hours and then the inhibitor was added to the medium culture, the NRU showed a reduction on the vacuolization (Figure 38).

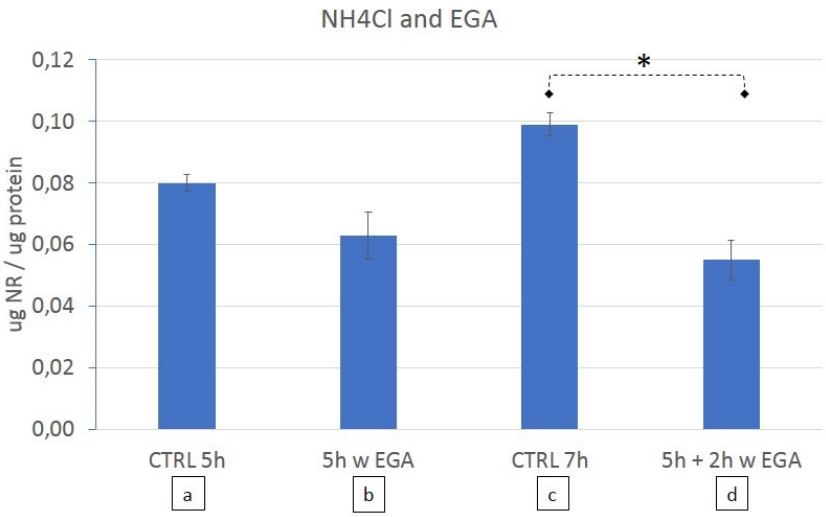

*Figure 38. Cells treated with NH_4Cl for 5 hours (a) or 7 hours (c), treated with NH_4Cl and EGA for 5 hours (b) or EGA added to the medium 5 hours after the vacuolization was promoted (d) and analyzed 2 hours later. Significance is related to respective control. Data are expressed as µg of neutral red per µg cell protein. * = p < 0.05.*

The analysis of BCF C- treated cell (Figure 39) reveal that EGA was able to decrease the vacuolation on cells treated with the inhibitor form the beginning of the experiment (Figure 39a vs b) but also on those which had already been intoxicated for 5 hours with BCF C- (Figure 39c vs d). Interestingly, EGA was able to induce a greater reduction of NRU result from later addiction into medium (Figure 39d) compared to the 5 hours BCF C- EGA-free (Figure 39a, compared with red asterisk).

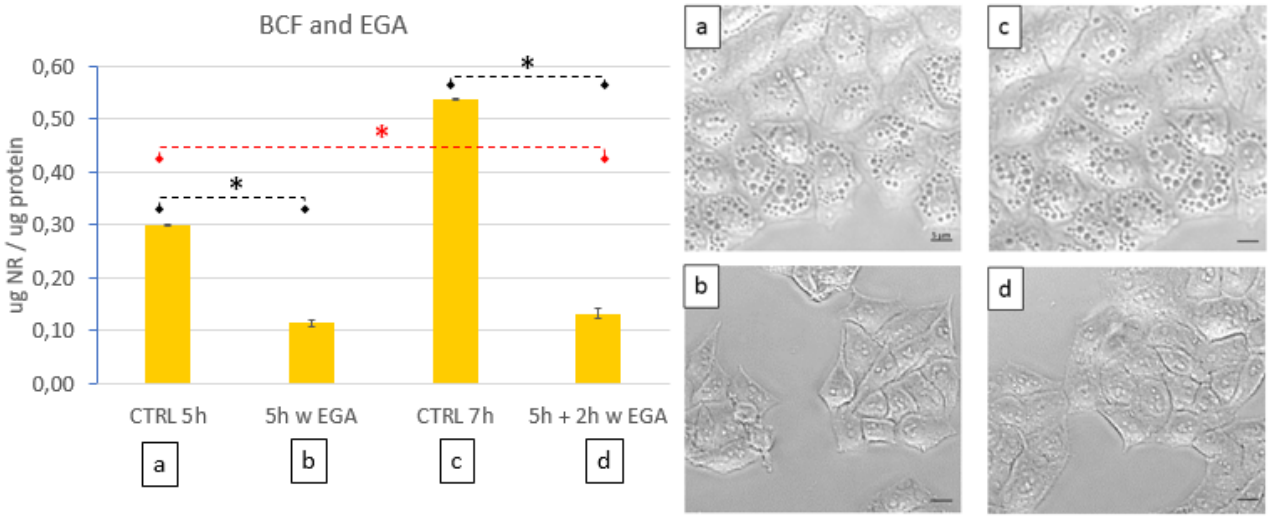

*Figure 39. Cells treated with BCF C- for 5 hours (a) or 7 hours (c), treated with BCF and EGA for 5 hours (b) or EGA added to the medium 5 hours after the vacuolization was promoted (d) and analyzed 2 hours later. The right panel shows corresponding images in light microscopy (60X magnification; bar, 5 µm). Significance is related to the respective control (black asterisk) or to the 5 hours BCF control (a versus d, red asterisk). Data are expressed as µg of neutral red per µg cell protein. * = p < 0.05.*

In CHL treated cells the same result was obtained: EGA was able to decrease vacuolization if added form the beginning of the experiment but also in cells where the vacuolization was already started (Figure 40). Moreover, the addition of EGA after five hours of vacuolation induced a reduction in vacuolization in 2 hours greater than the 5 hours control (Figure 40d compared to Figure 40a). Thus, the effect of the inhibitor in 2 hours on short-term vacuolization was greater than the untreated control.

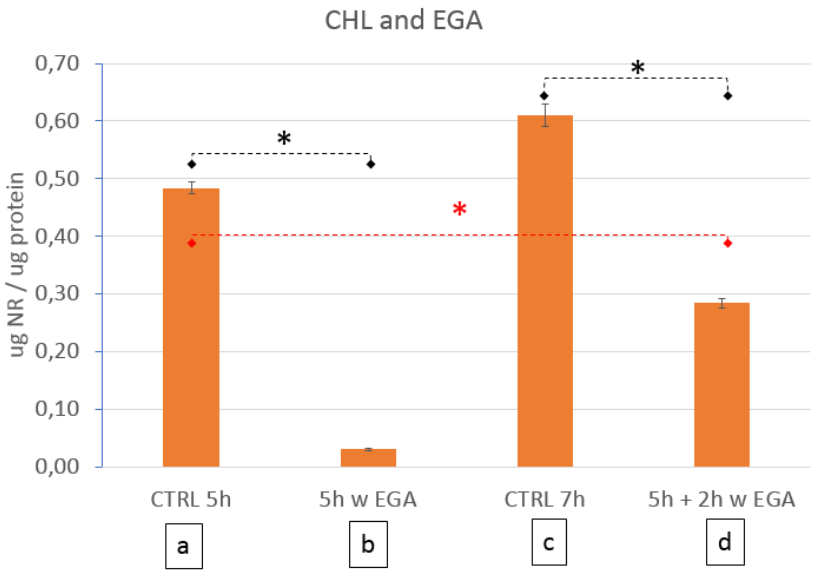

*Figure 40. Cells treated with CHL for 5 hours (a) or 7 hours (c), treated with CHL and EGA for 5 hours (b) or EGA added to the medium 5 hours after the vacuolization was promoted (d) and analyzed 2 hours later. Significance is related to corresponding control (black asterisk) or to the 5 hours CHL control (a versus d, red asterisk). Data are expressed as µg of neutral red per µg cell protein. * = p < 0.05.*

EGA effect on cells

Time-dependent effect

Starting from the information obtain throughout NRU assay, we deeper investigated EGA effect on cells. Firstly, we analyzed EGA preincubation time to effectively blocks the VacA-induced vacuolization.

We treated cell with EGA for a variable preincubation time, then cells were wash abundantly, and the vacuolization was promoted adding BCF C- to the medium. Cells were visualized at different time to check the vacuolization and images were taken after 24 hours of treatment.

In cells treated with a preincubation time (Figure 41) variable from 1 hour to 10 minutes, EGA was able to block the vacuolization. Furthermore, a preincubation time on ice (data not shown) did not interfere with EGA effects.

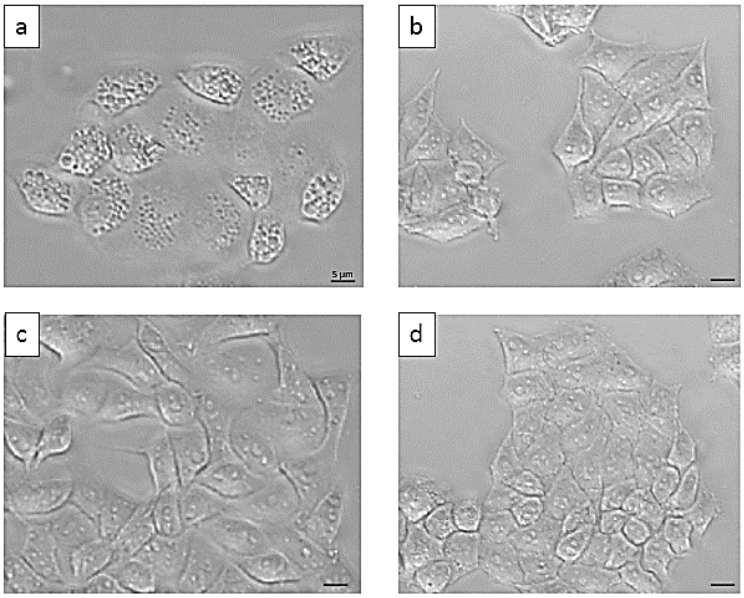

Figure 41. Cells treated with a) BCF C- or preincubated with EGA for b) 1 hour, c) 30 minutes d) 10 minutes and then intoxicated with BCF C- (60X magnification; bar, 5 µm).

Considering these results and the latest NRU results, we analyzed if EGA was able to revert the vacuoles.

In order to analyze the same cell before and after EGA treatment, we seeded cells on a µ-Dish 35 mm with a glass bottom and an imprinted 500 µm relocation grid. Hela cells were treated with BCF C- for 5 hours (Figure 42-1 and 2a) to promote vacuolization, then EGA was added directly to the medium and effect was evaluated 2 and 4 hours after the treatment in light microscopy.

As showed by the light microscopy images on the same cell at different time, EGA was able to promote the regression of the vacuoles (Figure 42). Moreover, the vacuoles reversion was time-dependent (Figure 42-1 and 2b compared to Figure 42- 1 and 2c). The same results (data not shown) was observed in cells treated with CHL.

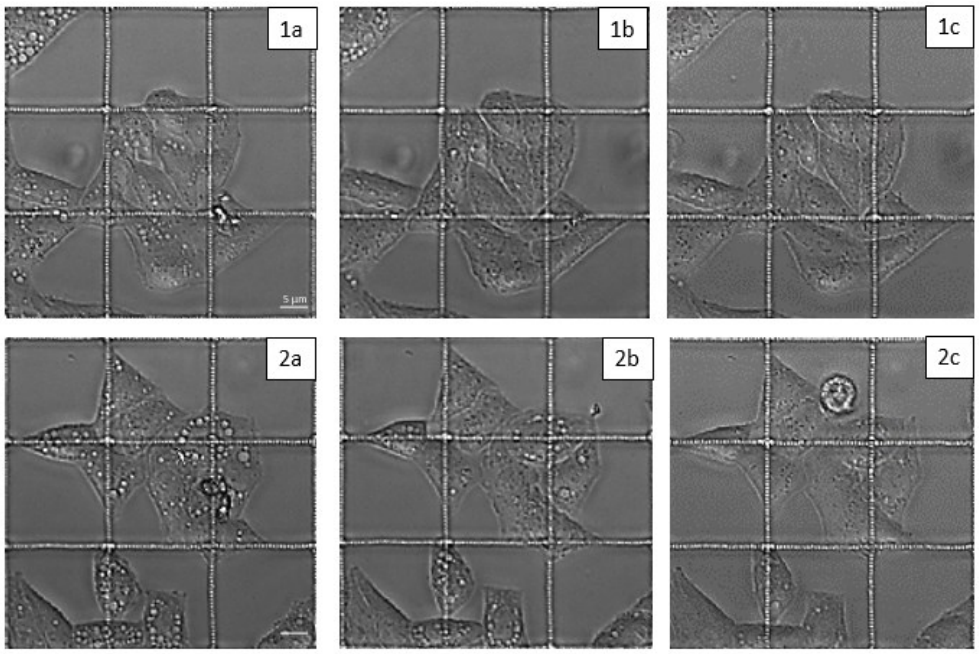

Figure 42. Cells treated for 5 hours with BCF C- (a) and then EGA was added to the medium to promote the reversion of the vacuoles. Images were taken after 2 hours (b) and 4 hours (c) of EGA action (60X magnification; bar, 5 µm).

pH analysis

Since that vacuoles arise from acidic compartments, in which VacA promote the swelling by forming a pore membrane channel, we investigated the possibility that EGA action on vacuoles could be related to pH alteration of acidic compartments.

To evaluate the pH alteration in cells we used AO, a metachromatic dye able to accumulate inside acid compartments, where becomes protonated and trapped. The constant influx of AO molecules results in increasing of AO concentration, aggregation and a red shift of emission and self-quenching. If the pH is altered or become basics, AO molecules can cross again the membrane of acid compartments due to the deprotonation (Lovelace & Cahill, 2007; Pierzyska-Mach et al., 2014). Considering its characteristic and action, AO is considered to be a good acidification indicator.

Firstly, we analyzed EGA effect on acid compartment in Hela cell BCF C- untreated, as a control. Preincubation time ranging from 1 hour to 10 minutes (Figure 43b, c, d), reveals a complete absence of red mark compared to the control (Figure 43a).

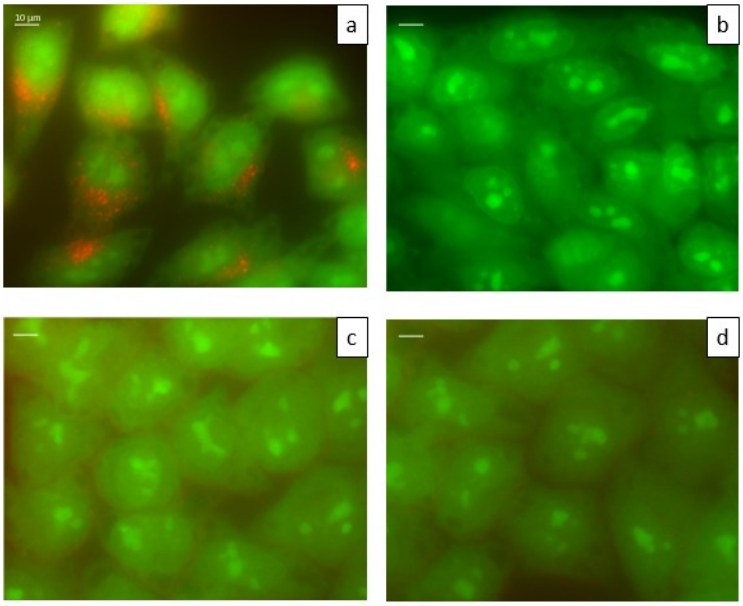

Figure 43. Cells stained with AO: control untreated (a) or preincubated with EGA for b) 1 hour, c) 30 minutes d) 10 minutes. The red staining identified the acidic compartments (60X magnification; bar, 10 µm).

Then we tested the AO staining in cell treated with BCF C- compared to cells preincubated with EGA for 1 hour before washing out and adding of BCF C- to the medium. The analysis was performed in short-term BCF C- treatment (5 hours) or long-term treatment as for NRU assay (o/n treatment). The AO staining was performed at the end of incubation time.

The vacuolization was inhibited as revealed both on light (data not shown) as for fluorescence microscopy (Figure 44b and d). The AO staining of vacuoles (Figure 44a and c), pronounced in the control EGA untreated, was absent in cells which have undergone preincubation time with EGA (Figure 44b and d). Interestingly, AO staining of acidic compartments were recognizable at 5 hours (Figure 44b) and even more marked at 16 hours (Figure 44d).

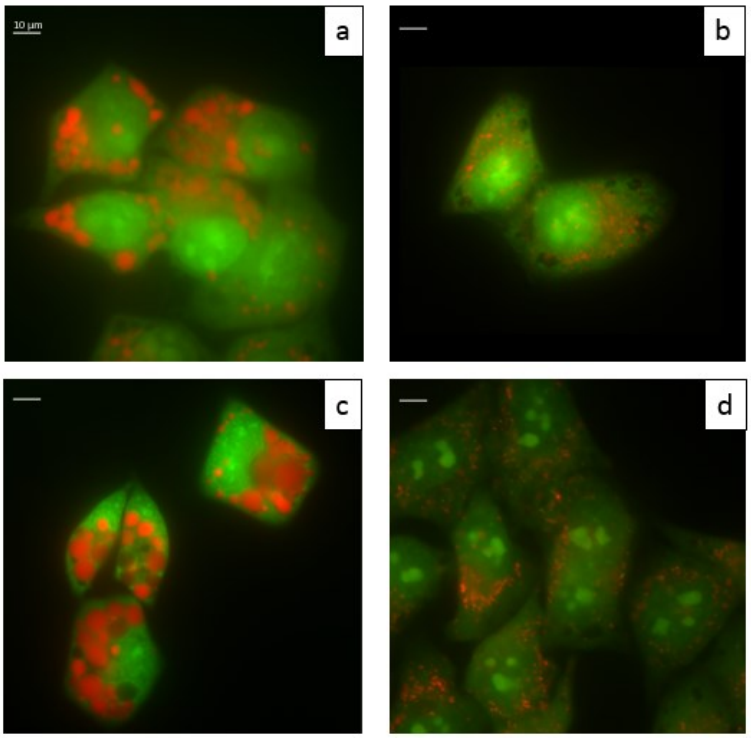

Figure 44. AO staining of cells treated with a) 5 hours of BCF C- b) 1 hour of EGA before 5 hours of BCF C- c) 16 hours of BCF C- c) 1 hour of EGA before 16 hours of BCF C- (60X magnification; bar, 10 µm).

Considering that AO revealed EGA reversible effect on pH of acidic compartments, we tested the possibility of vacuoles development after EGA wash out and cell recovery.

We treated cells with EGA for 1 hour, wash abundantly and left the cell recovered for 1 hour before adding BCF C- to promote the vacuoles development. The intoxication was allowed for 5 hours then we performed AO staining and NRU assay.

Both tests (NRU data not shown) revealed that, even if after recovery the staining of acidic compartments were comparable to the control (Figure 45d versus Figure 45a), the development of vacuoles was still blocked. The same result was obtained when the vacuolization was allowed for 16 hours (data not shown).

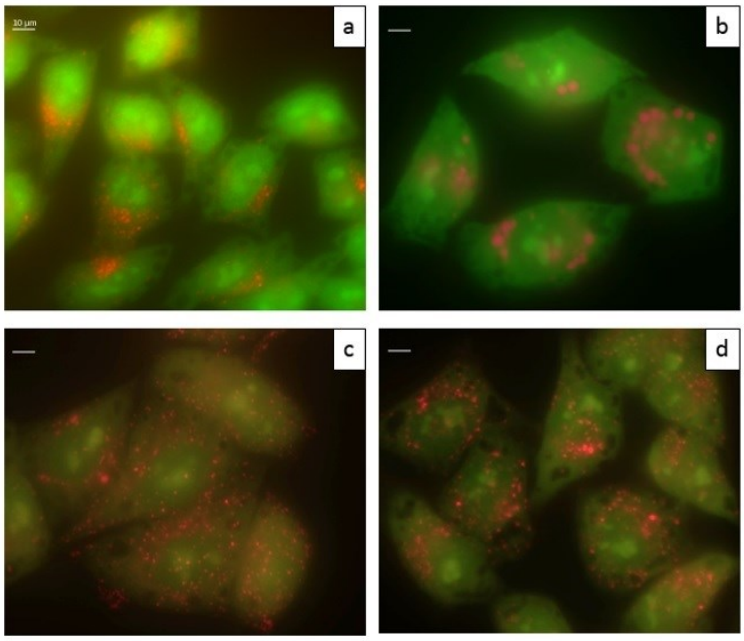

Figure 45. AO staining of cells a) left untreated or with b) 5 hours of BCF C-, c) 1 hour of EGA followed by 5 hours of BCF C- intoxication or c) 1 hour of EGA, 1 hour of cell recovery and 5 hours of BCF C- (60X magnification; bar, 10 µm).

Taking into account the ability of CHL to develop vacuoles similar to those VacA-induced, and that NRU reported that EGA abolish the CHL-induced vacuoles, we decided to replicate the AO experiment in CHL-treated Hela cells.

Cells treated with CHL for 5 hours developed vacuoles similar to those VacA-induced, even if smaller and much abundant, since that CHL does not needs to traffic inside the cell but diffuse spontaneously to the acidic compartments. AO stained the vacuoles, similar to those induced by VacA, with a red brilliant fluorescence (Figure 46b).

In cell preincubated with EGA for 1 hour, the CHL-induced vacuolization was abolished (Figure 46c). In addition, in cells preincubated with EGA for 1 hour, allowed to recover for the same time and then CHL treated (Figure 46d) the vacuolization was not visible. The same result was obtained with NRU analysis and no statically significant variation were found among the two conditions (Figure 46). Moreover, in both conditions, the one which recovered and the other which did not recovered, the acidic compartments were marked with AO staining comparable to the control left EGA-free (Figure 46b and c compared to Figure 46a).

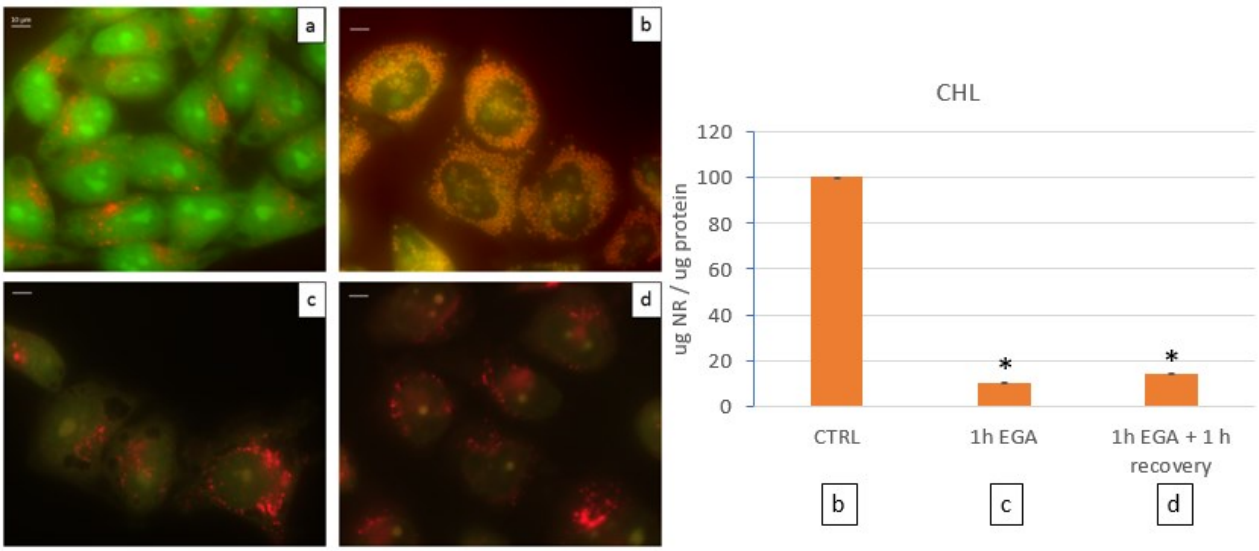

*Figure 46. AO staining of cells a) left untreated or with b) 5 hours of CHL, c) 1 hour of EGA followed by 5 hours of CHL or c) 1 hour of EGA, 1 hour of recovery and 5 hours of CHL (60X magnification; bar, 10 µm). Right panel shows NRU analysis performed 5 hours after the same treatment. Data are expressed as rate of the corresponding control. * = p < 0.05.*

Endosomal analysis

Considering the possibility that EGA could alter the maturation of EEs into LEs, we quantified their two markers respectively EEA1 and Rab7, in cells preincubated with EGA in combination with different treatment or recovery period.

We analyzed cells untreated as a control, preincubated for 1 hour with EGA, preincubated with EGA and allowed to recover for 1 hour or for 16 hours, incubated with BCF C- for 16 hours or preincubated with EGA for 1 hour and treated with BCF C- for 16 hours.

At the end of every treatments, cells were washed with washing buffer and lysate on ice for 30 minutes. Then samples were centrifugate, measured and diluted in SDS buffer. The protein concentration was determined using colorimetric assay and 50 µg of proteins were separated to SDS-PAGE and immunoblotting with anti-EEA1 and anti-Rab7 antibody and detected with enhanced chemiluminescence technique (Figure 47a).

Quantification (Figure 47b) of the two markers revealed that EEA1 was increased when EGA was added inside the medium instead Rab7 was reduced, even though these results were not statistic significant. When cells were allowed to fully recover (as for 1-hour EGA preincubation treatment followed by 16 hours of cell recovery) quantification of both markers were comparable to the control. In cells preincubated with EGA and then treated with 16 hours of BCF C-, vacuoles were not developed but the level of EEA1 was comparable to the control instead Rab7 was slightly reduced.

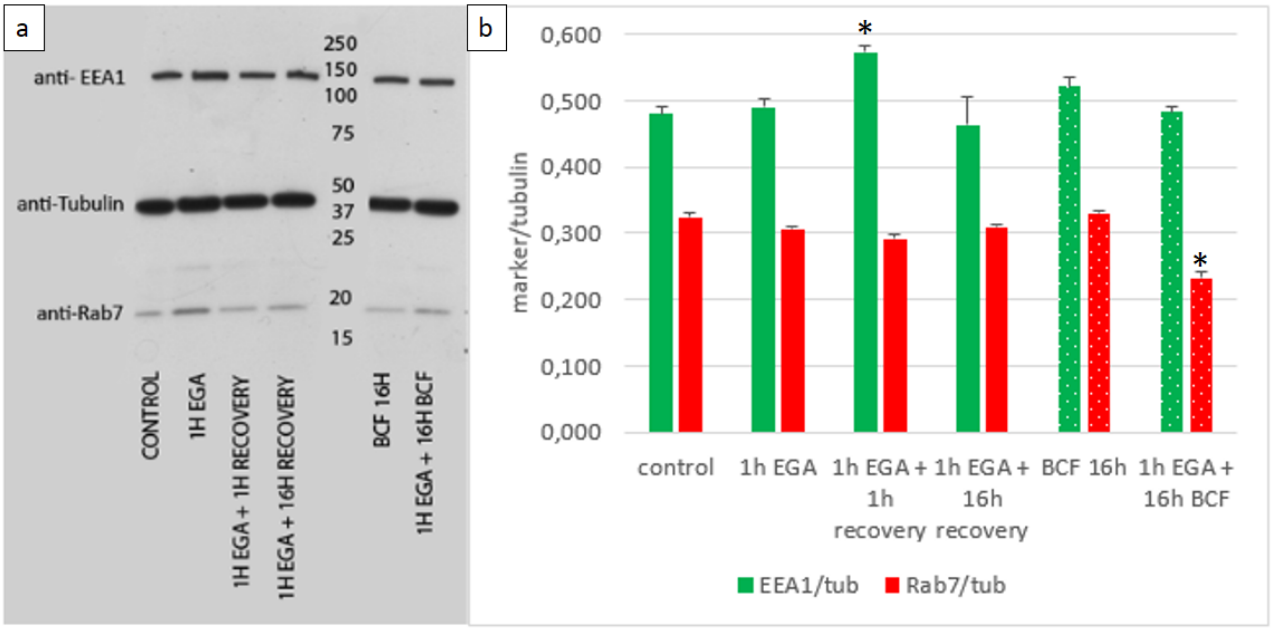

*Figure 47. a) Immunoblot anti-EEA1, tubulin and Rab7 of samples treated with EGA and controls. b) Quantification of EEA1 and Rab7 related to corresponding tubulin. The dot bar identifies the samples treated with BCF C- for 16 hours. * = p < 0.05. Green: EEA1/tubulin, Red: Rab7/tubulin.*

Time course analysis

Protocol development and CTxB analysis

In order to investigate the intracellular trafficking of VacA and EGA effect on toxin movement inside cells, we first focused our attention on transport analysis.

Considering that CTx and VacA have some structural similarities and that CTxB is an entasblished tool to study intracellular trafficking (Cho et al., 2012; Guimaraes et al., 2011; Matsudaira et al., 2015), we used CTxB-Alexa555 to develop a reliable incubation protocol and as a comparison on VacA intracellular trafficking. CTxB-Alexa555 was used by several groups to study, for istance, endocytic pathway (Dang et al., 2012; Howes et al., 2010), the properties of cholesterol-dependent domains (Gaus et al., 2006) and CTx internalization and trafficking (Blagojevi et al., 2008; Day & Kenworthy, 2012).

We tried two different kind of approach: the pulse-and-chase and the binding-on-ice protocol.

The first protocol requires a short incubation time with the compound (pulse) then, cells were washed abundantly, and the intracellular trafficking was study throughout IF analysis after an established period of internalization (chase).

As the name suggests, the binding-on-ice protocol require a preincubation time on ice. Endocytosis, which is a temperature-dependent process, is blocked during the toxin incubation step, while it is

possible to saturate the binding sites for the toxin receptors at the PM (Todar, 2009). Once cells are removed from ice, washed copiously to discard unbound ligand and put again at 37°C, the endocytosis is reactivated, and ligand starts entering the cell. At the end of the incubation cells are fixed, permeabilized, and stained for markers: Golgin97 for TGN, Giantin for Cis-Golgi and Calnexin AF18 as ER marker.

Firstly, HeLa cells were intoxicated with CTxB-Alexa555 in a pulse-and-chase protocol. Cells were washed with warmed HBSS, place at 37°C for 45 minutes then the toxin was added and intoxication was promoted for 30 minutes. At the end of the period, cells were washed with warm medium and incubation was promoted for short period of time (1 hour) or long-time period (5 hours). In both time point analysis, cells were preincubated with HBSS and then moved to complete medium, because Golgi analysis revealed sign of distress, showed as alteration of morphology with both markers (Figure 48-1b and 2b) when incubated with HBSS for longer period of time. Instead preincubation time with HBSS and intoxication time with complete medium revealed a Golgi structure (Figure 48-1c and 2c) comparable to the control HBSS untreated (Figure 48-1a and 2a).

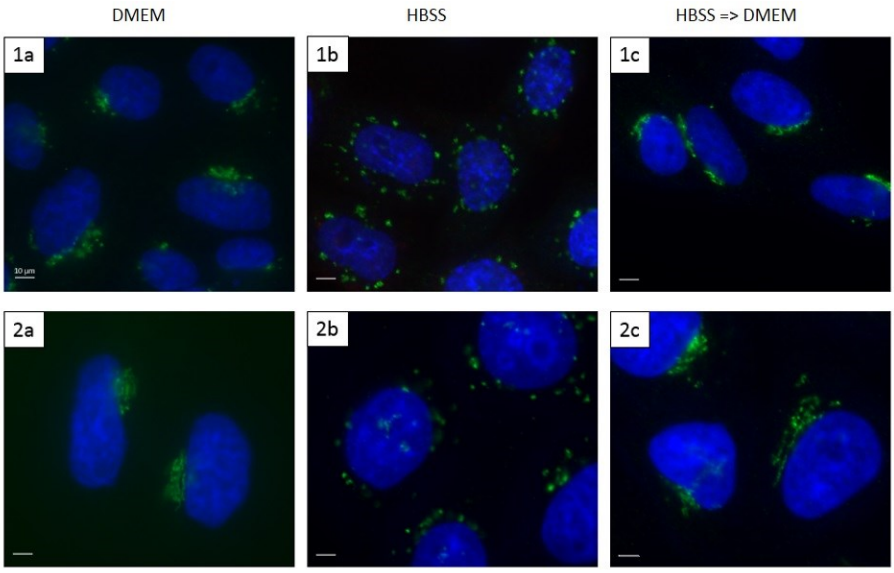

Figure 48. Hela cells incubated with a) complete medium b) HBSS for all the experiment or c) preincubated with HBSS and then moved to complete medium. IF performed after 4 hours of internalization. In green 1) TGN b) Cis-Golgi. 60X magnification (bar, 10 µm). Nuclei are depicted in blue.

We founded that only a small rate of CTxB was internalized and later moved from the TGN to the ER in a 5 hours time analysis. For this reason, the analysis performed on the colocalizations between the organelles and CTxB, showed a low number of points of colocalization and a low number of cells marked.

Next we investigated the binding-on-ice approach. Cells were washed with cold HBSS and placed on ice at 4°C for 45 minutes, then the toxin was added and binding was allowed for 30 minutes still on ice. At the end of the binding period, cells were washed with warm medium and place again at 37°C for 1 hour or 5 hours internalization, after which IF was performed.

The binding-on-ice protocol showed an increase of colocalization points between CTxB and organelles (Figure 49), compared to the pulse-and-chase approach.

As for the TGN, when analyzed in the two time points, we noticed a reduction of approximately 50% of the number of cells which had at least one point of colocalization and an equal reduction in the number of colocalization, of approximately a point for cell (1 hour versus 5 hours).

Regarding the cis-Golgi analysis, the number of cells with at least one point of colocalization at 1 hour was further reduced at 5 hours (from 33% of cells with at least one point to 24%).

ER colocalization showed the presence of the toxin in ER of virtually all cells analyzed (92% cells marked) after 1 hour, which reduces to 62% cells marked at 5 hours analysis. The average number of points for the totality of the examined cells showed a reduction of about one third: analysis at 1 hour revealed an avarage number of coholocalization for cell of about 1,29 for TGN, 0,44 for Cis-Golgi and ER 6,43 futher reducing at 5 hour analysis 0,52, 1,03 and 2,44 respectively (total number of cell counted 100/condition).

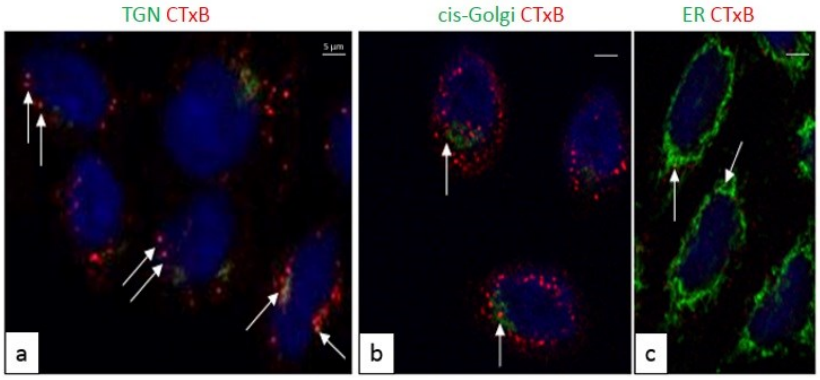

Figure 49. Binding-on-ice intoxication of cells with CTxB-Alexa555 (red). IF performed after 1 hour of internalization. In green a) TGN, b) Cis-Golgi and c) ER. White arrows enhanced colocalization points. 60X magnification (bar, 5 µm), nuclei are depicted in blue.

To further investigate the data obtained with binding-on-ice protocol we treated cells with BFA, which is a fungal metabolite produced by *Eupenicillium brefeldianum*, which interferes with anterograde transport by disrupting the Golgi apparatus. When the Golgi structure collapse, all the

Golgi components redistribute into the ER or the cytoplasm, which are not altered by BFA (Doms et al., 1989; Ito et al., 2012; Ward et al., 2001).

Cell treated with BFA throughout the experiment, showed a complete disassembly of Golgi apparatus (Figure 50-2a and 2b) but the toxin can successful reach the ER (Figure 50-2d), which was morphologically unaltered. The analysis on the effect of BFA on CTxB trafficking showed that, at Golgi level, the trafficking is greatly altered while the percentage of cells showing at least one point of colocalization in ER level remains stable at 1 hour, even if the average number of colocalizations per cells is reduced.

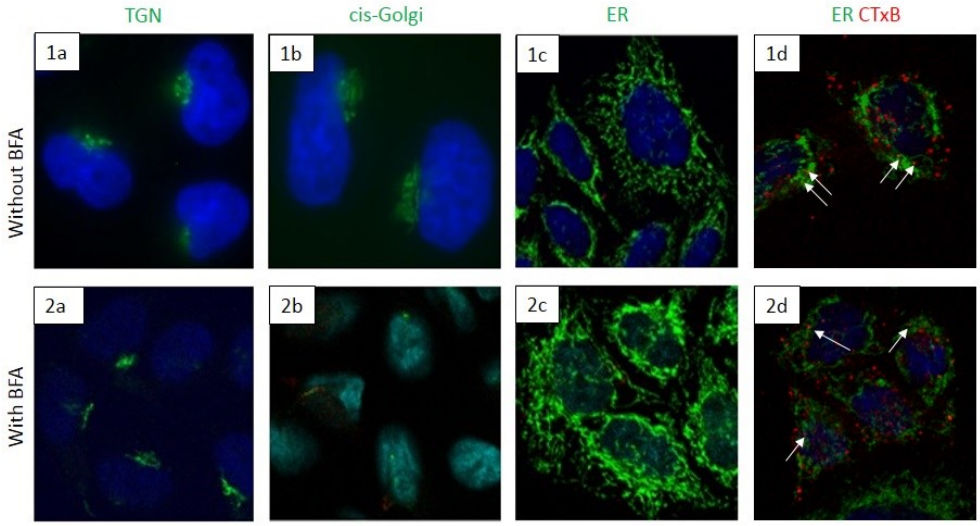

Figure 50. Cells treated with BFA (2) compared to the control (1). In green a) TGN, b) Cis-Golgi, c and d) ER. d) CTxB-Alexa 555 (red) was added to cells with binding-on-ice protocol and white arrows enhanced colocalization points with ER (green). IF was performed after 1 hour of internalization60X magnification (bar, 5 µm), nuclei are depicted in blue.

VacA trafficking inside the cell

We used the same two approaches for VacA trafficking analysis, even though we analyzed cells at 30 minutes versus 1 hour, considering the different time-dependent trafficking of VacA. We used acid activated purified and concentrated VacA previously prepared to exclude any interference from other BCF components. Furthermore, since that FBS could affect VacA trafficking, we used medium supplemented only with glutamine (thus without FBS) for all the experiment. Golgi morphology analysis (Figure 51) revealed no alteration comparing to complete medium.

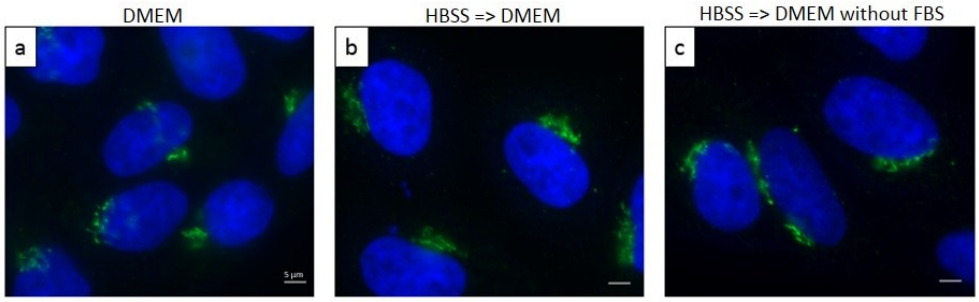

Figure 51. Hela cells incubated with a) complete medium or preincubated with b) HBSS and then moved to b) complete medium or c) medium supplemented only with glutamine. IF performed after 4 hours of internalization (TGN, green; nuclei, blue). 60X magnification (bar, 5 µm).

Trafficking analysis was performed investigating VacA colocalization with transient transfected mitochondria or with IF analysis of TGN, Cis-Golgi or ER.

The analysis with the pulse-and-chase protocol used for CTxB-Alexa555 with VacA pulse at 37°C, revealed that toxin amount which was able to reach intracellular environment was very small compared with VacA volume added. For this reason, we obtained a low number of points of colocalization with all markers.

Instead the binding-on-ice protocol analyzed at two-time points (30 minutes versus 1h) suggested a retrograde movement from TGN to ER, analogous to other bacterial toxins as CTxB. This type of trafficking was supported by an increase of number of colocalizations per cell from TGN to ER (Figure 52).

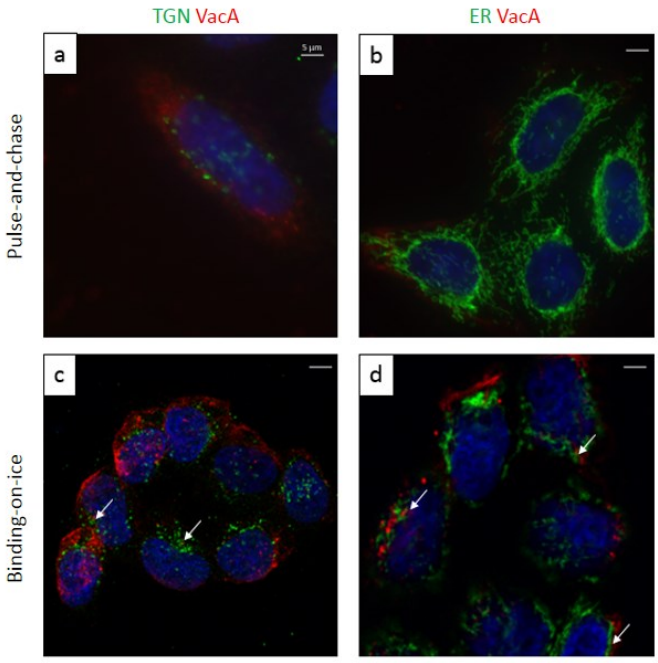

Figure 52. Pulse-and-chase (a, b) versus binding-on-ice (c, d) protocol of intoxication of Hela cells with VacA (red). IF performed after 1 hour of internalization. In green a, c) TGN b, d) ER. White arrows enhanced colocalization points. 60X magnification (bar, 5 µm), nuclei are depicted in blue.

Starting from these preliminary data and considering EGA effects on vacuolization, we next analyzed EGA ability to induce alterations in VacA internalization and trafficking.

Considering the effects of other inhibitors on organelles morphology and structure, we first analyzed EGA related morphological changes. IF analysis of the different organelles (TGN, Golgi, ER, LEs) revealed that EGA did not altered their structure (data not shown).

Then, we analyzed EGA ability to alter VacA binding. We used binding-on-ice protocol as for the internalization, but cells were fixed right after binding period. EGA was added to cells 1 hour before the intoxication and was maintained throughout the experiment.

IF analysis performed with confocal microscopy revealed that VacA amount allowed to bind in presence of EGA (Figure 53-b) was comparable to the control EGA-free (Figure 53-a). Besides, VacA amount per cell detectable was comparable in both conditions.

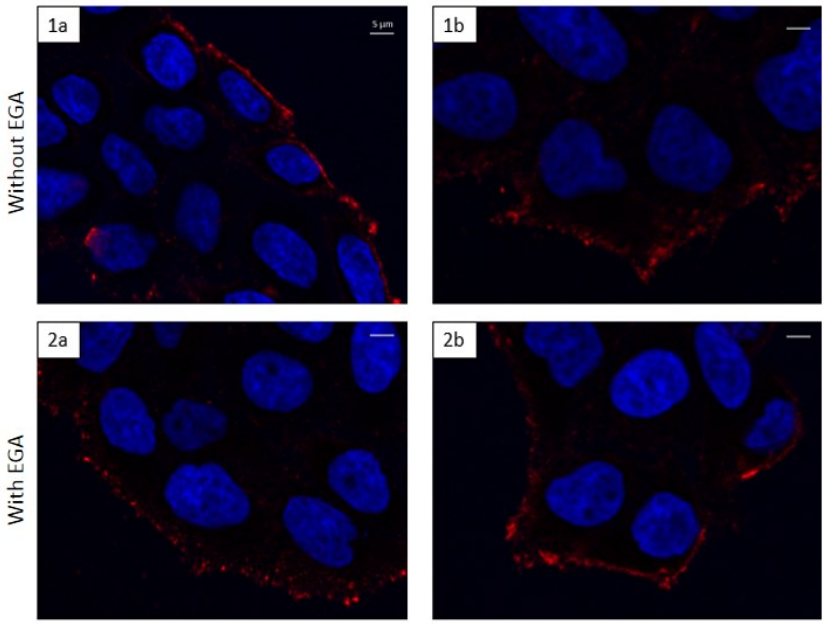

Figure 53. Binding on the PM of VacA (red) in control (1) or in presence of EGA (2). 60X magnification (bar, 5 µm), nuclei are depicted in blue.

The intracellular trafficking analysis in cell treated with EGA showed an increase in colocalization point at 4 hours with ER and mitochondria and, on the contrary, a reduction of colocalization with Golgi apparatus and slightly with LEs (Figure 54).

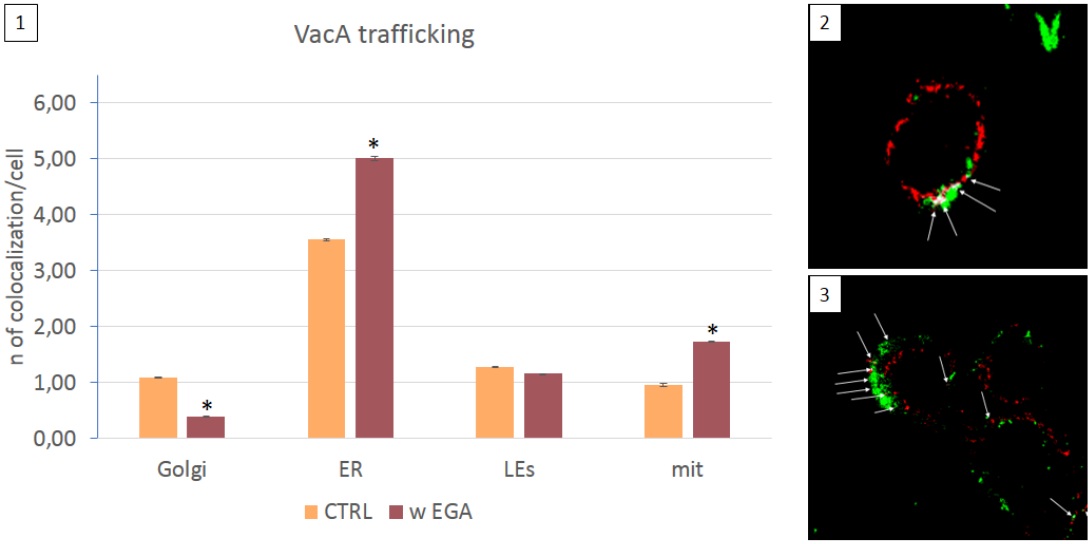

*Figure 54. Colocalization analysis of VacA trafficking in cell treated with EGA. Data are expressed as rate of number of colocalization per cell. * = p < 0.05. Example of colocalization mask obtained to quantify the colocalization between VacA (green) and mitochondria (2 red) or ER (3 red).*

DISCUSSION

Inclusion bodies are typical of many pathological conditions, such as neurodegenerative, muscular and liver disorder (Kopito, 2000). They are likely to have a role in the induction of the disease, but their origin before leading to the development of explicit symptoms has not yet been clarified. PaCSs are newly identified cytoplasmic structures, ubiquitin and proteasome enriched, that are candidate as a starting or intermediate step in aggregates development (Solcia et al., 2014). Considering the importance of intracellular trafficking and a correct processing for cellular physiology (Tokarev et al., 2009), we investigated the differences and similarity between PaCSs and other three aggregates (LBs, JUNQs and IPODs).

Our data indicated that PaCSs and LBs are different intracellular inclusions, even if they both share characteristic glycogen and laforin antibodies positivity. Moreover, these results suggest that areas in which LBs are present are marked in the same way in mice of different ages, but the amount of laforin present is proportional to age (e.g. younger mice shown less deposit). This would explain the consequent increase in symptoms related to enlarged deposition of laforin or malin. Considering the possibility that LBs could be the outcome of the evolution of other bodies, such as PaCSs, it could be helpful to analyze mice younger than 7 weeks to better understand their development.

As regard the existence of a relationship between PaCS and JUNQ or IPOD, we were able to reproduce both JUNQ and IPOD in HEK and Hela cells and analyzed them throughout ICC and TEM. Even if these aggregates share some features and components (as polyubiquitinated proteins or proteasome systems) our results indicate that PaCSs are different from all structures analyzed, considering overall ultrastructural and immunoreactivity characteristics. Regarding the localization in ICC analysis of the antibody 20S and FK1 in IPOD-transfected HeLa cells, which marks the edge of the aggregate, it could be due to a permeabilization problem, which does not allow the antibody to mark IPOD inside, or it could be effectively stained only the border.

Aggregates-transfected HeLa cells, which in physiological condition constitutively express PaCSs, analyzed throughout TEM showed the absence of this type of aggregate: no PaCSs were detected inside the cells showing IPOD and/or JUNQ. Moreover, the analysis of consecutive semithin fixed resin sections revealed that cells which have PaCSs do not have IPOD and vice-versa. This seems to indicate that these aggregates are mutually exclusive. We can speculate that it could be due to an alteration following the development of the transfected-induce aggregates, due to their disappearance or may not be linked. Moreover, considering the common functions of aggregates inside cytoplasm (i.e. misfolded proteins and component sequestration) and their potential toxicity,

it could be due to cell response to stressor without wasting of energy by forming aggregates with the same function or to limit possible cytotoxic risks.

Considering that inside PaCSs, bacterium products such as VacA are accumulated together with polyubiquitin proteins and proteasome components (Necchi et al., 2010), we investigated the possibility that VacA could be ubiquitinated before being accumulated inside PaCSs. VacA ubiquitination could be a tool of the cell to prevent its cytotoxic effects or to block its vacuolation action.

We investigated VacA level of ubiquitination using His-Ub-VacA and metal affinity purification following the protocol developed by Doye and colleagues (Doye et al., 2012). In order to enhance the amount of His-Ub-VacA inside cells, it was necessary to treat cells with a proteasome inhibitor: to this purpose we added MG132 (20 μM) 6 hours before lysis, which blocks the proteasomal degradation of polyubiquitinated proteins.

By immunoblot analysis with anti-VacA specific antibody, we identified two VacA-reactive bands in His-Ub tagged proteins sample. These two bands (distinguishable between 50 and 75 kDa) were lower that the classical molecular mass of mature VacA monomer (88 kDa). We can speculate that cells are able to proteolytic cleavage VacA, or maybe, that only one part of the mature VacA is allowed to escape vesicular compartments and reach its still unknown target. Other bacterial toxins use their B subunit to translocate into cell or its cytoplasm and reach the final target only with A subunit (Eierhoff et al., 2012; London, 1992; Sandvig et al., 2004). This would also support the idea that VacA represents the prototype of a new class (considering its pore forming function) of AB toxins (Boquet & Ricci, 2012). Moreover, we can also suppose that VacA inside cytoplasm is cleaved and/or ubiquitinated as a protective mechanism or under stresses condition, as suggested by the results obtained with MG132 treatment. It still needed to be investigate, how VacA reaches cytosol, possibly exploit ERAD pathway as suggested by the finding of Kern and colleagues which demonstrated that VacA, as CTxA1, colocalize with Sec61p system which is responsible for retro-translocation into the cytosol (Kern et al., 2015) and if cells intoxicated with the bacterium for different period (acute versus chronic intoxication) react as BCF treated cells.

Then we investigated the effect of trafficking inhibitor on VacA action. VacA-induced vacuolization is promoted by the toxin once its reach LEs (Papini et al., 1994) and for this reason, the toxin takes advantage of the endosomal system inside the cells. These inhibitors could prevent or reduce VacA

effect by blocking toxin trafficking inside cells at different steps. The commercial inhibitors used: BFA that blocks the anterograde transport (Barbier et al., 2012) and Retro-1 and 2 which are inhibitors of the retrograde transport between EEs and LEs (Park et al., 2012; Yang et al., 2016). Another commercial inhibitor used was EGA, effective on other toxins, never tested on VacA and with an unknown mechanism of action (Azarnia Tehran et al., 2015; Dixon et al., 2015; Gillespie et al., 2013; Schnell A, 2016; Schnell B, 2016; Slater et al., 2014). Other four inhibitors used (Ha-432 or Retro-1.1, Retro-2 cyclic, RN-3-122 or Retro-2.1 and Compound 20) were new experimental inhibitors.

This part of the study was carry out using NRU assay. Neutral red dye is a membrane-permeable weak base which accumulate inside vacuoles and NRU is a well-accepted methods for quantification of VacA activity (Cover et al., 1992; de Bernard et al., 1997; Ricci et al., 2002; Sun et al., 2010). We first tested inhibitors effect on early vacuolization (5 hours) and long-term BCF VacA^{+} action (o/n treatment). Furthermore, we evaluated their effect also on cells left untreated, cells treated with NH_4Cl, a weak base which induced mildly vacuolization, and cells treated with CHL, a lysosomotropic agent able to accumulate inside acidic organelles and promote the development of vacuoles similar to those VacA-induced (Hiruma & Kawakami, 2011). The main result from these first experiments was that, among the different inhibitors, EGA was able to virtually abolish VacA-induced vacuolization in both intoxication period. It was a prominent effect confirmed also in light microscopy: cells showed an almost absence of vacuoles without any sign of distresses correlated, even after 24 hours of BCF treatment.

Other inhibitors (such as Retro-1, Retro-2 cyclic and Compound 20) were able to reduce VacA effects in short and long-term treatment, suggesting that they are able to alter VacA accumulation inside endosome. Moreover, other inhibitors, like BFA, did not induced any significant variation on VacA action, even if their effect on other toxins, such as STx, is documented in the literature (Spooner et al., 2008). It could be due to an action at post-endosomal level of trafficking or the toxin could follow other pathways for endosomal accumulation, as the retrograde transport insensible to these kinds of inhibitors. There might be two or more parallel pathways exploited by VacA, depending on the amount of toxin which is internalized by the cell, as for other toxin such as CTx (Johannes & Popoff, 2008; Todar, 2009).

Considering the prominent effect of EGA on VacA-induced vacuoles, we evaluated its effect on CHL-induced vacuolation. CHL is a weak base which accumulates inside endosome, where it become protonated, increases osmotic pressure and promotes the development of vacuoles (Alvarez &

Sztul, 1999). Also in this case EGA was able to virtually abolish CHL-induced vacuolization at 7 hours. This could be due to an alteration of pH EGA-promoted, already suggested by other groups (Schnell B, 2016).

Since that EGA maintained throughout the experiment blocks vacuoles, we tested EGA effect added at later stage of the experiment. We evaluated three conditions: NH_4Cl, CHL or BCF treatment for 5 hours and then EGA addiction for 2 hours. EGA was able to induce a reduction of vacuoles in all conditions, compared to the control at 7 hours, and for CHL and BCF treatment showed a statistical significant reduction greater than the control EGA-free at 5 hours. This could imply that EGA is able not only to promote the reversion of vacuoles already develop, but also that is able to reduce cytotoxic stress with a more pronounced effect. These results were also established using µ-Dish 35 mm with a glass bottom and an imprinted 500 µm relocation grid. Using this approach, it was possible to follow single cell before and after EGA treatment. Light microscopy analysis confirmed that EGA was able to promote regression of the vacuoles in a time-dependent manner, for both VacA and CHL treatment.

Moreover, light microscopy analysis showed that maintaining EGA throughout the experiment was redundant. In fact, a preincubation time with EGA for a range of time starting from 1 hour to 10 minutes followed by inhibitor washing out, revealed that EGA could efficiently block VacA-induced vacuolization, as found out on LTx by previously finding (Gillespie et al., 2013). Finally, we tested with a preincubation time on ice whether temperature could affect EGA efficiency: we detected no alteration on blocking effect compared to a control with a preincubation time at 37°C.

Supposing that EGA could interfere with pH, as suggested by the efficiency blocks of other pH-dependent toxins (Slater et al., 2014), and considering the importance of a physiological endosomal acidification for VacA action, we used AO staining to analyze acid compartments in cells treated with EGA. AO is a metachromatic dye which is accumulated inside acid compartments and is trapped due to protonation (Lovelace & Cahill, 2007; Pierzyska-Mach et al., 2014). When pH is altered or become basic, AO molecules undergo to deprotonation and are able to cross again the membrane.

Firstly, we compared preincubation time with EGA ranging from 1 hour to 10 minutes to control left untreated. In all these conditions AO staining revealed the complete absence of red marks, suggesting a possible alteration of pH inside acid compartments.

Then we stained with AO, Hela cells BCF C- treated for the same time as NRU analysis (5 hours and o/n treatment). AO staining of vacuoles was clearly identifiable by red circle occupying almost all

the cytoplasm. Instead, cells that were preincubated with EGA for 1 hours showed a complete absence of vacuoles, as indicated by light microscopy results, but in both conditions acidic compartments were stained as a control EGA and BCF-free.

Starting from these results, we speculated that EGA pH alteration effect could be reversible. To confirm this hypothesis, we treated cells for 1 hour with EGA, promoted cell recovery for the same period and then performed the intoxication with BCF C-. Even if acid compartments were comparable to the control, AO staining revealed that in cell treated with EGA and left recovered, vacuoles were not developed after 16 hours of BCF treatment. Moreover, NRU results revealed that there were no statically significant differences between cells that have recovered and cells in which recovery was not allowed. Moreover, the same scenario was obtained in cell treated with CHL.

Considering these results, we can speculate that EGA effects on pH and on vacuoles are distinct or maybe, that the recovery time was insufficient to allow a fully restoration of EGA-induced modification inside acidic compartments, thus blocking VacA-induced vacuolization. This scenario could also explain why EGA have the same action on cell treated with CHL, which is a weak base that does not follow intracellular traffic but diffuses spontaneously following the concentration of hydrogen ions. Our third hypothesis is that EGA could prevent VacA trafficking from EEs to LEs, thus preventing changes link to acid pH, such as oligomerization (necessary to induced vacuolization), as previously supposed for LTx by Gillespie and collaborators (Gillespie et al., 2013).

To investigate this later hypothesis, we evaluated if EGA could alter the maturation of endosomes, thus preventing VacA or CHL to reach LEs. To this purpose, we analyzed through immunoblot analysis the level of EEA1 and Rab7, respectively markers for EEs and LEs, in different conditions. We investigated cell untreated as a control, preincubated for 1 hour with EGA, preincubated with EGA and allowed to recover for 1 hour or for 16 hours, preincubated with EGA for 1 hour and treated with BCF C- for 16 hours and its control EGA free. Quantification of the two markers revealed that, EGA 1 hour preincubation determined an increase level of EEA1 instead Rab7 was reduced. When cells were allowed to fully recover (as for 16 hours period) quantification of both markers were comparable to the control. The results of both markers from the different conditions allowed to recover, seems to indicate that cells are able to restore the organelles component, as for pH, in a time-dependent manner. Regarding the two BCF conditions, we can speculate that, even if vacuoles are not developed, the intoxication may interfere with the cell recovery, as suggested by the lower Rab7 level compared to its control.

The endosomal network is a sorting and trafficking system: it is responsible for the transport of a wide variety of cargo molecules inside cells. The trafficking between endosome and the ER is crucial for the physiological cellular metabolism, but is also exploit by pathogens such as bacteria and viruses. For instance, CTx after internalization reaches the TGN and moves efficiently to ER thanks to its subunit B, even if the Golgi apparatus is disrupted by BFA (Orlandi et al., 1993). In a process called retro-translocation, the toxins take advantage of Sec61p to escape ERAD, crossing the ER membrane and reach cytosol (Feng et al., 2004). Supporting this kind of movement is also the findings of Raiborg and colleagues (Raiborg et al., 2016) which described the newly discovered juxtaposition of ER and endosome membranes. The fission between endosomes and the ER allows molecules flowing and it could be a pathway exploited by VacA as other toxins.

Considering the data obtained from EGA effect on VacA, the finding concerning the ER contacts with multiple membranes and exploring the possibility that VacA could follow also a retrograde intracellular trafficking (Kern et al., 2015), explaining besides why different inhibitors could not act on VacA vacuoles induction, we focused our attention on VacA intracellular trafficking. Furthermore, since that CTx is a well-known AB toxin, the structural similarities between CTx and VacA (Boquet & Ricci, 2012) and that CTxB is an established tool to study intracellular trafficking (Cho et al., 2012; Guimaraes et al., 2011; Matsudaira et al., 2015), we used CTxB fluorescent marked with Alexa Fluor 555 to develop a reliable incubation protocol and as comparison of VacA intracellular trafficking. Although these toxins are internalized by different mechanisms, they might reach the same endosomal compartment and might then both be transported to the TGN (Wernick et al., 2010).

We tried two different kind of approach: the pulse-and-chase and binding-on-ice protocol. The results from CTxB trafficking analysis were obtained with binding-on-ice, because the pulse-and-chase approach allowed to recognize only a small amount of the toxin compared to the totality added to cells. Indeed, the blocks of endocytosis promoted by cold intoxication, associated with saturation of PM receptors and CTxB subsequently entry following cell heating, allowed an improvement in the analysis of colocalization.

The analysis at two-time points (1 hour and 5 hours) of the CTxB movement showed a trafficking of the toxin from the TGN to the ER, with a peak of almost the totality of the cells labeled for at least one point of colocalization between ER and CTxB. These results are in agreement with those reported in literature (Blagojevi et al., 2008; Feng et al., 2004). Moreover, cells treated with BFA, maintained throughout the experiment, showed a complete disassembly of the Golgi apparatus, visible as a morphological structure and as lower number of points of colocalization between the

Golgi and CTxB. CTxB was able to reach successfully ER, which is not affected by BFA and showed no alteration in its structure and in number of points of colocalization with the toxin. These data confirm what is reported in the literature by Ward and colleagues (Ward et al., 2001).

Starting from these results we analyzed VacA trafficking. The preliminary data obtained from the study of VacA trafficking with the same approaches, showed a higher number of cells with at least one point of colocalization with the binding-on-ice protocol compared to the pulse-and-chase approach, as for CTxB. This could be explained as for CTxB, considering the block of endocytosis as a result of incubation on ice which allows toxin saturation of membrane receptors and a subsequent single flow wave once cells are heated.

Furthermore, the total colocalization and the number of cells which showed at least one point of colocalization seems to suggest a retrograde movement from the TGN to ER, analogous to the trafficking of other bacterial toxins (McKenzie et al., 2009; Saimani & Kim, 2017), with a progressive increase of ER number of colocalizations per cell. This finding is in agreement with the results of Kern and colleagues, showing a possible trafficking of VacA to the ER, and also consistent with the data indicating that toxin can affect intracellular calcium signaling (Kern et al., 2015). This important role played by VacA allowed the toxin to disrupt T-cell activation and proliferation, therefore altering immune system response against the infection. VacA effect on calcium signaling level could be crucial for successful chronic colonization of the host's stomach (Foegeding et al., 2016).

Taking into account of VacA trafficking results, we next investigated whether EGA alterations of VacA-induced vacuolization were related to the toxin endocytosis and/or trafficking inside the cell. To this purpose, we firstly investigate EGA effect on VacA binding. Considering the results which showed that EGA effects was not affected by temperature, we used binding-on-ice protocol combined to a preincubation time with EGA and subsequently fixing cell after binding period, to evaluate the binding efficiency in cell EGA-free and in cell treated. Data showed that VacA amount allowed to bind in presence of EGA was comparable to the control left untreated, supporting the idea that EGA does not interfere with this primary step of intoxication, as for other toxins (Schnell B, 2016).

Then, considering the possibility that EGA blocks of vacuolization was related to the toxin inability to reach LEs, we analyzed intracellular trafficking at 4 hours in presence of preincubation time with EGA or n control cells. Our results showed an increase colocalization points per cell with ER and

mitochondria compared to the control EGA-free and a reduction with Golgi apparatus and LEs. A reduced number of colocalization points, which could correspond to a lower concentration of VacA inside LEs, could suggests that EGA promote VacA relocation to other organelles or to the cytoplasm, and could also explained the reduced vacuolization which NRU showed.

Taking together our results confirmed that EGA ability to block the effects of different toxins (Azarnia Tehran et al., 2015; Dixon et al., 2015; Gillespie et al., 2013; Schnell A, 2016; Schnell B, 2016; Slater et al., 2014) can also include VacA-induced vacuolization and maybe also its other cytotoxic effects.

CONCLUSION

In conclusion, this work elucidates several characteristics of the intracellular trafficking and processing of proteins inside human cells.

Firstly, we demonstrated that the newly described PaCS and three other aggregates (LB, JUNQ, IPOD) are different inclusions even if they share some similar positives and components. It still needed to be evaluate if LBs could developed from PaCSs. Moreover, they were not identifiable after plasmid trasfection of aggregation-prone proteins in cells where are constitutively present, suggesting that cells are able to express either PaCS or JUNQ or/and IPOD. It should be considered the possibility that this alteration could be a cell tool to avoid excessive aggregation of components in different areas of the cytoplasm (i.e. polyubiquitinated proteins inside PaCSs and JUNQ) or to reduce cytotoxic consequences. Further, it still needed to be investigated whether and how PaCSs components could be redistributed into other aggregates or are somehow eliminated.

Since that inside PaCSs of Hp-infected patients, VacA was found together with polyubiquitin proteins and proteasome components, we next evaluate if VacA is ubiquitinated inside cells. Our results suggest that a certain amount of VacA is ubiquitinated inside cell, supporting the idea that vacuoles are only an intermediate step of the toxin action supporting the idea that the toxin could escape ERAD and reach the cytoplasm where it could be ubiquitinated, to prevent its cytotoxic effect and promote degradation, and maybe later accumulated inside PaCSs.

Focusing our attention on VacA action we analyzed the effect of eight different trafficking inhibitors. Even though some of them were able to promote a statistical significant reduction of VacA-induced vacuolization, the prominent effect was performed by EGA (Figure 55), which virtually abolished the toxin activity in all experiments.

EGA is a newly studied inhibitor with a powerful effect on several toxins, which belongs to the AB family of toxins. VacA is key factor of Hp successful intoxication, and considering its structure, it has been suggested that VacA could represents the prototype of a new class of AB toxins (Boquet & Ricci, 2012). This hypothesis is supported by EGA protective effect developed on AB toxins and VacA intoxicated cells. Following this scenario and considering our results, we can speculate that EGA effects on vacuolation could be related to modification of oligomers assembly or EGA preventing VacA to access acidified endosomes, as supposed by Gillespie for LTx (Gillespie et al., 2013).

Moreover, our data suggest that EGA was able to reduce VacA-induced vacuolization on cells in which the vacuolization was already developed. This could be due to its pH-alteration ability or could be a relocation effects of VacA consequently to EGA treatment. Our results showed also that, in cells

where EGA was washed out and cells allowed to recover, acid compartments were stained in a comparable manner as the control, suggesting a reversible effect on pH. This could explained why Gillespie and colleagues did not find out any alteration in acid organelles pH when analyzed cell treated with EGA with a fluorescent lysotracker dye (Gillespie et al., 2013).

Additionally, our results with binding-on-ice approach support the idea that VacA can exploit the retrograde movement to reach ER and that EGA can alter the toxin trafficking, preventing VacA to reach LEs and relocated the toxin to other organelles. Considering the results on EGA's pH reversible effect and the persistent blocks of vacuolization even after cell recovery, we can speculate that these two effects are distinct. Moreover, since that EGA could also blocks CHL-induced vacuolization, further studies are needed to understand the exact EGA target and mechanisms of action, but its characteristic and effect on different toxins associated with a low toxicity in mouse model (Azarnia Tehran et al., 2015) make it look like a potent inhibitor and interesting tool to develop a therapeutics strategy against bacterial toxins.

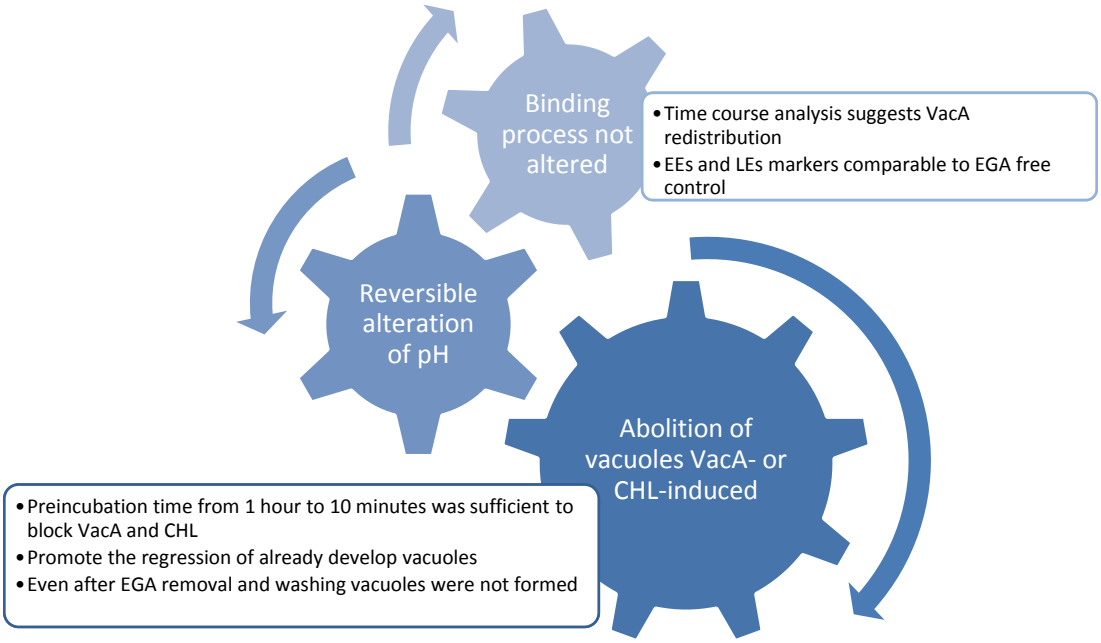

Figure 55. Summary of EGA effects elucidated by this study.

BIBLIOGRAPHY

Ahn, H. J., & Lee, D. S. (2015). Helicobacter pylori in gastric carcinogenesis. *World Journal of Gastrointestinal Oncology*, *7*(12), 455–65.

Akada, J. K., Aoki, H., Torigoe, Y., Kitagawa, T., Kurazono, H., Hoshida, H., Nishikawa, J., Terai, S., Matsuzaki, M., Hirayama, T., Nakazawa, T., Akada, R., & Nakamura, K. (2010). Helicobacter pylori CagA inhibits endocytosis of cytotoxin VacA in host cells. *Disease Models & Mechanisms*, *3*(9–10), 605–17.

Alberts, B., Johnson, A., Lewis, J., Raff, M., Roberts, K., & Walter, P. (2005). *Molecular Biology of the Cell* (Vol. 2410).

Alvarez-Miranda, E. A., Sinnl, M., & Farhan, H. (2015). Alteration of Golgi structure by stress: A link to neurodegeneration? *Frontiers in Neuroscience*, *9*(435), 1–13.

Alvarez, C., & Sztul, E. S. (1999). Brefeldin A (BFA) disrupts the organization of the microtubule and the actin cytoskeletons. *European Journal of Cell Biology*, *78*(1), 1–14.

Amen, T., & Kaganovich, D. (2015). Dynamic droplets: The role of cytoplasmic inclusions in stress, function, and disease. *Cellular and Molecular Life Sciences*, *72*(3), 401–415.

Amieva, M. R., & El-Omar, E. M. (2008). Host-Bacterial Interactions in Helicobacter pylori Infection. *Gastroenterology*, *134*(1), 306–323.

Argent, R. H., Thomas, R. J., Letley, D. P., Rittig, M. G., Hardie, K. R., & Atherton, J. C. (2008). Functional association between the Helicobacter pylori virulence factors VacA and CagA. *Journal of Medical Microbiology*, *57*(2), 145–150.

Atherton, J. C. (2006). The pathogenesis of Helicobacter pylori- induced gastroduodenal diseases. *Annual Review of Pathology: Mechanisms of Disease*, *1*(1), 63–96.

Azarnia Tehran, D., Zanetti, G., Leka, O., Lista, F., Fillo, S., Binz, T., Shone, C. C., Rossetto, O., Montecucco, C., Paradisi, C., Mattarei, A., & Pirazzini, M. (2015). A Novel Inhibitor Prevents the Peripheral Neuroparalysis of Botulinum Neurotoxins. *Scientific Reports*, *5*, 17513.

Backert, S., & Tegtmeyer, N. (2010). The versatility of the Helicobacter pylori vacuolating cytotoxin VacA in signal transduction and molecular crosstalk. *Toxins*, *2*(1), 69–92.

Bagola, K., & Sommer, T. (2008). Protein Quality Control: On IPODs and Other JUNQ. *Current Biology*, *18*(21), 1019–1021.

Bannykh, S. I., Nishimura, N., & Balch, W. E. (1998). Getting into the Golgi. *Trends in Cell Biology*, *8*(1), 21–25.

Barbier, J., Bouclier, C., Johannes, L., & Gillet, D. (2012). Inhibitors of the cellular trafficking of ricin. *Toxins*, *4*(1), 15–27.

Bersuker, K., Hipp, M. S., Calamini, B., Morimoto, R. I., & Kopito, R. R. (2013). Heat shock response activation exacerbates inclusion body formation in a cellular model of huntington disease. *Journal of Biological Chemistry*, *288*(33), 23633–23638.

Bharati, K., & Ganguly, N. K. (2011). Cholera toxin : A paradigm of a multifunctional protein Cholera toxin: an historical introduction. *Indian Journal Of Medical Research*, *133*(2), 179–187.

Blagojevi, G., Mahmutefendi, H., Ku, N., Toma, M. I., & Lu, P. (2008). Endocytic Trafficking of Cholera Toxin in Balb 3T3 Cells. *Croatica Chemica Acta*, *81*(1), 8–10.

Blaser, M. J., & Atherton, J. C. (2004). Helicobacter pylori persistence: Biology and disease. *Journal*

of Clinical Investigation, *113*(3), 321–333.

Boquet, P., & Ricci, V. (2012). Intoxication strategy of Helicobacter pylori VacA toxin. *Trends in Microbiology*, *20*(4), 165–174.

Boquet, P., & Ricci, V. (2014). Bacterial Exotoxins. *Reference Module in Biomedical Sciences* (Third Edit). Elsevier.

Boquet, P., Ricci, V., Galmiche, A., & Gauthier, N. C. (2003). Gastric cell apoptosis and H. pylori: has the main function of VacA finally been identified? *Trends in Microbiology*, *11*(9), 408–410.

Calore, F., Genisset, C., Casellato, A., Rossato, M., Codolo, G., Scorrano, L., & Bernard, M. De. (2010). Endosome–mitochondria juxtaposition during apoptosis induced by H. pylori VacA. *Cell Death Differ*, *17*(11), 1707–1716.

Chan, E. C., Chen, K. T., & Lin, Y. L. (1996). Vacuolating toxin from Helicobacter pylori activates cellular signaling and pepsinogen secretion in human gastric adenocarcinoma cells. *FEBS Letters*, *399*(1–2), 127–130.

Chia, P. Z. C., Gunn, P., & Gleeson, P. A. (2013). Cargo trafficking between endosomes and the trans-Golgi network. *Histochemistry and Cell Biology*, *140*(3), 307–315.

Cho, J. A., Chinnapen, D. J.-F., Aamar, E., Welscher, Y. M. t., Lencer, W. I., & Massol, R. (2012). Insights on the trafficking and retro-translocation of glycosphingolipid-binding bacterial toxins. *Frontiers in Cellular and Infection Microbiology*, *2*, 1–6.

Chong, D. C., Paton, J. C., Thorpe, C. M., & Paton, A. W. (2008). Clathrin-dependent trafficking of subtilase cytotoxin, a novel AB5 toxin that targets the endoplasmic reticulum chaperone BiP. *Cellular Microbiology*, *10*(3), 795–806.

Chung, C., Olivares, A., Torres, E., Yilmaz, O., Cohen, H., & Perez-Perez, G. (2010). Diversity of VacA intermediate region among Helicobacter pylori strains from several regions of the world. *Journal of Clinical Microbiology*, *48*(3), 690–696.

Clemens, J., Shin, S., Sur, D., Nair, G. B., & Holmgren, J. (2011). New-generation vaccines against cholera. *Nature Reviews Gastroenterology & Hepatology*, *8*(12), 701–710.

Conner, S. D., & Schmid, S. L. (2003). Regulated portals of enrty into the cell. *Nature*, *422*(March), 37–43.

Correa, P., Piazuelo, M. B., & Camargo, M. C. (2004). The future of gastric cancer prevention. *Gastric Cancer*, *7*(1), 9–16.

Cover, T. L. (1998). An intracellular target for Helicobacter pylori vacuolating toxin. *Trends in Microbiology*, *6*(4), 127-8-9.

Cover, T. L., & Blanke, S. R. (2005). Helicobacter pylori VacA, a paradigm for toxin multifunctionality. *Nature Reviews. Microbiology*, *3*(4), 320–332.

Cover, T. L., Hanson, P. I., & Heuser, J. E. (1997). Acid-induced dissociation of VacA, the Helicobacter pylori vacuolating cytotoxin, reveals its pattern of assembly. *Journal of Cell Biology*, *138*(4), 759–769.

Cover, T. L., Tummuru, M. K. R., Cao, P., Thompson, S. A., & Blaser, M. J. (1994). Divergence of genetic sequences for the vacuolating cytotoxin among Helicobacter pylori strains. *Journal of Biological Chemistry*, *269*(14), 10566–10573.

Cover, T. L., Vaughn, S. G., Cao, P., & Blaser, M. J. (1992). Potentiation of Helicobacter pylori Vacuolating Toxin Activity by Nicotine and Other Weak Bases. *Oxford University Press*, *166*(5),

1073–1078.

Dang, P., Smythe, E., & Furley, J. W. (2012). TAG1 Regulates the Endocytic Trafficking and Signaling of the Semaphorin3A Receptor Complex. *Journal of Neuroscience*, *32*(30), 10370–10382.

Day, C. a., & Kenworthy, A. K. (2012). Mechanisms Underlying the Confined Diffusion of Cholera Toxin B-Subunit in Intact Cell Membranes. *PLoS ONE*, *7*(4), e34923.

de Bernard, M., Arico, B., Papini, E., Rizzuto, R., Grandi, G., Rappuoli, R., & Montecucco, C. (1997). Helicobacter pylori toxin VacA induces vacuole formation by acting in the cell cytosol. *Molecular Microbiology*, *26*(4), 665–674.

De Bernard, M., Burroni, D., Papini, E., Rappuoli, R., Telford, J., & Montecucco, C. (1998). Identification of the Helicobacter pylori VacA toxin domain active in the cell cytosol. *Infection and Immunity*, *66*(12), 6014–6016.

Dixon, S. D., Huynh, M. M., Tamilselvam, B., Spiegelman, L. M., Son, S. B., Eshraghi, A., Blanke, S. R., & Bradley, K. A. (2015). Distinct roles for CdtA and CdtC during intoxication by cytolethal distending toxins. *PLoS ONE*, *10*(11), 1–16.

Djekic, A., & Müller, A. (2016). Review the immunomodulator vaca promotes immune tolerance and persistent helicobacter pylori infection through its activities on T-cells and antigen-presenting cells. *Toxins*, *8*(6), 1–9.

Doms, R. W., Russ, G., & Yewdell, J. W. (1989). Brefeldin A redistributes resident and itinerant Golgi proteins to the endoplasmic reticulum. *Journal of Cell Biology*, *109*(1), 61–72.

Doye, A., Mettouchi, A., & Lemichez, E. (2012). Assessing Ubiquitylation of Rho GTPases in Mammalian Cells. *Methods in Cell Biology*, *827*, 97–105.

Driouich, A., Zhang, G. F., & Staehelin, L. A. (1993). Effect of brefeldin A on the structure of the Golgi apparatus and on the synthesis and secretion of proteins and polysaccharides in sycamore maple (Acer pseudoplatanus) suspension-cultured cells. *Plant Physiology*, *101*(4), 1363–73.

Duran, J., Gruart, A., García-Rocha, M., Delgado-García, J. M., & Guinovart, J. J. (2014). Glycogen accumulation underlies neurodegeneration and autophagy impairment in lafora disease. *Human Molecular Genetics*, *23*(12), 3147–3156.

Eierhoff, T., Stechmann, B., & Römer, W. (2012). Pathogen and Toxin Entry – How Pathogens and Toxins Induce and Harness Endocytotic Mechanisms. In B. Ceresa (Ed.), *Molecular Regulation of Endocytosis* (p. 466). InTech.

England, J. L., & Kaganovich, D. (2011). Polyglutamine shows a urea-like affinity for unfolded cytosolic protein. *FEBS Letters*, *585*(2), 381–384.

Feng, Y., Jadhav, A. P., Rodighiero, C., Fujinaga, Y., Kirchhausen, T., & Lencer, W. I. (2004). Retrograde transport of cholera toxin from the plasma membrane to the endoplasmic reticulum requires the trans-Golgi network but not the Golgi apparatus in Exo2-treated cells. *EMBO Reports*, *5*(6), 596–601.

Fleck, C. A. (2006). Differentiating MMPs, Biofilm, Endotoxins, Exotoxins, and Cytokines. *Adv Skin Wound Care*, *19*(2), 77–81.

Foegeding, N. J., Caston, R. R., McClain, M. S., Ohi, M. D., & Cover, T. L. (2016). An overview of Helicobacter pylori VacA toxin biology. *Toxins*, *8*(6), 1–21.

Galmiche, A., Rassow, J., Doye, A., Cagnol, S., Chambard, J. C., Contamin, S., de Thillot, V., Just, I., Ricci, V., Solcia, E., Van Obberghen, E., & Boquet, P. (2000). The N-terminal 34 kDa fragment of

Helicobacter pylori vacuolating cytotoxin targets mitochondria and induces cytochrome c release. *The EMBO Journal*, *19*(23), 6361–70.

Gaus, K., Le Lay, S., Balasubramanian, N., & Schwartz, M. A. (2006). Integrin-mediated adhesion regulates membrane order. *Journal of Cell Biology*, *174*(5), 725–734.

Gauthier, N. C., Monzo, P., Gonzalez, T., Doye, A., Oldani, A., Gounon, P., Ricci, V., Cormont, M., & Boquet, P. (2007). Early endosomes associated with dynamic F-actin structures are required for late trafficking of H. pylori VacA toxin. *Journal of Cell Biology*, *177*(2), 343–354.

Gauthier, N. C., Ricci, V., Gounon, P., Doye, A., Tauc, M., Poujeol, P., & Boquet, P. (2004). Glycosylphosphatidylinositol-anchored Proteins and Actin Cytoskeleton Modulate Chloride Transport by Channels Formed by the Helicobacter pylori Vacuolating Cytotoxin VacA in HeLa Cells. *Journal of Biological Chemistry*, *279*(10), 9481–9489.

Gentry, M. S., Worby, C. A., & Dixon, J. E. (2005). Insights into Lafora disease: malin is an E3 ubiquitin ligase that ubiquitinates and promotes the degradation of laforin. *Proc Natl Acad Sci U S A*, *102*(24), 8501–8506.

Giacomello, M., Hudec, R., & Lopreiato, R. (2011). Huntington's disease, calcium, and mitochondria. *BioFactors*, *37*(3), 206–218.

Gillespie EJ., Ho CL., Balaji K., Clemens DL., Deng G., Wang YE., Elsaesser HJ., Tamilselvam B., Gargi A., Dixon SD., France B., Chamberlain BT., Blanke SR., Cheng G., de la Torre JC., Brooks DG., Jung ME., Colicelli J., Damoiseaux R., Bradley KA. (2013). Selective inhibitor of endosomal trafficking pathways exploited by multiple toxins and viruses. *Proceedings of the National Academy of Sciences of the United States of America*, *110*(50), E4904-12.

Girard, E., Chmiest, D., Fournier, N., Johannes, L., Paul, J. L., Vedie, B., & Lamaze, C. (2014). Rab7 is functionally required for selective cargo sorting at the early endosome. *Traffic*, *15*(3), 309–326.

Glover, J. R., & Lindquist, S. (1998). Hsp104, Hsp70, and Hsp40: A novel chaperone system that rescues previously aggregated proteins. *Cell*, *94*(1), 73–82.

Goehler H., Lalowski M., Stelzl U., Waelter S., Stroedicke M., Worm U., Droege A., Lindenberg KS., Knoblich M., Haenig C., Herbst M., Suopanki J., Scherzinger E., Abraham C., Bauer B., Hasenbank R., Fritzsche A, Ludewig AH., Büssow K., Coleman SH., Gutekunst CA., Landwehrmeyer BG., Lehrach H., Wanker EE. (2004). A protein interaction network links GIT1, an enhancer of huntingtin aggregation, to Huntington's disease. *Molecular Cell*, *15*(6), 853–865.

Guimaraes, C. P., Carette, J. E., Varadarajan, M., Antos, J., Popp, M. W., Spooner, E., Brummelkamp, T. R., & Ploegh, H. L. (2011). Identification of host cell factors required for intoxication through use of modified cholera toxin. *Journal of Cell Biology*, *195*(5), 751–764.

Han, Y., Moon, H., You, B., & Park, W. (2011). The effect of MG132, a proteasome inhibitor on HeLa cells in relation to cell growth, reactive oxygen species and GSH. *Oncology Reports*, *25*, 223–230.

Hatakeyama, M. (2004). Oncogenic mechanisms of the Helicobacter pylori CagA protein. *Nature Reviews. Cancer*, *4*(9), 688–694.

Hatakeyama, M. (2017). Structure and function of Helicobacter pylori CagA, the first-identified bacterial protein involved in human cancer. *Proc. Jpn. Acad.*, *93*, 196–219.

Hazell, S. L., Lee, A., Brady, L., & Hennessy, W. (1986). Campylobacter pyloridis and gastritis: association with intercellular spaces and adaptation to an environment of mucus as important

factors in colonization of the gastric epithelium. *The Journal of Infectious Diseases*, *153*(4), 658–663.

Hazes, B., & Read, R. J. (1997). Accumulating evidence suggests that several AB- toxins subvert the endoplasmic reticulum-associated protein degradation pathway to enter target cells. *Biochemistry*, *36*(37), 11051–11054.

Henkel, J. S., Baldwin, M. R., & Barbieri, J. T. (2010). Toxins from bacteria. *Experientia*, *100*, 1–29.

Herrera, V., & Parsonnet, J. (2009). Helicobacter pylori and gastric adenocarcinoma. *Clinical Microbiology and Infection*, *15*(11), 971–976.

Herszényi, L., & Tulassay, Z. (2010). Epidemiology of gastrointestinal and liver tumors. *European Review for Medical and Pharmacological Sciences*, *14*(4), 249–258.

Hiruma, H., & Kawakami, T. (2011). Characteristics of weak base-induced vacuoles formed around individual acidic organelles. *Folia Histochemica et Cytobiologica*, *49*(2), 272–279.

Howes MT., Kirkham M., Riches J., Cortese K., Walser PJ, Simpson F., Hill MM., Jones A., Lundmark R., Lindsay MR., Hernandez-Deviez DJ., Hadzic G., McCluskey A., Bashir R., Liu L., Pilch P., McMahon H., Robinson PJ., Hancock JF., Mayor S., Parton RG. (2010). Clathrin-independent carriers form a high capacity endocytic sorting system at the leading edge of migrating cells. *Journal of Cell Biology*, *190*(4), 675–691.

Hu, Y.-B., Dammer, E. B., Ren, R.J., & Wang, G. (2015). The endosomal-lysosomal system: from acidification and cargo sorting to neurodegeneration. *Translational Neurodegeneration*, *4*(1), 18.

Huotari, J., & Helenius, A. (2011). Endosome maturation. *The EMBO Journal*, *30*(17), 3481–500.

IARC. (2012). Biological Agents. *IARC Monogr Eval Carcinog Risks Hum*, *100B*, 1–443.

Ito, Y., Uemura, T., Shoda, K., Fujimoto, M., Ueda, T., & Nakano, A. (2012). cis-Golgi proteins accumulate near the ER exit sites and act as the scaffold for Golgi regeneration after brefeldin A treatment in tobacco BY-2 cells. *Molecular Biology of the Cell*, *23*(16), 3203–3214.

Johannes, L., & Popoff, V. (2008). Tracing the Retrograde Route in Protein Trafficking. *Cell*, *135*(7), 1175–1187.

Johannes, L., & Wunder, C. (2011). Retrograde transport: two (or more) roads diverged in an endosomal tree? *Traffic*, *12*(8), 956–962.

Johnson, L. S., Dunn, K. W., Pytowski, B., & McGraw, T. E. (1993). Endosome acidification and receptor trafficking: bafilomycin A1 slows receptor externalization by a mechanism involving the receptor's internalization motif. *Molecular Biology of the Cell*, *4*(12), 1251–66.

Johnston, J. A., Ward, C. L., & Kopito, R. R. (2012). Aggresomes:a cellular response to misfolded proteins. *Cell*, *143*(7), 1883–1898.

Junaid, M., Linn, A. K., Javadi, M. B., Al-Gubare, S., Ali, N., & Katzenmeier, G. (2016). Vacuolating cytotoxin A (VacA) - A multi-talented pore-forming toxin from Helicobacter pylori. *Toxicon*, *118*, 27–35.

Kaganovich, D., Kopito, R., & Frydman, J. (2008). Misfolded proteins partition between two distinct quality control compartments. *Nature*, *454*, 1088–1095.

Kern, B., Jain, U., Utsch, C., Otto, A., Busch, B., Jiménez-Soto, L., Becher, D., & Haas, R. (2015). Characterization of Helicobacter pyloriVacA-containing vacuoles (VCVs), VacA intracellular trafficking and interference with calcium signalling in T lymphocytes. *Cellular Microbiology*,

17(12), 1811–1832.

Kim, I. J., & Blanke, S. R. (2012). Remodeling the host environment: modulation of the gastric epithelium by the Helicobacter pylori vacuolating toxin (VacA). Frontiers in Cellular and Infection Microbiology, 2(37), 1–18.

Kim, S. S., Ruiz, V. E., Carroll, J. D., & Moss, S. F. (2011). Helicobacter pylori in the pathogenesis of gastric cancer and gastric lymphoma. Cancer Letters, 305(2), 228–238.

Kopito, R. R. (2000). Aggresomes, inclusion bodies and protein aggregation. Trends in Cell Biology, 10(12), 524–530.

Kuipers, E. J. (1997). Helicobacter pylori and the risk and management of associated diseases. *Aliment Pharmacol Ther*, *11*, 71–88.

Kulp, A., & Kuehn, M. J. (2012). Biological Functions and Biogenesis of Secreted Bacterial Outer Membrane Vesicles. *Annu Rev Microbiol.*, 163–184.

Kumari, S., Mg, S., & Mayor, S. (2010). Endocytosis unplugged: multiple ways to enter the cell. *Cell Research*, *20*(3), 256–275.

Lee, D. H. (1998). Proteasome inhibitors: Valuable new tools for cell biologists. *Trends in Cell Biology*, *8*(10), 397–403.

Lencer, W. I., & Tsai, B. (2003). The intracellular voyage of cholera toxin: Going retro. *Trends in Biochemical Sciences*, *28*(12), 639–645.

Leunk, R. D., Johnson, P. T., David, B. C., Kraft, W. G., & Morgan, D. R. (1988). Cyto-Toxic Activity in Broth-Culture Filtrates of Campylobacter-Pylori. *Journal of Medical Microbiology*, *26*(2), 93–99.

Lippincott-Schwartz, J., Yuan, L. C., Bonifacino, J. S., & Klausner, R. D. (1989). Rapid redistribution of Golgi proteins into the ER in cells treated with brefeldin A: evidence for membrane cycling from Golgi to ER. *Cell*, *56*(5), 801–813.

London, E. (1992). How bacterial protein toxins enter celis: the role of partiai unfoiding in membrane transiocation. *Molecular Microbiology*, *6*, 3277–3282.

Lönnroth, I., & Holmgren, J. (1973). Subunit Structure of Cholera Toxin. *J. Gen. Microbiol.*, *76*, 417–427.

Lovelace, M. D., & Cahill, D. M. (2007). A rapid cell counting method utilising acridine orange as a novel discriminating marker for both cultured astrocytes and microglia. *Journal of Neuroscience Methods*, *165*(2), 223–229.

Lowry, O., Rosebrough, N., Farr, A., & Randall, R. (1951). Protein measurement with the Folin phenol reagent. *The Journal of Biological Chemistry*, *193*(1), 265–275.

Mani, A., & Gelmann, E. P. (2005). The ubiquitin-proteasome pathway and its role in cancer. *Journal of Clinical Oncology*, *23*(21), 4776–4789.

Marlink, K. L., Bacon, K. D., Sheppard, B. C., Ashktorab, H., Smoot, D. T., Cover, T. L., Deveney, C. W., & Rutten, M. J. (2003). Effects of Helicobacter pylori on intracellular Ca2+ signaling in normal human gastric mucous epithelial cells. *Am J Physiol Gastrointest Liver Physiol*, *285*(1), G163–G176.

Marshall, B. (2008). Helicobacter pylori--a Nobel pursuit? *Canadian Journal of Gastroenterology = Journal Canadien de Gastroenterologie*, *22*(11), 895–6.

Matsudaira, T., Niki, T., Taguchi, T., & Arai, H. (2015). Transport of the cholera toxin B-subunit from recycling endosomes to the Golgi requires clathrin and AP-1. *Journal of Cell Science*, *128*(16),

3131–3142.

McClain, M. S., Schraw, W., Ricci, V., Boquet, P., & Cover, T. L. (2000). Acid activation of Helicobacter pylori vacuolating cytotoxin (VacA) results in toxin internalization by eukaryotic cells. *Molecular Microbiology*, *37*(2), 433–442.

McKenzie, J., Johannes, L., Taguchi, T., & Sheff, D. (2009). Passage through the Golgi is necessary for Shiga toxin B subunit to reach the endoplasmic reticulum. *FEBS Journal*, *276*(6), 1581–1595.

Mera, R., Fontham, E. T. H., Bravo, L. E., Bravo, J. C., Piazuelo, M. B., Camargo, M. C., & Correa, P. (2005). Long term follow up of patients treated for Helicobacter pylori infection. *Gut*, *54*(11), 1536–1540.

Minassian, B. A. (2001). Lafora's disease: Towards a clinical, pathologic, and molecular synthesis. *Pediatric Neurology*, *25*(1), 21–29.

Mishev, K., Dejonghe, W., & Russinova, E. (2013). Small molecules for dissecting endomembrane trafficking: A cross-systems view. Chemistry and Biology, 20(4), 475–486.

Miyazaki, Y., Mizumoto, K., Dey, G., Kudo, T., Perrino, J., Chen, L., Meyer, T., & Wandless, T. J. (2016). A method to rapidly create protein aggregates in living cells. Nature Communications, 7, 11689.

Miyashita, S. I., Sagane, Y., Suzuki, T., Matsumoto, T., Niwa, K., & Watanabe, T. (2016). "Non-Toxic" Proteins of the Botulinum Toxin Complex Exert In-vivo Toxicity. Scientific Reports, 6(1), 31043.

Moldavski, O., Amen, T., Levin-Zaidman, S., Eisenstein, M., Rogachev, I., Brandis, A., Kaganovich, D., & Schuldiner, M. (2015). Lipid Droplets Are Essential for Efficient Clearance of Cytosolic Inclusion Bodies. Developmental Cell, 33(5), 603–610.

Montagna, D., Sommi, P., Necchi, V., Vitali, A., Montini, E., Turin, I., Ferraro, D., Ricci, V., & Solcia, E. (2017). Different Polyubiquitinated Bodies in Human Dendritic Cells: IL-4 Causes PaCS During Differentiation while LPS or IFNα Induces DALIS During Maturation. Scientific Reports, (April), 1–13.

Müller, D. J., Janovjak, H., Lehto, T., Kuerschner, L., & Anderson, K. (2002). Observing structure, function and assembly of single proteins by AFM. Progress in Biophysics and Molecular Biology, 79(1–3), 1–43.

Necchi, V., Balduini, A., Noris, P., Barozzi, S., Sommi, P., di Buduo, C., Balduini, C. L., Solcia, E., & Pecci, A. (2013). Ubiquitin/proteasome-rich particulate cytoplasmic structures (PaCSs) in the platelets and megakaryocytes of ANKRD26-related thrombocytopenia. Thrombosis and Haemostasis, 109(2), 263–271.

Necchi, V., Candusso, M. E., Tava, F., Luinetti, O., Ventura, U., Fiocca, R., Ricci, V., & Solcia, E. (2007). Intracellular, Intercellular, and Stromal Invasion of Gastric Mucosa, Preneoplastic Lesions, and Cancer by Helicobacter pylori. *Gastroenterology*, *132*(3), 1009–1023.

Necchi, V., Sommi, P., Ricci, V., & Solcia, E. (2010). In vivo accumulation of Helicobacter pylori products, NOD1, ubiquitinated proteins and proteasome in a novel cytoplasmic structure. *PLoS ONE*, *5*(3).

Necchi, V., Sommi, P., Vitali, A., Vanoli, A., Savoia, A., Ricci, V., & Solcia, E. (2014). Polyubiquitinated proteins, proteasome, and glycogen characterize the particle-rich cytoplasmic structure (PaCS) of neoplastic and fetal cells. *Histochemistry and Cell Biology*, *141*(5), 483–497.

Niu, T.-K., Andrea C. Pfeifer, Jennifer Lippincott-Schwartz, & Jackson, C. L. (2005). Dynamics of GBF1, a Brefeldin A-Sensitive Arf1 Exchange Factor at the Golgi. *Molecular Biology of the Cell*, *16*(8),

1–13.

Odumosu, O., Nicholas, D., Yano, H., & Langridge, W. (2010). AB toxins: A paradigm switch from deadly to desirable. *Toxins*, *2*(7), 1612–1645.

Ogrodnik, M., Salmonowicz, H., Brown, R., Turkowska, J., Średniawa, W., Pattabiraman, S., Amen, T., Abraham, A. chen, Eichler, N., Lyakhovetsky, R., & Kaganovich, D. (2014). Dynamic JUNQ inclusion bodies are asymmetrically inherited in mammalian cell lines through the asymmetric partitioning of vimentin. *Proceedings of the National Academy of Sciences of the United States of America*, *111*(22), 8049–54.

Ohnishi, N., Yuasa, H., Tanaka, S., Sawa, H., Miura, M., Matsui, A., Higashi, H., Musashi, M., Iwabuchi, K., Suzuki, M., Yamada, G., Azuma, T., & Hatakeyama, M. (2008). Transgenic expression of Helicobacter pylori CagA induces gastrointestinal and hematopoietic neoplasms in mouse. *Proceedings of the National Academy of Sciences of the United States of America*, *105*(3), 1003–1008.

Oldani, A., Cormont, M., Hofman, V., Chiozzi, V., Oregioni, O., Canonici, A., Sciullo, A., Sommi, P., Fabbri, A., Ricci, V., & Boquet, P. (2009). Helicobacter pylori counteracts the apoptotic action of its VacA toxin by injecting the CagA protein into gastric epithelial cells. *PLoS Pathogens*, *5*(10), e1000603.

Orlandi, P. A., Curran, P. K., & Fishman, P. H. (1993). Brefeldin A blocks the response of cultured cells to cholera toxin. Implications for intracellular trafficking in toxin action. *Journal of Biological Chemistry*, *268*(16), 12010–12016.

Palade, G. E. (1975). Intracellulaar aspects of the process of protein synthesis. *Science*, *189*, 347–358.

Palframan, S. L., Kwok, T., & Gabriel, K. (2012). Vacuolating cytotoxin A (VacA), a key toxin for Helicobacter pylori pathogenesis. *Frontiers in Cellular and Infection Microbiology*, *2*, 1–9.

Panasiewicz, M., Domek, H., Hoser, G., Kawalec, M., & Pacuszka, T. (2003). Structure of the ceramide moiety of GM1 ganglioside determines its occurrence in different detergent-resistant membrane domains in HL-60 cells. *Biochemistry*, *42*(21), 6608–6619.

Papini, E., De Bernard, M., Milia, E., Bugnolit, M., Zerialt, M., Rappuolit, R., & Montecucco, C. (1994). Cellular vacuoles induced by Helicobacter pylon originate from late endosomal compartments. *Proceedings of the National Academy of Sciences*, *91*, 9720–9724.

Park, J. G., Kahn, J. N., Tumer, N. E., & Pang, Y.-P. (2012). Chemical Structure of Retro-2, a Compound That Protects Cells against Ribosome-Inactivating Proteins. *Scientific Reports*, *2*, 631.

Parkin, D. M. (2006). The global health burden of infection-associated cancers in the year 2002. *International Journal of Cancer*, *118*(12), 3030–3044.

Peek, R. M., Blaser, M. J., Jr, R. M. P., & Blaser, M. J. (2002). Helicobacter pylori and gastrointestinal tract adenocarcinomas. *Nature Reviews. Cancer*, *2*(January), 28–37.

Peek, R. M., & Crabtree, J. E. (2006). Helicobacter infection and gastric neoplasia. *Journal of Pathology*, *208*(2), 233–248.

Personnic, N., Brlocher, K., Finsel, I., & Hilbi, H. (2016). Subversion of Retrograde Trafficking by Translocated Pathogen Effectors. *Trends in Microbiology*, *24*(6), 450–462.

Peterson, J. W. (1996). Bacterial Pathogenesis. In Samuel Baron (Ed.), *Medical Microbiology* (4th ed., pp. 1–20). Galveston (TX): University of Texas Medical Branch at Galveston.

Pierzyska-Mach, A., Janowski, P. A., & Dobrucki, J. W. (2014). Evaluation of acridine orange, LysoTracker Red, and quinacrine as fluorescent probes for long-term tracking of acidic vesicles. *Cytometry Part A*, *85*(8), 729–737.

Progida, C., Cogli, L., Piro, F., De Luca, A., Bakke, O., & Bucci, C. (2010). Rab7b controls trafficking from endosomes to the TGN. *Journal of Cell Science*, *123*(9), 1480–1491.

Raiborg, C., Wenzel, E. M., Pedersen, N. M., & Stenmark, H. (2016). ER-endosome contact sites in endosome positioning and protrusion outgrowth. *Biochemical Society Transactions*, *44*(2), 441–446.

Raju, D., & Jones, N. L. (2010). Methods to monitor autophagy in H. pylori vacuolating cytotoxin A (VacA)-treated cells. *Autophagy*, *6*(1), 138–143.

Ramachandran, G. (2014). Gram-positive and gram-negative bacterial toxins in sepsis: a brief review. *Virulence*, *5*(1), 213–8.

Rassow, J., & Meinecke, M. (2012). Helicobacter pylori VacA: A new perspective on an invasive chloride channel. *Microbes and Infection*, *14*(12), 1026–1033.

Ricci, V. (2016). Relationship between vaca toxin and host cell autophagy in helicobacter pylori infection of the human stomach: A few answers, Many questions. *Toxins*, *8*(7).

Ricci, V., Ciacci, C., Zarrilli, R., Sommi, P., Tummuru, M. K., Del Vecchio Blanco, C., Bruni, C. B., Cover, T. L., Blaser, M. J., & Romano, M. (1996). Effect of Helicobacter pylori on gastric epithelial cell migration and proliferation in vitro: role of VacA and CagA. *Infect Immun*, *64*(7), 2829–2833.

Ricci, V., Galmiche, A., Doye, A., Necchi, V., Solcia, E., & Boquet, P. (2000). High cell sensitivity to Helicobacter pylori VacA toxin depends on a GPI-anchored protein and is not blocked by inhibition of the clathrin-mediated pathway of endocytosis. *Molecular Biology of the Cell*, *11*(11), 3897–909.

Ricci, V., Sommi, P., Cova, E., Fiocca, R., Romano, M., Ivey, K., Solcia, E., & Ventura, U. (1993). Na+,K+-ATPase of gastric cells. *FEBS*, *334*(2), 158–160.

Ricci, V., Sommi, P., Fiocca, R., Necchi, V., Romano, M., & Solcia, E. (2002). Extracellular pH modulates Helicobacter pylori-induced vacuolation and VacA toxin internalization in human gastric epithelial cells. *Biochemical and Biophysical Research Communications*, *292*(1), 167–174.

Ricci, V., Sommi, P., Fiocca, R., Romano, M., Solcia, E., & Ventura, U. (1997). Helicobacter pylori vacuolating toxin accumulates within the endosomal-vacuolar compartment of cultured gastric cells and potentiates the vacuolating activity of ammonia. *Journal of Pathology*, *183*, 453–459.

Romano, M., Ricci, V., & Zarrilli, R. (2006). Mechanisms of Disease: Helicobacter pylori-related gastric carcinogenesis—implications for chemoprevention. *Nature Clinical Practice Gastroenterology & Hepatology*, *3*(11), 622–632.

Saimani, U., & Kim, K. (2017). Traffic from the endosome towards trans-Golgi network. *European Journal of Cell Biology*, *96*(2), 198–205.

Sandvig, K., Spilsberg, B., Lauvrak, S. U., Torgersen, M. L., Iversen, T.-G., & van Deurs, B. (2004). Pathways followed by protein toxins into cells. *International Journal of Medical Microbiology*, *293*(7–8), 483–490.

Sandvig, K., & Van Deurs, B. (2002). Transport of protein toxins into cells: Pathways used by ricin, cholera toxin and Shiga toxin. *FEBS Letters*, *529*(1), 49–53.

Schindelin J., Arganda-Carreras I., Frise E., Kaynig V., Longair M., Pietzsch T., Preibisch S., Rueden C., Saalfeld S., Schmid B., Tinevez JY., White DJ., Hartenstein V., Eliceiri K., Tomancak P., Cardona A. (2012). Fiji: an open source platform for biological image analysis. *Nature Methods*, *9*(7), 676–682.

Schmitz, A., Herrgen, H., Winkeler, A., & Herzog, V. (2000). Cholera toxin is exported from microsomes by the Sec61p complex. *Journal of Cell Biology*, *148*(6), 1203–1212.

Schnell A: Schnell, L., Mittler, A. K., Mattarei, A., Tehran, D., Montecucco, C., & Barth, H. (2016). Semicarbazone EGA inhibits uptake of diphtheria toxin into human cells and protects cells article from intoxication. *Toxins*, *8*(7), 1–9.

Schnell B: Schnell, L., Mittler, A. K., Sadi, M., Popoff, M. R., Schwan, C., Aktories, K., Mattarei, A., Tehran, D. A., Montecucco, C., & Barth, H. (2016). EGA protects mammalian cells from clostridiumdifficile CDT, clostridium perfringens iota toxin clostridium botulinum C2 toxin. *Toxins*, *8*(4).

Schreiber, S., Bücker, R., Groll, C., Garten, D., Scheid, P., Gatermann, S., Josenhans, C., Bu, R., Azevedo-vethacke, M., Friedrich, S., & Suerbaum, S. (2005). Rapid Loss of Motility of Helicobacter pylori in the Gastric Lumen In Vivo Rapid Loss of Motility of Helicobacter pylori in the Gastric Lumen In Vivo. *Infection and Immunity*, *73*(3), 1–7.

Scott, C. C., Vacca, F., & Gruenberg, J. (2014). Endosome maturation, transport and functions. *Seminars in Cell and Developmental Biology*, *31*, 2–10.

Segal, E. D., Cha, J., Lo, J., Falkow, S., & Tompkins, L. S. (1999). Altered states: involvement of phosphorylated CagA in the induction of host cellular growth changes by Helicobacter pylori. *Proceedings of the National Academy of Sciences of the United States of America*, *96*(25), 14559–14564.

Seto, K., Hayashi-Kuwabara, Y., Yoneta, T., Suda, H., & Tamaki, H. (1998). Vacuolation induced by cytotoxin from Helicobacter pylori is mediated by the EGF receptor in HeLa cells. *FEBS Letters*, *431*(3), 347–350.

Sewald, X., Fischer, W., & Haas, R. (2008). Sticky socks: Helicobacter pylori VacA takes shape. *Trends in Microbiology*, *16*(3), 89–92.

Shames, S. R., & Finlay, B. B. (2012). Bacterial effector interplay: A new way to view effector function. *Trends in Microbiology*, *20*(5), 214–219.

Sivan, G., Weisberg, A. S., Americo, J. L., & Moss, B. (2016). Retrograde Transport from Early Endosomes to the Trans-Golgi Network Enables Membrane Wrapping and Egress of Vaccinia Virions. *Journal of Virology*, *90*(19), JVI.01114-16.

Slater, L. H., Clatworthy, A. E., & Hung, D. T. (2014). Bacterial toxins and small molecules elucidate endosomal trafficking. *Trends in Microbiology*, *22*(2), 53–55.

Snider, R. M., McKenzie, J. R., Kraft, L., Kozlov, E., Wikswo, J. P., & Cliffel, D. E. (2010). The effects of cholera toxin on cellular energy metabolism. *Toxins*, *2*(4), 632–648.

Solcia, E., Sommi, P., Necchi, V., Vitali, A., Manca, R., & Ricci, V. (2014). Particle-Rich Cytoplasmic Structure (PaCS): Identification, Natural History, Role in Cell Biology and Pathology. *Biomolecules*, *4*(3), 848–861.

Sommi, P., Necchi, V., Vitali, A., Montagna, D., De Luigi, A., Salmona, M., Ricci, V., & Solcia, E. (2013). PaCS is a novel cytoplasmic structure containing functional proteasome and inducible by

cytokines/trophic factors. *PLoS ONE*, *8*(12).

Sommi, P., Ricci, V., Fiocca, R., Necchi, V., Romano, M., Telford, J. L., Solcia, E., & Ventura, U. (1998). Persistence of Helicobacter pylori VacA toxin and vacuolating potential in cultured gastric epithelial cells. *Am J Physiol*, *275*(4 Pt 1), G681-688.

Sommi, P., Ricci, V., Fiocca, R., Romano, M., Ivey, K. J., Cova, E., Solcia, E., & Ventura, U. (1996). Significance of ammonia in the genesis of gastric epithelial lesions induced by Helicobacter pylori: an in vitro study with different bacterial strains and urea concentrations. *Digestion*, *57*(5), 299–304.

Spooner, R. A., Watson, P., Smith, D. C., Boal, F., Amessou, M., Johannes, L., Clarkson, G. J., Lord, J. M., Stephens, D. J., & Roberts, L. M. (2008). The secretion inhibitor Exo2 perturbs trafficking of Shiga toxin between endosomes and the trans-Golgi network. *The Biochemical Journal*, *414*(3), 471–84.

Stechmann, B., Bai, S. K., Gobbo, E., Lopez, R., Merer, G., Pinchard, S., Panigai, L., Tenza, D., Raposo, G., Beaumelle, B., Sauvaire, D., Gillet, D., Johannes, L., & Barbier, J. (2010). Inhibition of retrograde transport protects mice from lethal ricin challenge. *Cell*, *141*(2), 231–242.

Stenmark, H. (2009). Rab GTPases as coordinators of vesicle traffic. *Nature Reviews. Molecular Cell Biology*, *10*(8), 513–25.

Stringer, D. (2010). The role of ubiquitination within the endocytic pathway. *Theses and Dissertations*.

Sun J., Wu Y., Su Z., Liu Z., Su B., Liu Z., Liu W., Zhao H., Tana., Bateer., Eshita Y., Chi B., Zhao L., Fang X., Hao W., Wu S., Bian J., Chen J., Ouyang X. (2010). The role of small molecular weight compounds to increase vacuolation induced by VacA toxin in vitro. *Toxicology in Vitro*, *24*(5), 1373–1378.

Sundrud, M. S., Torres, V. J., Unutmaz, D., & Cover, T. L. (2004). Inhibition of primary human T cell proliferation by Helicobacter pylori vacuolating toxin (VacA) is independent of VacA effects on IL-2 secretion. *Proceedings of the National Academy of Sciences*, *101*(20), 7727–7732.

Sycuro, L. K., Pincus, Z., Gutierrez, K. D., Biboy, J., Chelsea, A., Vollmer, W., & Salama, N. R. (2011). Relaxation of peptidoglycan cross-linking promotes Helicobacter pylori's helical shape and stomach colonization. *Cell*, *141*(5), 822–833.

Takalo, M., Salminen, A., Soininen, H., Hiltunen, M., & Haapasalo, A. (2013). Protein aggregation and degradation mechanisms in neurodegenerative diseases. *American Journal of Neurodegenerative Disease*, *2*(1), 1–14.

Tan, S., Noto, J. M., Romero-Gallo, J., Peek, R. M., & Amieva, M. R. (2011). Helicobacter pylori perturbs iron trafficking in the epithelium to grow on the cell surface. *PLoS Pathogens*, *7*(5).

Todar, K. (2009). Todar's Online Textbook of Bacteriology. *Todar's Online Textbook of Bacteriology*, 1–580.

Tokarev, A. A., Alfonso, A., & Segev, N. (2009). *Overview of Intracellular Compartments and Trafficking Pathways*. *Landes Bioscience*.

Tombola, F., Oregna, F., Brutsche, S., Szabò, I., Del Giudice, G., Rappuoli, R., Montecucco, C., Papini, E., & Zoratti, M. (1999). Inhibition of the vacuolating and anion channel activities of the VacA toxin of Helicobacter pylori. *FEBS Letters*, *460*(2), 221–225.

Torres, V. J., Ivie, S. E., McClain, M. S., & Cover, T. L. (2005). Functional properties of the p33 and

p55 domains of the Helicobacter pylori vacuolating cytotoxin. *Journal of Biological Chemistry*, *280*(22), 21107–21114.

Turnbull, J., Girard, J. M., Lohi, H., Chan, E. M., Wang, P., Tiberia, E., Omer, S., Ahmed, M., Bennett, C., Chakrabarty, A., Tyagi, A., Liu, Y., Pencea, N., Zhao, X., Scherer, S. W., Ackerley, C. A., & Minassian, B. A. (2012). Early-onset Lafora body disease. *Brain*, *135*(9), 2684–2698.

Utsch, C., & Haas, R. (2016). Vaca's induction of vaca-containing vacuoles (VCVs) and their immunomodulatory activities on human T cells. *Toxins*, *8*(6).

Valles-Ortega, J., Duran, J., Garcia-Rocha, M., Bosch, C., Saez, I., Pujadas, L., Serafin, A., Canas, X., Soriano, E., Delgado-Garcia, J. M., Gruart, A., & Guinovart, J. J. (2011). Neurodegeneration and functional impairments associated with glycogen synthase accumulation in a mouse model of Lafora disease. *EMBO Molecular Medicine*, *3*(11), 667–681.

Vinion-Dubiel, A. D., McClain, M. S., Czajkowsky, D. M., Iwamoto, H., Ye, D., Cao, P., Schraw, W., Szabo, G., Blanke, S. R., Shao, Z., & Cover, T. L. (1999). A dominant negative mutant of Helicobacter pylori vacuolating toxin (VacA) inhibits VacA-induced cell vacuolation. *Journal of Biological Chemistry*, *274*(53), 37736–37742.

Ward, T. H., Polishchuk, R. S., Caplan, S., Hirschberg, K., & Lippincott-Schwartz, J. (2001). Maintenance of Golgi structure and function depends on the integrity of ER export. *The Journal of Cell Biology*, *155*(4), 557–570.

Watson, P., Jones, A. T., & Stephens, D. J. (2005). Intracellular trafficking pathways and drug delivery: Fluorescence imaging of living and fixed cells. *Advanced Drug Delivery Reviews*, *57*(1 SPEC. ISS), 43–61.

Weisberg, S. J., Lyakhovetsky, R., Werdiger, A., Gitler, a. D., Soen, Y., & Kaganovich, D. (2012). Compartmentalization of superoxide dismutase 1 (SOD1G93A) aggregates determines their toxicity. *Proceedings of the National Academy of Sciences*, *109*(39), 15811–15816.

Wernick, N. L. B., Chinnapen, D. J. F., Cho, J. A., & Lencer, W. I. (2010). Cholera toxin: An intracellular journey into the cytosol by way of the endoplasmic reticulum. *Toxins*, *2*(3), 310–325.

Willhite, D. C., & Blanke, S. R. (2004). Helicobacter pylori vacuolating cytotoxin enters cells, localizes to the mitochondria, and induces mitochondrial membrane permeability changes correlated to toxin channel activity. *Cellular Microbiology*, *6*(2), 143–154.

Wong, B. C.-Y., Lam, S. K., Wong, W. M., Chen, J. S., Zheng, T. T., Feng, R. E., Lai, K. C., Hu, W. H. C., Yuen, S. T., Leung, S. Y., Fong, D. Y. T., Ho, J., Ching, C. K., & Chen, J. S. (2004). Helicobacter pylori eradication to prevent gastric cancer in a high-risk region of China: a randomized controlled trial. *JAMA : The Journal of the American Medical Association*, *291*(2), 187–194.

Yahiro, K., Hirayama, T., Moss, J., & Noda, M. (2016). New insights into VacA intoxication mediated through its cell surface receptors. *Toxins*, *8*(5), 1–12.

Yang, B., Ming, X., Abdelkafi, H., Pons, V., Michau, A., Gillet, D., Cintrat, J.-C., Barbier, J., & Juliano, R. (2016). Retro-1 Analogues Differentially Affect Oligonucleotide Delivery and Toxin Trafficking. *ChemMedChem*, *11*(22), 2506–2510.

Yukako Fujinaga, Wolf, A. A., Rodighiero, C., Wheeler, H., Tsai, B., Larry Allen, M. G. J., Rapoport, T., Holmes, R. K., & Lencer, W. I. (2004). Gangliosides That Associate with Lipid Rafts Mediate Transport of Cholera and Related Toxins from the Plasma Membrane to Endoplasmic Reticulm. *Molecular Biology of the Cell*, *15*(April), 3751–3737.

Zarrilli, R., Ricci, V., & Romano, M. (1999). Molecular response of gastric epithelial cells to Helicobacter pylori-induced cell damage. *Cellular Microbiology*, *1*(2), 93–99.